MHz - Tomoscopy

D1.2

Realization and characterization of the crystals for MHz-TOMOSCOPY prototype

Project information

Project full title	MHz rate mulTiple prOjection X-ray MicrOSCOPY
Project acronym	MHz-TOMOSCOPY
Grant agreement no.	101046448
Instrument	EIC Pathfinder Open
Duration	42 months
Website	https://tomoscopy.eu/

Deliverable information

Deliverable no.	1.2
Deliverable title	Realization and characterization of the crystals for MHz-TOMOSCOPY prototype (diamond crystals)
Deliverable responsible	INFN
Related Work-Package/Task	WP1
Type (e.g. report; other)	Diamond crystals

Funded by the European Union

MHz - Tomoscopy

Author(s)	A. Mazzolari L. Malagutti M. Romagnoni
Dissemination level	
Document Version	1.0
Date	31/03/2025
Download page	

Document information

Version no.	Date	Author(s)	Comment
1	31/03/2025	**A. Mazzolari** L. Malagutti M. Romagnoni F. Cescato	Initial version

Funded by
the European Union

Abstract

This report presents a comprehensive account of the realization and characterization processes undertaken for the silicon and diamond crystals employed in the MHz-TOMOSCOPY prototype.
In the silicon section, the crystals have been both fabricated and rigorously characterized using advanced techniques. The fabrication process involved state-of-the-art photolithography, anisotropic wet chemical etching, and the integration of precision strain relief cuts to produce high-quality, thin silicon membranes. These membranes were subsequently evaluated using white-light interferometry and 3D optical profilometry to ensure uniform thickness, low surface roughness, and precise geometric parameters. High-resolution X-ray diffraction was further employed to verify the crystallographic orientation, confirming that the silicon crystals meet the demanding quality requirements for X-ray interaction studies.
Subsequently, the report discusses the diamond crystals. Initially, the sole supplier capable of fulfilling the project's requirements was the Institute for Super Hard Materials in Moscow; however, geopolitical constraints necessitated the establishment of alternative supply channels through international collaborations with private companies and research institutes. The diamond crystals are produced via a High Pressure High Temperature (HPHT) process and adhere to rigorous specifications, including a IIa purity grade, low surface roughness, and carefully tailored geometrical and assembly criteria to prevent mechanical stress during mounting.
The diamond crystals were procured and then meticulously characterized. Comprehensive interferometric measurements were performed to determine their lateral dimensions and thickness, while 3D optical profilometry was used to assess surface roughness at the nanometric level. High-resolution X-ray diffraction provided accurate determination of crystallographic orientation and miscut angles, and X-ray topography offered direct imaging of the lattice to detect any dislocations in the active area.
It is important to underline that the crystallographic specifications of the crystals were defined by DESY, ensuring that both silicon and diamond components adhere to the requirements for the project. The advanced characterization capabilities demonstrated in this study confirm the successful realization of high-quality crystal components essential for the success of the MHz-TOMOSCOPY prototype.

Funded by
the European Union

Table of Contents

Funded by
the European Union

Funded by
the European Union

1. Silicon crystals.

Manufacturing of silicon crytals of relevance to the project has been entrusted to INFN and the University of Ferrara (UniFe), both of which possess extensive infrastructure dedicated to the processing of high-quality crystals. These institutions have significant experience in the fabrication of silicon components, having previously developed crystals with (100) orientation for use at CERN within the UA9 collaboration, where they were employed for particle beam deflection studies.

Compared to the state of the art, the TOMOSCOPY project introduces a substantial advancement by requiring the fabrication of silicon crystals with crystallographic orientations different from (100), such as (111), (110), (311), (331), and (211). This requirement presents a major technological challenge, as it necessitates a comprehensive revision of the conventional processing techniques typically used in the silicon microelectronics industry, which is almost exclusively based on (100)-oriented wafers.

The processing of crystals for X-ray interaction applications demands extremely high crystallographic quality. This level of perfection cannot be achieved through conventional mechanical methods, which induce lattice damage and dislocations. Instead, the fabrication must rely entirely on chemical-based processing techniques. Silicon chemistry is known for its strong anisotropy, a property that has been extensively exploited in microelectronics. However, these techniques are optimized for (100) orientation and do not directly translate to other crystallographic directions.

Consequently, the development of silicon crystals for TOMOSCOPY requires the creation of novel processing methodologies and the formulation of innovative chemical recipes tailored to less conventional orientations. These advancements aim to preserve crystalline integrity, ensure dimensional precision, and enable the reliable production of high-performance components for beam–crystal interaction studies.

1.2 Silicon crystals requirements.

During the early phases of the project, INFN and the University of Ferrara (UNIFE) maintained a proactive dialogue with DESY to support the timely definition of the technical specifications for the silicon crystals. Although this process required longer than initially expected, the final specifications were formally established by DESY in April 2024. In the meantime, it was carried out

a series of preliminary studies and mechanical validation tests using silicon samples already available at INFN, to advance the development activities while awaiting the final design requirements.

The first prototype consisted of a thin, free-standing silicon foil approximately 15 µm thick. While this solution was relatively simple to produce, it proved to be mechanically unstable. During early tests, it became evident that once mounted on the precision goniometers of the experimental setup, the crystal was highly sensitive to environmental mechanical vibrations. This compromised both its alignment stability and measurement reliability.

To address these limitations, a second design was tested, in which the thin silicon membrane was embedded within a thicker support frame. The presence of the frame significantly improved mechanical robustness and facilitated safe handling of the crystal. However, this configuration introduced new challenges: mechanical stress originating from the clamping area was found to propagate into the active membrane region, affecting its structural and functional stability. Moreover, beam exposure during operation led to measurable heating of the crystal, which raised further concerns for long-term performance.

To mitigate these effects, a strain relief cut was introduced, mechanically decoupling the membrane from the frame and thus isolating the active region from external stresses. Additionally, the membrane thickness was reduced to below 25 µm, in line with the agreed design specifications. This updated configuration successfully eliminated stress propagation effects while maintaining structural integrity.

Nevertheless, thermal issues persisted. Despite the improved mechanical performance, the membrane continued to exhibit heating under beam irradiation. As a result, it was decided to further reduce the silicon thickness to below 10 µm, in order to minimize energy absorption and thermal load during operation.

In order to meet the experimental objectives of the project—particularly those related to the study of beam–crystal interactions under various lattice configurations—it is necessary to fabricate silicon membranes with a variety of crystallographic orientations. Specifically, crystals must be produced with surface orientations along the (111), (110), (311), (100), (331), and (211) planes. This range of orientations is essential for exploring direction-dependent phenomena and optimizing the interaction geometry between the x-ray beam and the crystal lattice. The fabrication process must therefore be

adaptable to wafers with these specific orientations, while maintaining the same standards of thickness uniformity, mechanical integrity, and stress isolation previously described.

Figure 1 shows the structural design of a silicon crystal featuring a central thin membrane ("Active area") surrounded by a mechanically robust support region. The **active area**, highlighted in light grey, corresponds to the functional membrane through which the particle beam passes. This region has a nominal **width of at least 6 mm** and a **height greater than 3 mm**, providing sufficient aperture for beam transmission and interaction studies.

Figure 1 Schematic layout of the silicon crystal. The thin active membrane (5 mm width, >3 mm height) is mechanically isolated from the clamping area by a laser-defined strain-relief cut, ensuring stress-free operation.

Encircling the membrane is a frame containing a **strain-relief cut structure**, represented as a thin gap. This mechanically isolates the active area from the surrounding structure, preventing stress transmission from external fixtures. This feature is critical to maintaining the mechanical stability and planarity of the membrane during mounting and operation.

The outer **clamping area**, shown in dark grey, serves as the mechanical interface between the crystal and the experimental holder. This region is intentionally thicker to ensure robustness and facilitate safe handling. Thanks to the presence of the strain-relief cut, mechanical stress arising from clamping is effectively prevented from reaching the active region.

Funded by
the European Union

1.3 Materials and Methods

1.3.1 Wafer preparation and masking.

The starting substrates are (100)-oriented, 500 µm thick silicon wafers produced via the Czochralski (CZ) method. CZ-grown wafers are chosen over Float-Zone (FZ) alternatives due to their higher crystalline uniformity—a factor that is critical for process reproducibility and mechanical integrity in thin membrane fabrication. Importantly, the wafers used in this study are intrinsic (i.e., undoped), which avoids the introduction of unwanted impurity profiles and ensures compatibility with standard etching recipes.

The wafers are classified as prime grade, denoting the highest industry standard in terms of surface quality, low defect density, and dimensional precision. They exhibit ultra-tight geometric specifications, including a Total Thickness Variation (TTV) of less than 1 µm, minimal bow and warp, and highly planar surfaces. These features are essential for achieving uniform etching and producing large-area membranes with consistent thickness. Furthermore, the wafers are certified by the supplier to be free of crystallographic dislocations, ensuring high mechanical reliability and optimal performance during their interaction with X-Ray beams.
A dielectric mask layer—either silicon nitride or silicon oxide—is deposited on the front side via low-pressure chemical vapor deposition (LPCVD) or plasma-enhanced CVD (PECVD), with a typical thickness of 400 nm.

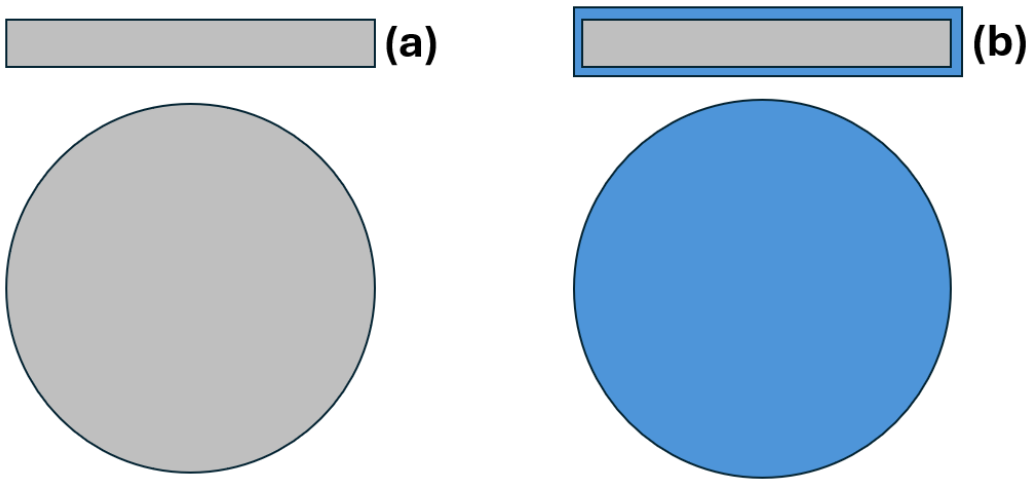

Figure 2. (a) illustration of a silicon wafer. Top: cross section, bottom top view. (b) wafer is coated with a thin layer of dielectric film used as further etching mask

1.3.2 Crystallographic orientation

High-Resolution X-ray Diffraction (HRXRD) is an essential analytical method employed to precisely determine the crystallographic orientation of crystals. By examining diffraction patterns resulting from the interaction of monochromatic X-rays with the crystal lattice, HRXRD provides accurate assessments of crystallographic orientation and angular misorientation with respect to physical surface. This technique enables precise characterization of crystallographic planes, including identification of deviations from ideal orientations (miscut angle, see Figure 3a) and evaluation of structural coherence within the silicon lattice. The measurement setup foreseen a high-resolution X-Ray diffractometer (Panalytical X'Pert^3 MRD) (see figure 3b) coupled with a high-resolution custom-made autocollimator. Measurement approach have been already described in [4].

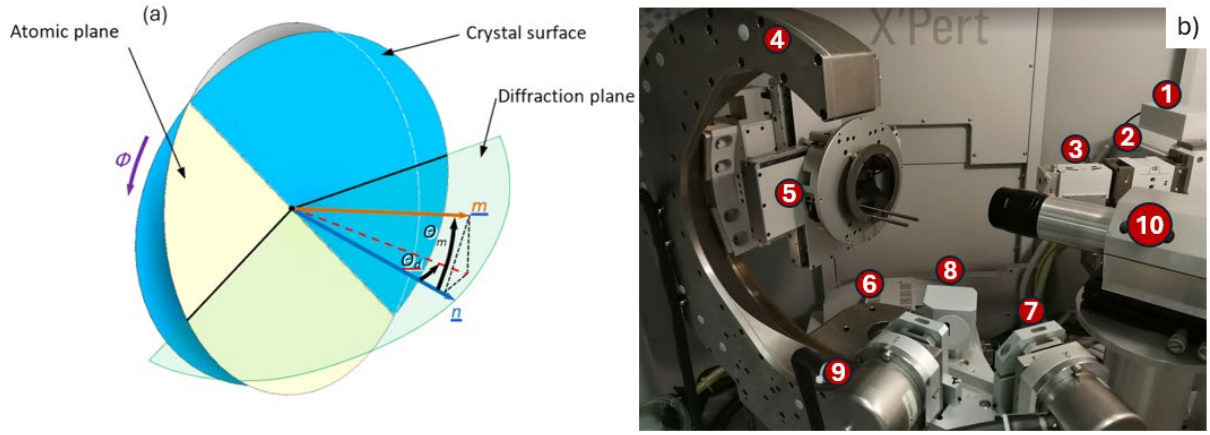

Figure 3 (a) Geometrical model of a crystal illustrating the crystallographic plane (yellow) with its normal m, inclined by the miscut angle Θ_m relative to the surface normal n of the crystal (surface shown in blue). (b) Photograph of a wafer on the high-resolution X-ray diffractometer for the measurement of miscut angles. X-Rays are generated in a conventional x-ray tube (1), collected by a Goebel mirror (2) and directed to a 4-bounce monochromator based on (220) germanium crystals (3). The sample is mounted on a high resolution stage capable of XYZ movements, which is mounted on a Eulerian cradle (4), which is mounted on a high-resolution goniometer (6). Diffracted x-ray beam can be collected by an analyzer crystal based on 3 bounce on (220) germanium (8) and then directed to a detector (9), or can be directly collected by a detector (9). An autocollimator (10) is used to characterize the angular motions and enhance accuracy and precision of the measurement down to 0.0001 deg.

The system employs a conventional X-ray tube source, where X-rays are generated by bremsstrahlung radiation produced by electrons incident on a copper anode. The emitted X-rays are subsequently monochromatized and collimated by a Göbel mirror, followed by a four-bounce monochromator utilizing four successive reflections from (220)-oriented germanium crystals. The setup allows measurements of surface orientation (miscut angle) with accuracy and precision down to 2 µrad, a value ~25000 times better than the requirements (see figure 3b). As an example, Figure 4 shows miscut angle measured on a wafer along different directions.

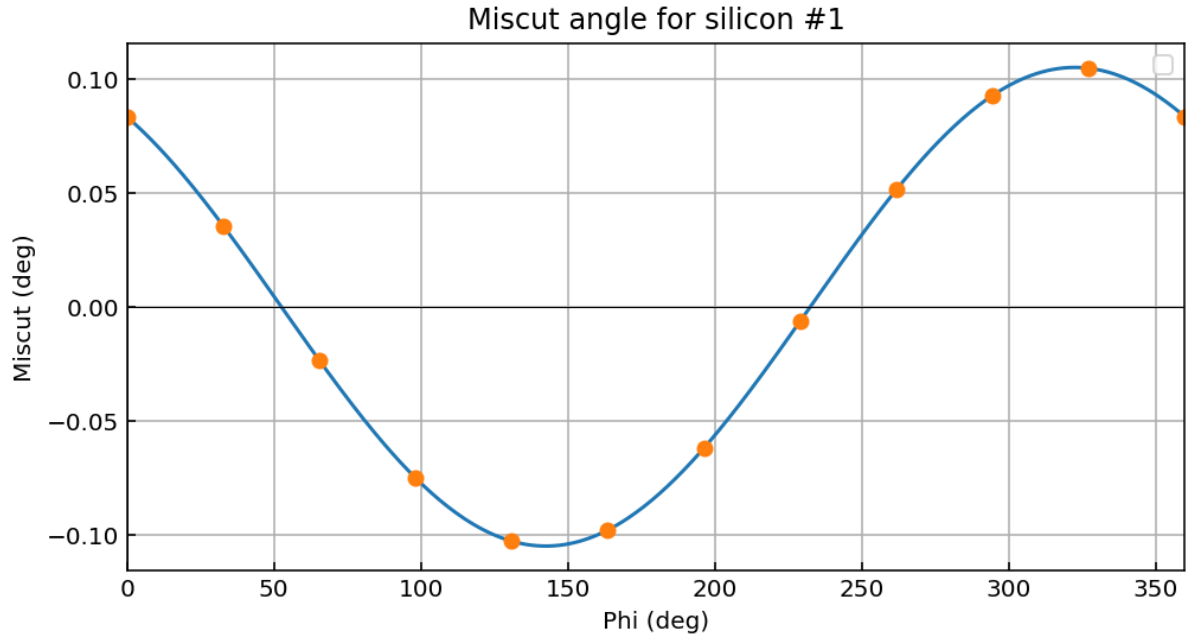

Figure 4: Example of a miscut angle measurement of a silicon wafer

Miscut of the wafers from which membranes are machined is measured after their coating with masking layer, and before the following the subsequent manufacturing steps.

1.3.3 Photolithography.

A first layer of positive-tone photoresist is spin-coated and soft-baked according to the manufacturer's specifications. Photolithographic exposure is carried out using a mask aligner and a photomask defining small square openings (~1 mm). After development, the pattern is transferred to the dielectric layer by means of buffered HF wet etching.

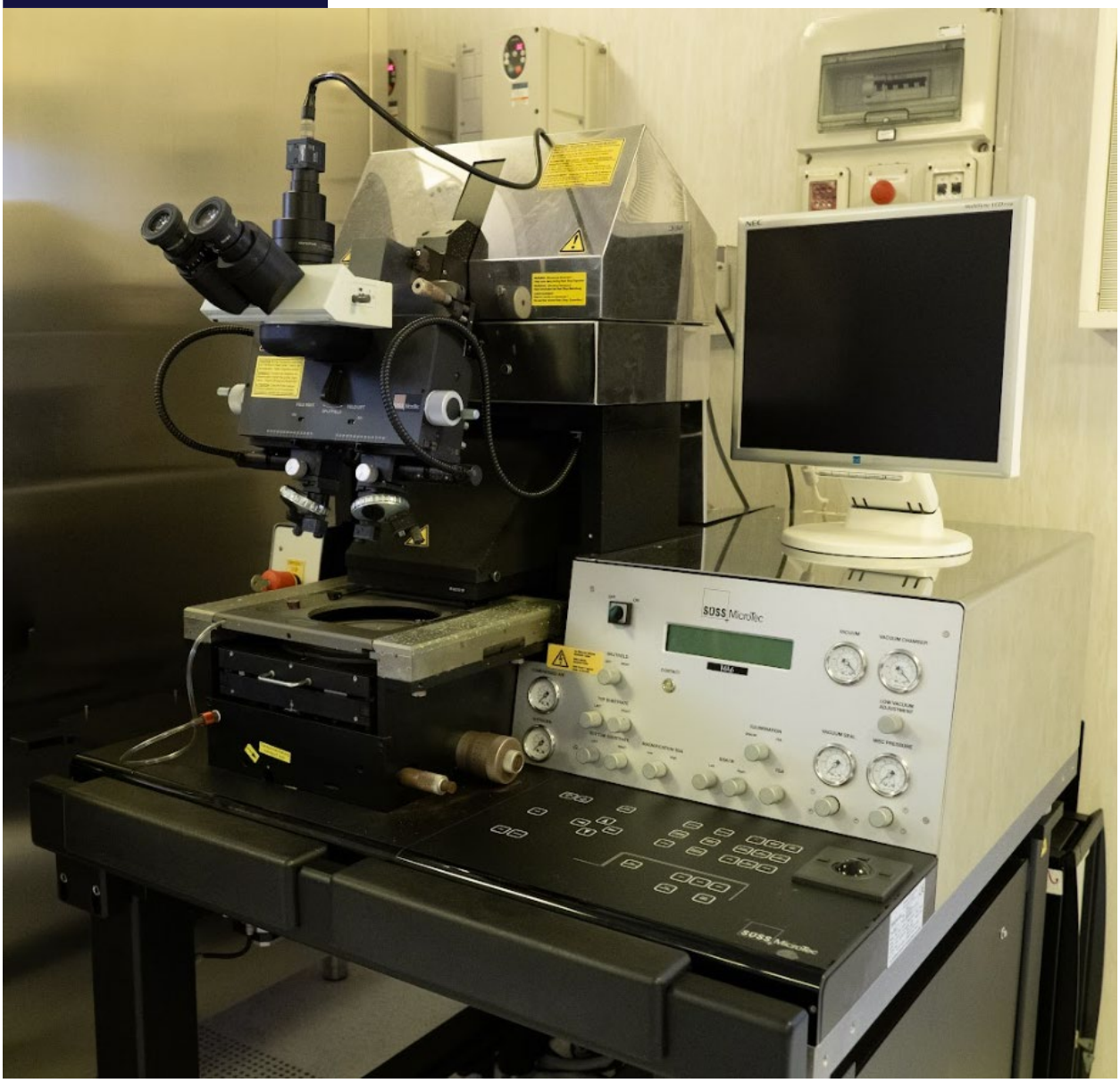

Figure 5 Photolitography equipment

1.3.4 Wet chemical etching.

The wafer is immersed in a basic solution—either potassium hydroxide (30% w/w KOH in deionized water) or tetramethylammonium hydroxide (TMAH, 25%)—to perform anisotropic etching along the (100) crystallographic planes. The process is conducted at room temperature (~22 °C) to enhance process stability and controllability. Under these conditions, the etch rate is approximately 0.8 µm/hour, leading to a total etching duration of about three weeks per wafer. In order to maintain a constant temperature during such prolonged processing, the etching bath is integrated into a custom-built water-

jacketed reactor. The water temperature is actively regulated through an external recirculating chiller, ensuring a stable thermal environment throughout the etching cycle. This thermal stability contributes significantly to achieving uniform membrane thickness across the wafer and between different batches.

An innovative, ad hoc chemical recipe—specifically developed for this project and not previously reported in the literature—has been formulated to enable extremely smooth etched surfaces, with surface roughness in the nanometer range. Such low roughness levels are critical for ensuring uniform thickness throughout the membrane area, particularly when targeting final thicknesses of just a few microns. The recipe has also been carefully optimized to guarantee thickness uniformity within ±1 µm across the entire membrane, addressing the stringent requirements of the application.

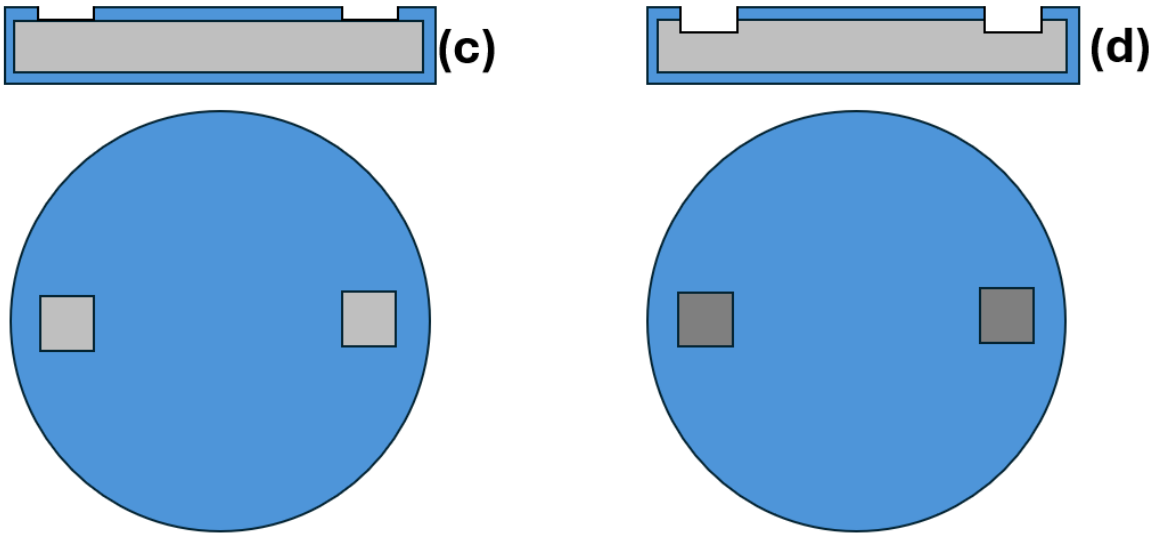

Figure 6. (c) Patterning and selective etching of the silicon nitride layer (blue) through small photoresist-defined openings (light grey). (d) First wet etching step: shallow cavities (~20 µm) are formed in the silicon beneath the exposed areas (dark grey), preparing the structure for subsequent deep etching. Labels follows from figure 2.

1.3.5 Second lithography and deep etching.

Following the first etching step, a second photolithographic process defines larger openings (typically 6×6 mm^2 to 8×8 mm^2), aligned to overlap the previously defined smaller windows. A second wet etching step is carried out under the same thermal and chemical conditions. As the small openings have already been partially etched, they reach the backside of the wafer earlier,

serving as a visual and procedural reference for process monitoring. Etching is deliberately stopped before complete perforation, leaving a thin silicon membrane a few microns thick.

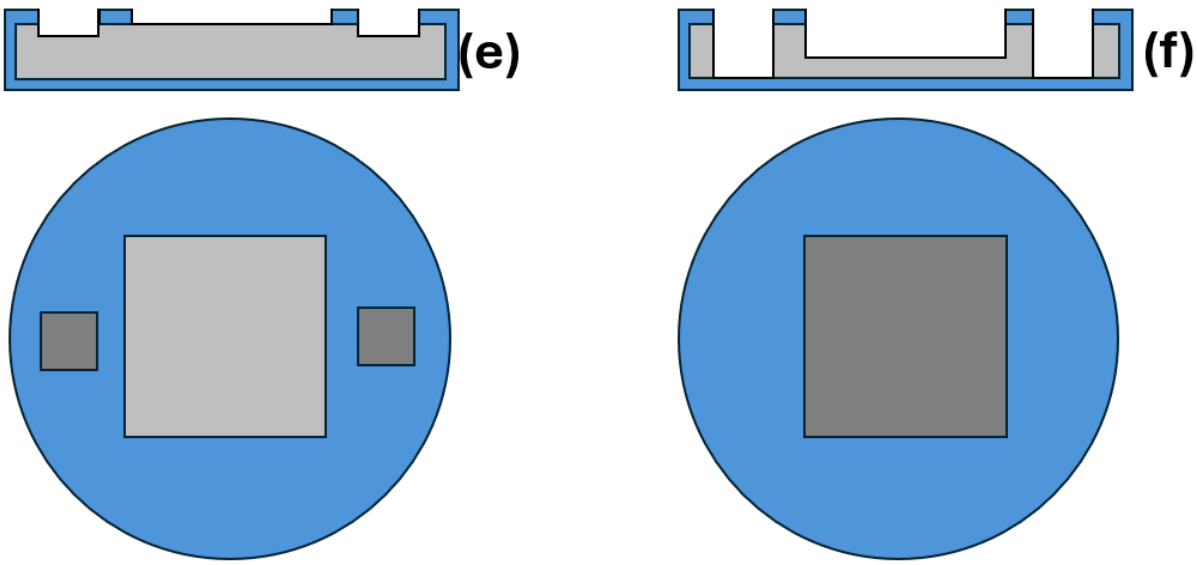

Figure 7 (e) A second photolithography step opens larger square windows (light grey), initiating the second etching phase. Both the new large openings and the previously etched small ones are exposed to the etchant. (f) As the second etching proceeds, the membrane begins to form (dark grey); the small windows, already partially etched, reach the backside of the wafer earlier, indicating the process is approaching completion. Labels follow from figure 4.

1.3.6 Mask removal and final cleaning.

After the desired membrane thickness is achieved, the residual dielectric mask is removed using diluted hydrofluoric acid (HF, 5–10%). The wafer is then rinsed in deionized water and dried with nitrogen.

1.3.7 Custom tooling and process control.

Due to the mechanical fragility of the membranes, a set of custom fixtures and containers was specifically developed to support the chemical processing steps. These include beakers, wafer holders, and reagent handling tools, all produced via 3D printing in polypropylene. To ensure full chemical compatibility and water tightness, dedicated printing recipes were developed and optimized internally. These recipes show in Figure 8, guarantee resistance to aggressive chemical agents such as potassium hydroxide (KOH) and tetramethylammonium hydroxide (TMAH), while maintaining mechanical integrity and sealing performance. The tools were designed in-house and

engineered to provide safe, stress-free handling of delicate samples during prolonged etching procedures.

Figure 8 – Photo of some of custom-designed polypropylene containers and holders developed for the safe handling and chemical processing of fragile silicon membranes. All components were 3D printed in-house and optimized for compatibility with KOH and TMAH solutions, enabling stress-free wafer manipulation during long-duration etching cycles.

1.3.8 Thickness monitoring.

Etch depth and final membrane thickness were monitored throughout the process using white-light interferometry (Ametek Zygo NX2), which offers nanometric resolution and ensures process repeatability across different wafers.

1.3.9 Strain relief design and manufacturing.

To ensure mechanical decoupling between the active membrane and the supporting frame, a dedicated strain relief cut is introduced into the final crystal structure. This feature is obtained by means of precision laser scribing, to define a peripheral groove below the membrane area. The laser marker allows for localized material modification with minimal thermal load, producing a controlled mechanical discontinuity between the membrane and the external frame. This design effectively isolates the active area from mechanical stresses that may arise during mounting or handling. By concentrating deformation in the relief zone, the membrane remains

essentially stress-free, preserving its structural integrity and ensuring stable performance during subsequent use or characterization.

1.3.10 Cleanroom environment.

All fabrication steps—including lithography, masking, etching, and cleaning—were carried out in an ISO class 5 cleanroom to minimize particle contamination and ensure high process reliability. Operating under cleanroom conditions is particularly critical during photolithographic steps, as these define the geometry and alignment of the etched structures. Equally important is maintaining cleanroom conditions during the wet etching processes: performing etching in a controlled environment significantly reduces the risk of metallic contamination in the etching bath or on the wafer surface. Such contamination, even at trace levels, can lead to non-uniform etch rates and result in surface roughening or membrane thickness variations. By avoiding these defects, cleanroom operation contributes to the production of high-quality, uniform silicon membranes suitable for high-precision applications.

1.3.11 Sample singulation.

From a single processed wafer, multiple membrane samples are obtained, each corresponding to a patterned region defined during photolithography. Once the etching and strain relief cut processes are completed, the wafer is sectioned into individual units through mechanical dicing. This step is carried out using a precision wafer saw equipped with a diamond blade, allowing accurate separation along predefined lines while preserving the structural integrity of each membrane. Proper fixturing and low cutting forces are employed to minimize mechanical stress and prevent damage to the thin, fragile structures during the separation process.

Funded by
the European Union

1.4 Silicon crystals individual datasheets

We below summarize the main properties of the manufactured silicon crystals

Technical characteristics		Crystallographic Orientation	
		{100}	{100}
Crystal thickness	Thickness, µm	9.30	9.45
Active area	Length x Width, mm	6.4 x 6.4	6.4 x 6.4
Miscut angle	Degrees	0.1051	0.2433

To ensure full traceability and support thorough quality evaluation, a dedicated datasheet has been compiled for each individual silicon crystal fabricated within the scope of this project. These datasheets report the key characteristics of each crystal, including geometry, thickness, surface roughness, and crystallographic orientation. Each document is accompanied by measurement data and graphical outputs obtained through white-light interferometry, infrared thickness profiling, and high-resolution X-ray diffraction. This structured documentation enables a rigorous comparison between the fabricated items and the project specifications, offering a transparent record of each crystal's properties, manufacturing history, and compliance status.

Funded by
the European Union

1.4.1 Datasheet for the crystal Silicon #1

MHz-Tomoscopy

Grant Agreement 101046448

Datasheet for the crystal Silicon #1

Crystal main features

Crystal orientation: (100)
Crystal active area thickness: 9.3 µm
Strain relief cut: yes
Maximum miscut: 0.1051 degrees
Surface roughness: 50 nm
Dislocations: absent

Crystals geometry

Crystals lateral sizes are verified through a 3D optical profilometer (Zygo NX2), whose working principle relies on white-light interferometry. 6.4 × 6.4 mm^2, precisely defined through photolithographic and etching processes.

Figure 9 representative photo of silicon membrane (crystal silicon #1) mounted on its holder

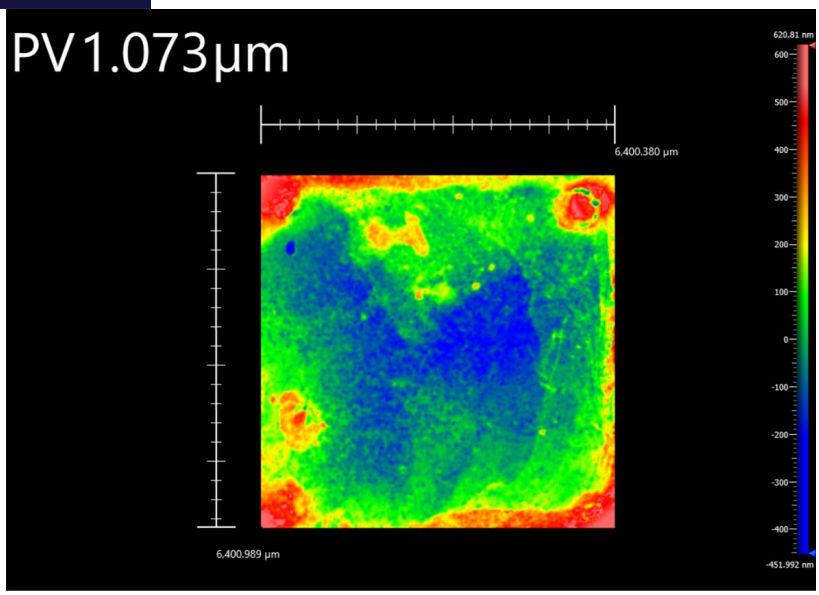

Figure 10. (a) Surface map of the entire active area of silicon crystal sample #1. (b) Detailed view of the surface within the red rectangle highlighted in (a), corresponding to a 6.4 × 6.4 mm^2 region.

Surface roughness

Surface mirror have a mirror-like aspect. Surface roughness is measured through a 3D optical profilometer (Zygo NX2) operating at 100X magnification. Measured value is about ~45 nm. Measurement is carried out on 20 sites and average value is estimated.

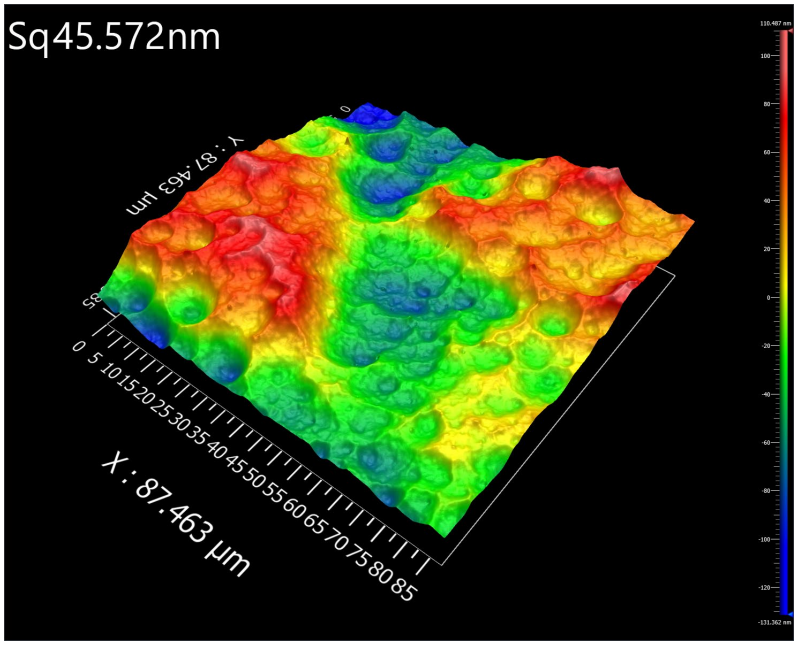

Figure 11. An example of measurement of surface roughness for sample crystal silicon #1

Funded by
the European Union

Crystallographic orientation

Miscut angle, i.e. the angle between the crystal main surface and the atomic planes have been measured through a High-Resolution X-ray Diffraction (Panalytical X'Pert^3 MRD) coupled to a custom-made autocollimator. Maximum miscut angle is 0.1051 degrees.

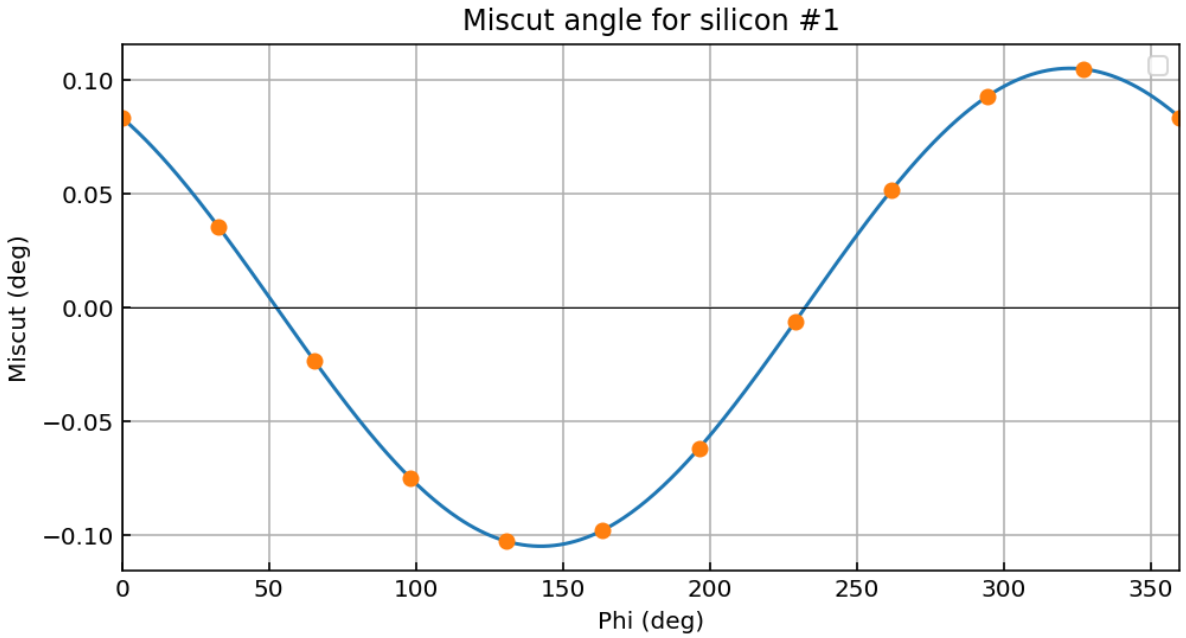

Figure 12. Miscut angle for sample silicon #1. Maximum value reaches 0.1051 degree.

Funded by
the European Union

MHz-Tomoscopy

Grant Agreement 101046448

Datasheet for the crystal Silicon #2

Crystal main features
Crystal orientation: (100)
Crystal active area thickness: 9.45 µm
Strain relief cut: yes
Maximum miscut: 0.2433 degrees
Surface roughness: 40 nm
Dislocations: absent

Crystals geometry
Crystals lateral sizes are verified through a 3D optical profilometer (Zygo NX2), whose working principle relies on white-light interferometry. 6.4 × 6.4 mm^2, precisely defined through photolithographic and etching processes.

Figure 13 representative photo of silicon membrane (crystal silicon #1) mounted on its holder

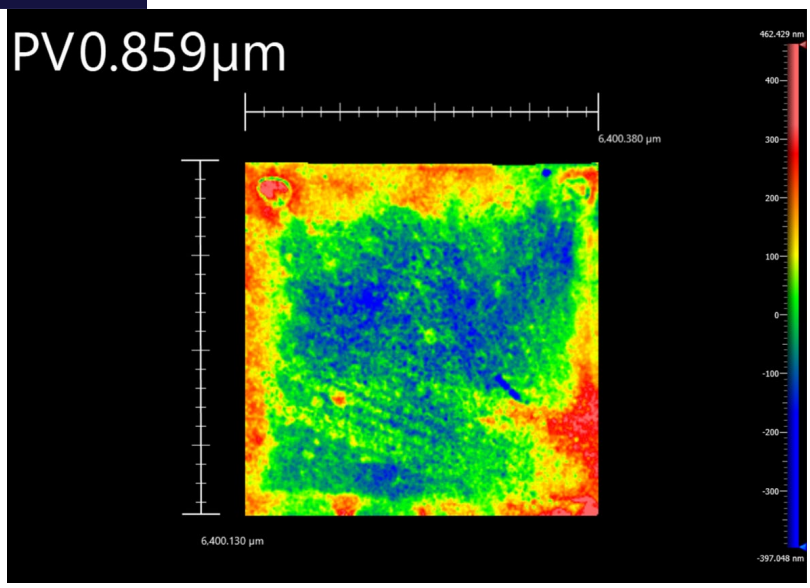

Figure 14. (a) Surface map of the entire active area of silicon crystal sample #1. (b) Detailed view of the surface within the red rectangle highlighted in (a), corresponding to a 6.4 × 6.4 mm^2 region.

Surface roughness

Surface mirror have a mirror-like aspect. Surface roughness is measured through a 3D optical profilometer (Zygo NX2) operating at 100X magnification. Measured value is about ~35 nm. Measurement is carried out on 20 sites and average value is estimated.

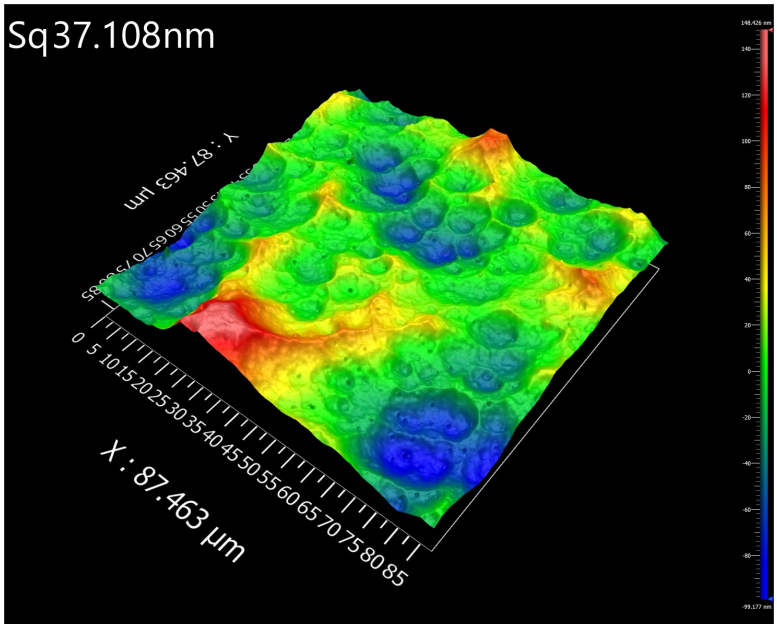

Figure 15. An example of measurement of surface roughness for sample crystal silicon #2

Funded by
the European Union

Crystallographic orientation

Miscut angle, i.e. the angle between the crystal main surface and the atomic planes have been measured through a High-Resolution X-ray Diffraction (Panalytical X'Pert^3 MRD) coupled to a custom-made autocollimator. Maximum miscut angle is 0.2433 degrees.

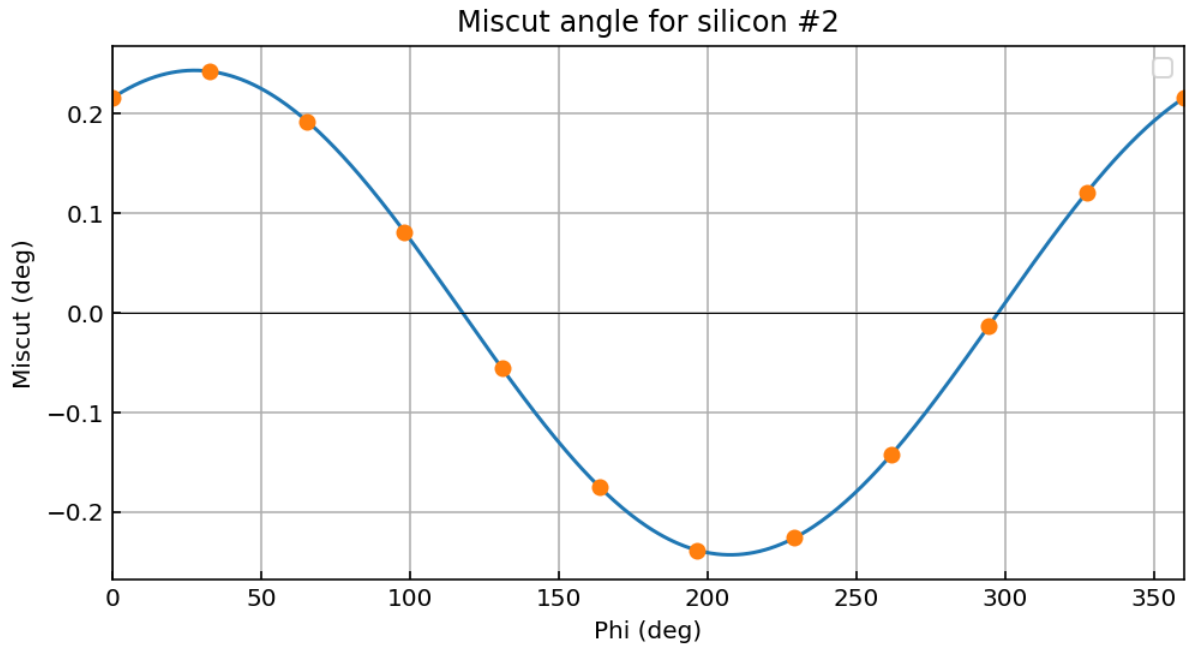

Figure 16. Miscut angle for sample silicon #2. Maximum value reaches 0.2433 degrees.

Funded by
the European Union

1.5 Silicon crystal: future outlooks

In conclusion, the silicon crystals were successfully fabricated using advanced photolithography, anisotropic wet chemical etching, and precision strain relief cuts, yielding thin membranes characterized by uniform thickness and extremely low surface roughness. Subsequent evaluations through white-light interferometry, 3D optical profilometry, and high-resolution X-ray diffraction confirmed full compliance with the stringent technical specifications required for X-ray interaction studies. The crystals were mounted into dedicated holders specifically designed to preserve structural integrity and isolate them from mechanical stresses. Given the delayed finalization of specifications for crystals with orientations other than (100), their production is currently being finalized. Furthermore, the possibility of patenting the developed manufacturing processes is presently under evaluation. These results underscore the team's expertise in developing and characterizing innovative, high-quality silicon components, which are pivotal for the success of the MHz-TOMOSCOPY prototype.

Funded by
the European Union

2. Diamond crystals

We outlines the procurement and characterization process of diamond crystals, which are relevant to the project's objectives. Initially, the Institute for Super Hard Materials (TISNCM) in Moscow, Russia, was the only supplier capable of meeting the requirements. However, due to the conflict between Russia and Ukraine, the need to identify alternative suppliers arose. In response, global collaborations were established with private companies and research institutes, including universities and specialized laboratories in the growth and machining of diamond crystals for scientific applications.
Simultaneously, the technical specifications for the crystals and their metallic supports were defined in collaboration with DESY and Lund University. The required features include the HPHT growth method, a IIa purity grade, precise crystallographic orientations, surfaces with roughness below 50 nm, and active areas with controlled dislocation counts. Detailed geometric parameters and assembly criteria were set to ensure the integrity of the active region during both mounting and subsequent handling.
Finally, the crystals were ordered from XRNanotech (Switzerland) and underwent rigorous quality control at INFN-Ferrara, using characterization protocols derived from extensive experience in producing crystalline optics for particle accelerators.
This report encapsulates the strategic and technical approach adopted to ensure the success of the project, highlighting both the logistical challenges and the innovative solutions implemented on an international scale.

2.1 Diamonds market search

In the scientific field, it was well known that the Institute for Super Hard Materials (TISNCM) in Moscow, Russia was the only supplier capable of fulfilling the project's requirements. Due to war between Ukraine and Russia contacts with this institute was interrupted. Initially, efforts were directed toward constructing a supply chain specifically suited for the production of the diamond crystals of interest, with TISNCM as the primary target. However, due to the conflict between Russia and Ukraine, established collaborations with Russian institutes were disrupted, necessitating the search for alternative suppliers. Consequently, global contacts were established with private companies and research institutes specializing in the growth and machining of diamond crystals for scientific applications. To this end, multiple contacts—via remote meetings and email exchanges—were conducted with various suppliers and research institutes to assess their capabilities and to establish a viable supply chain. The following is a list of companies and institutes with which significant exchanges were held to understand their capacities and to set up a supply chain.

- Research institutes:
    1. TISNCM (Russia)
    2. University of Johannesburg (South Africa)
    3. State Key Lab of Superhard Materials (China)
    4. Ucranian Institute for Super Hard Materials - ISM NAS (Ukraine)
    5. Henan Polytechnic University
    6. Guangxi University of Science and Technology
- Private companies:
    1. NDT Company (Russia)
    2. Almax (Germany)
    3. Sumitomo (Japan)
    4. XRNanotech (Switerland)
    5. Flawless technical diamonds (USA)

2.2 Definition of diamonds technical specifications

Meanwhile, the specifications for the crystals—developed independently of the aforementioned challenges—were established in collaboration with DESY (Dr.

Patrik Vagovic and his team) and Lund University (Prof. Pablo Villanueva Perez and his team). These specifications were finalized by DESY in mid-April 2023. Additionally, the design of the metal supports for the crystals was defined in cooperation with SUNA Precision GMBH (Dr. Alke Meents and his team) in early September 2024.

Below we summarize the specifications for the crystals and the associated metallic supports

1) **Crystal Growth Method**: High Pressure High Temperature (HPHT)
2) **Purity Grade**: IIa (as defined by the International Institute of Diamond Grading & Research).
3) **Angle between the crystal's physical surface and the atomic plane**: The crystallographic orientation of the main surface is indicated in table I: the major surfaces of the crystal must be parallel to the atomic planes of the crystal within 3 degrees along any direction.
4) **Surface Roughness of both major surfaces (Ra)**: less than 50 nm.
5) **Active Area**: each crystal must have an "active area" whose dimensions and location in the crystal geometry are indicated in Table I. This area must be characterized by a dislocation count of less than or equal to 10.
6) **Crystal Geometry and Crystallographic Orientation**: the geometry and crystallographic orientation of the crystals are defined by Figure 17 and Table 1. In Figure 17, the red lines indicate two cuts, internationally known as "strain relief cuts," which serve to prevent the propagation of stress from the region where the crystal is held to the active area of the crystal itself. The cuts must not exceed 50 microns in width and have a length, in millimeters, equal to w-0.5, where w is the length of the crystal expressed in millimeters (see Table 1). For these cuts, a wall taper of less than 10 degrees is acceptable.

   Any variations to the geometry can be discussed and approved both in the bidding phase and in the implementation phase, as long as the presence of an active area with dimensions not less than indicated in Table I is maintained, and the presence of "strain relief cuts" is maintained also.

Funded by
the European Union

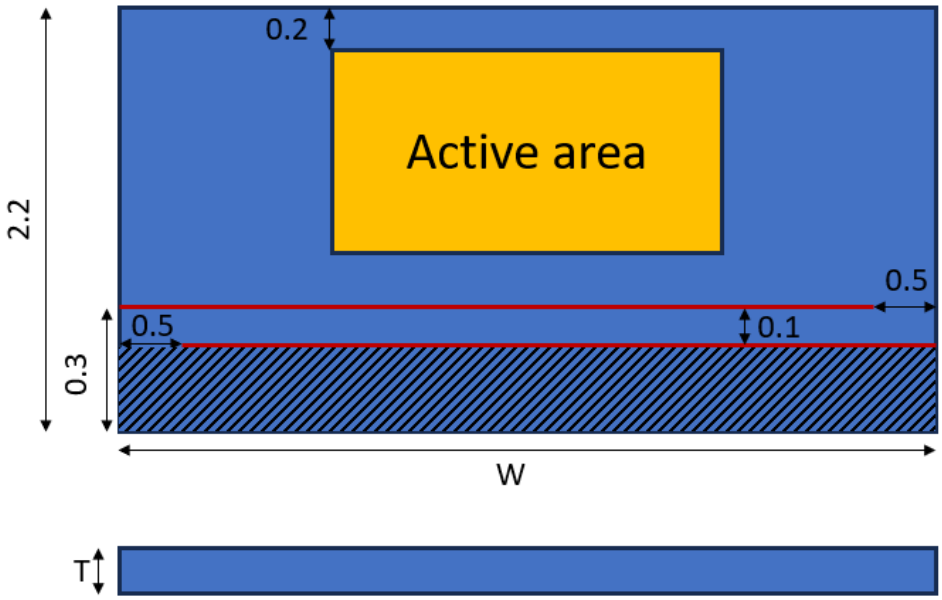

Figure 17: Representation of the geometry of the relevant crystals. The values of width (w) and thickness (T) are indicated in Table I. The dimensions provided are expressed in millimeters.

Crystallographic orientation	Length (W, mm)	Thickness (T, µm)	Size of active area		Quantity
			Width, mm	**Length, mm**	
111±3°	5	≤80	≥1.5	≥3	2
110±3°	4	≤100	≥1.5	≥3	2
311±3°	4	≤100	≥1.5	≥3	1
211±3°	4	≤100	≥1.5	≥3	1
331±3°	4	≤100	≥1.5	≥3	1
511±3°	4	≤100	≥1.5	≥3	1

Table I: Definition of the geometric characteristics of the crystals and their respective quantities. The crystallographic orientation of the first column refers to the orientation of the main surface of each crystal.

Funded by the European Union

7) **Quantity**: The quantities for each type of crystal are specified in Table 1.
8) **Supports for the Crystals**: Each crystal must be accompanied by an aluminum frame that ensures the ability to handle the crystal.
9) **Crystal Assembly**: Each crystal must be mounted in its respective frame, possibly with accessories for fastening also made of aluminum. The assembly must be carried out in such a way that only the region beneath the "strain relief cuts" is in contact with the frame itself (dashed region in figure 1).

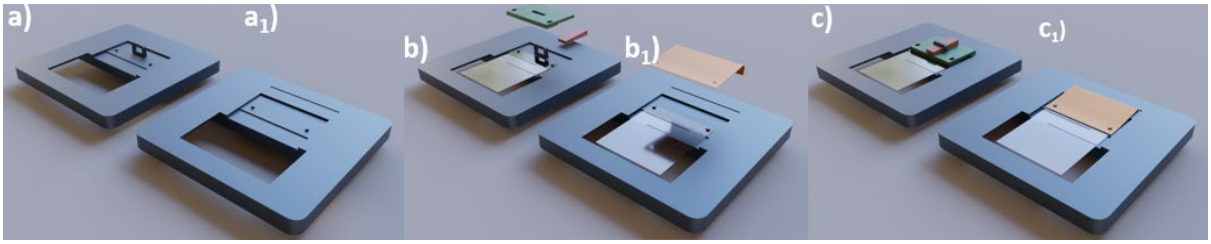

Figure 18: mounting schemes of the crystals on an aluminum frame are illustrated. (a-a1) Aluminum frame without crystal. (b-b1) Frame with the crystal placed on it. The crystal locking elements are depicted above the crystal itself (blue and purple in scheme b, and pink in scheme b1). (c-c1) Crystals assembled in their respective frames.

10) **Deformation of the active region**: After mounting on the frame, the active region of each crystal must not be affected by deformations compared to when the crystal is in its free state.

Funded by
the European Union

2.3 Diamonds purchase and validation

2.3.1 Diamonds purchase

Crystals were ordered at the company XRNanotech (Switerland) on 14-Dec-2023 and received by INFN at the end of November 2024, with almost three month of delay with respect to the delivery date initially foreseen by the supplier.

Figure 19: photo of purchased crystals inside their boxes.

Crystals were delivered contained in boxes suitable for transportation along long distances (see Figure 19). These boxes are advanced packaging solutions engineered specifically for safely transporting delicate items. They integrate a protective membrane —a resilient polymer layer—that acts as a shock absorber and barrier against environmental stresses such as vibrations, impacts, and moisture. This membrane is carefully designed to cushion the contents, ensuring that fragile materials remain secure during handling and transit. These boxes offer both structural rigidity and flexibility, making them ideal for high-risk shipments.

Each box is clearly labeled with the crystallographic orientation of the diamond crystal and its thickness. This labeling system ensures a unique identification of the contents, allowing for immediate verification of both the type and dimensions of the diamond crystal contained within. The precise information provided on each label minimizes handling errors, streamlines inventory management, and supports rigorous quality control throughout the transportation and storage processes.

Funded by
the European Union

2.3.2 Crystals diamond validation

Compliance with the tender specifications was certified by the supplier and verified at INFN-Ferrara empowering a protocol previously employed by the INFN for the manufacturing and characterization of crystalline optics in particle accelerators worldwide [1] — facilities where the requirements are considerably more stringent than those set for this project.

Annex 1 at the end of this report is to report on the characteristics evaluated by the supplier.

2.3.2.1 **Diamonds geometry**

Geometry of each crystal is characterized by a strain relief cut, which assures that stress from the clamping region does not propagate to the active area of the crystal, interacting with X-rays. Crystals are indeed set into an aluminum frame and hold in position by a small clamp. Adoption of a strain relief structure is a standard for crystals whose deformation is sensitive to mounting conditions and typically used at synchrotrons and XFEL facilities [2].

Crystals sizes are verified through a 3D optical profilometer, whose working principle relies on white-light interferometry [3]. This is an advanced optical measurement technique that leverages a broadband, low-coherence light source to accurately capture detailed surface profiles and minute distance variations. In this method, a beam of white light is split into two paths: one is directed toward a reference mirror, and the other is directed toward the test surface. Due to the low coherence of white light, interference fringes form only when the optical path difference between these two beams is extremely small. This selective interference enables precise localization of the fringes, which are then recorded by a detector. By scanning the sample or adjusting the reference mirror, the system acquires data that allows for the reconstruction of a three-dimensional surface profile with sub-nanometer-scale resolution. This capability makes white light interferometry especially valuable for applications such as measuring surface roughness, step heights, and other intricate features. Moreover, the non-contact nature of the technique minimizes any risk of damaging delicate surfaces, making it a preferred choice in industries like semiconductor manufacturing, materials science, and optical component testing. Through this technology we could get information related to crystals lateral sizes, surface roughness and thickness [4].

Figure 4 illustrates an example of the results of the white-light interferometric characterization (in this case (331) oriented crystal with nominal thickness ≤ 100 µm). Panel 4a presents a topological map of the surface, from which the lateral dimensions of the crystal can be determined. Panel 4b displays a detailed map of the crystal thickness over the active area, (in this case the crystal results to be 98.8 µm thick with a thickness variation of just ±1.5 µm, in perfect agreement with specifications). Table 2 summarizes the measured lateral sizes and thickness of the available crystals.

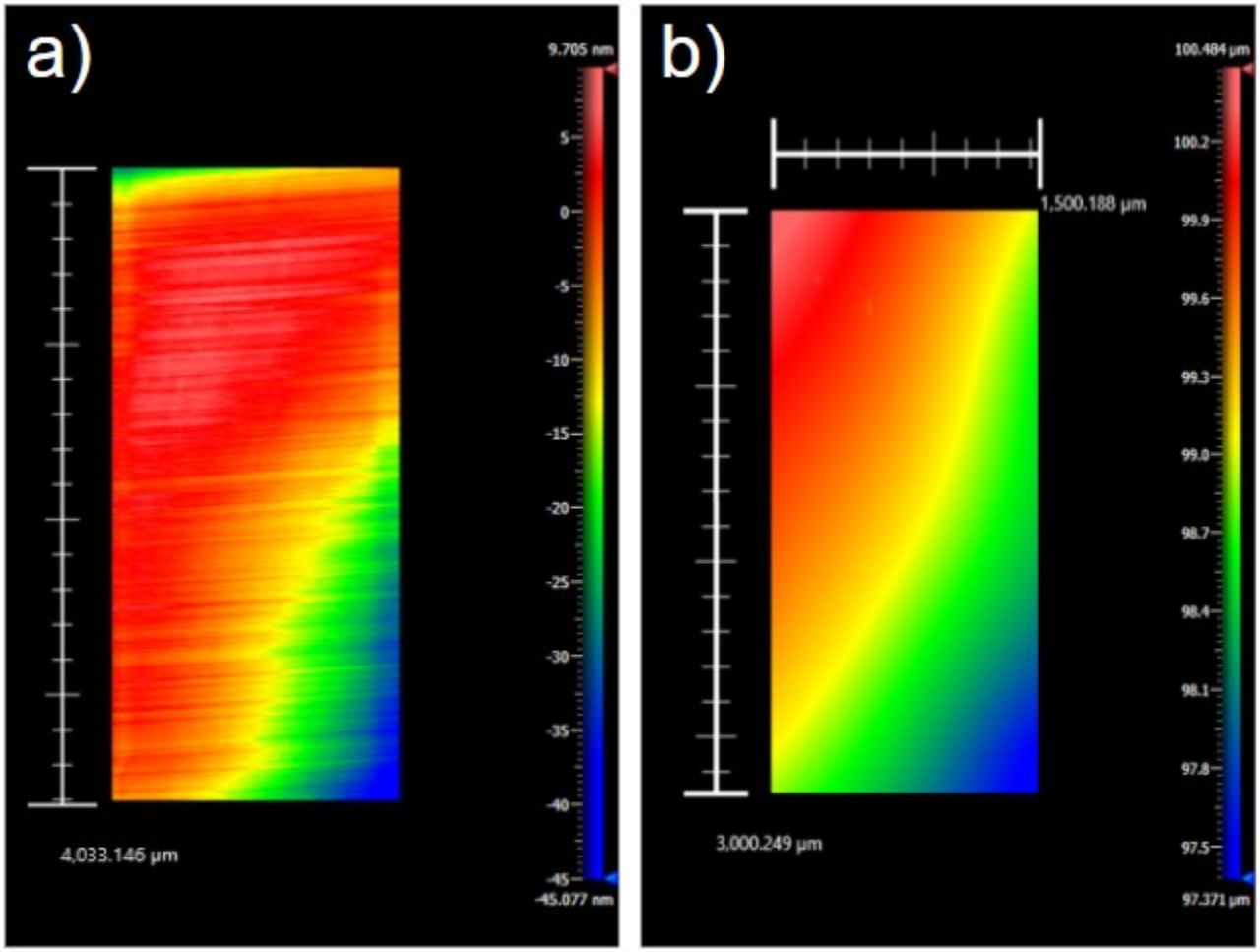

Figure. 20 (a) White light interferometric reconstruction of surface topology used to verify crystal lateral sizes. Darken region highlights the active region (b) Map of crystal thickness filtered over its active area (3x1.5 mm^2) over the central area.

Further confirmation of crystal thickness comes from measurement through a LISE-LI system developed by Fogale Nanotech, which operates on the principle of low coherence infrared interferometry, also known as partial coherence interferometry. It functions by comparing the optical group delays between two interferometer arms: one containing the object to be measured and the

other incorporating a reference delay line with a movable mirror. The system is illuminated by a broadband near-infrared super-luminescent diode centered at 1310 nm. Due to the limited temporal coherence of the light source, interference occurs only when the optical path lengths in both arms match within the coherence length, which is typically around 25 µm. As the reference mirror is scanned, the system detects the position at which the group delays coincide by identifying the peak of the interferometric fringe envelope. This allows for the precise, non-contact measurement of the absolute position and thickness of transparent layers or air gaps, achieving accuracies on the order of ±100 nm. Differently from white light interferometry, which provides a map with a lateral resolution of ~ 12 µm, this tool provides an average thickness value of areas of about 100 µm. Moreover, the result of the measurement is just displayed on the software driving the tool, without a plot to show.

2.3.2.2 Diamonds surface roughness

Surface roughness quantification is achieved by processing the three-dimensional topographic data reconstructed from the interference signal recorded at 100X magnification and is defined as:

$$Sq = \sqrt{\frac{1}{A}\iint_A \left[z(x,y) - \underline{z}\right]^2 dxdy} \qquad \text{Eq. 1}$$

where $\underline{z}$ is the mean surface height over the area A, and $z(x,y)$ is the local height.

The vertical accuracy and precision, which in our tool reaches sub-nanometric levels, allows for the extraction of surface roughness over the field of view (87.4x87.4 µm^2). Figure 21 shows a typical measurement result.

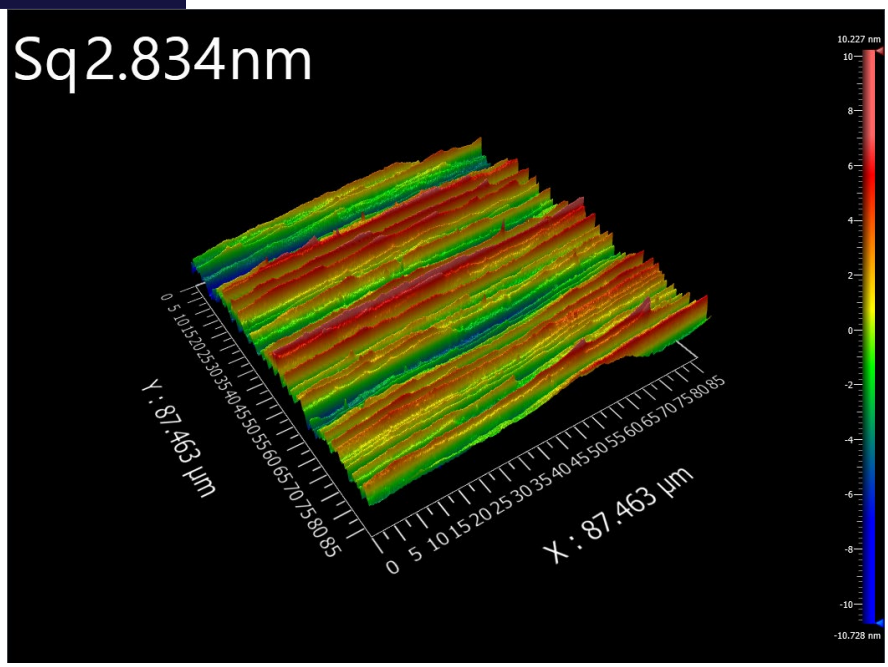

Figure 21. Surface roughness measurement acquired using White Light Interferometry (WLI). The color-coded height map represents the topography of the scanned area (87.457 µm × 87.457 µm), with red corresponding to surface peaks and blue to valleys. The root mean square roughness (Sq) is measured to be 2.7 nm, indicating a high-quality surface finish. The observed linear features suggest an anisotropic surface texture, likely resulting from polishing process.

Sample #	Crystallographic orientation		Length (mm)		Thickness (µm)			Roughness (nm)		Compliance
	Expected	**Measured**	**Expected**	**Measured**	**Expected**	**Measured (WLI)**	**Measured (LISE)**	**Expected**	**Measured**	
1	(111)	(111)	5	5.02	≤ 80	N.A.	79.4	< 50	0.7	Yes
2	(111)	(111)	5	5.04	≤ 80	79.20	79.3	< 50	0.7	Yes
3	(110)	(110)	4	4.02	≤ 100	96.85	96.8	< 50	3.9	Yes
4	(110)	(110)	4	4.03	≤ 100	98.97	98.8	< 50	0.4	Yes
5	(311)	(311)	4	4.12	≤ 100	99.30	99.2	< 50	0.3	Yes
6	(211)	(211)	4	4.02	≤ 100	77.12	77.1	< 50	1.14	Yes
7	(331)	(331)	4	4.03	≤ 100	99.13	99.2	< 50	2.7	Yes
8	(511)	(511)	4	4.01	≤ 100	97.8	97.9	< 50	2.9	Yes

Table 2. Geometric characteristics of the diamond crystals in terms of lateral sizes, thickness and surface roughness.

Funded by the European Union

2.3.2.3 Diamonds crystallographic orientation

High-Resolution X-ray Diffraction (HRXRD) is an essential analytical method employed to precisely determine the crystallographic orientation of crystals. By examining diffraction patterns resulting from the interaction of monochromatic X-rays with the crystal lattice, HRXRD provides accurate assessments of crystallographic orientation and angular misorientation with respect to physical surface. This technique enables precise characterization of crystallographic planes, including identification of deviations from ideal orientations (miscut angle, see Figure 22a) and evaluation of structural coherence within the diamond lattice. The measurement setup foreseen a high-resolution X-Ray diffractometer (Panalytical X'Pert^3 MRD) (see figure 6b) coupled with a high-resolution custom-made autocollimator. Measurement approach have been already described in [1].

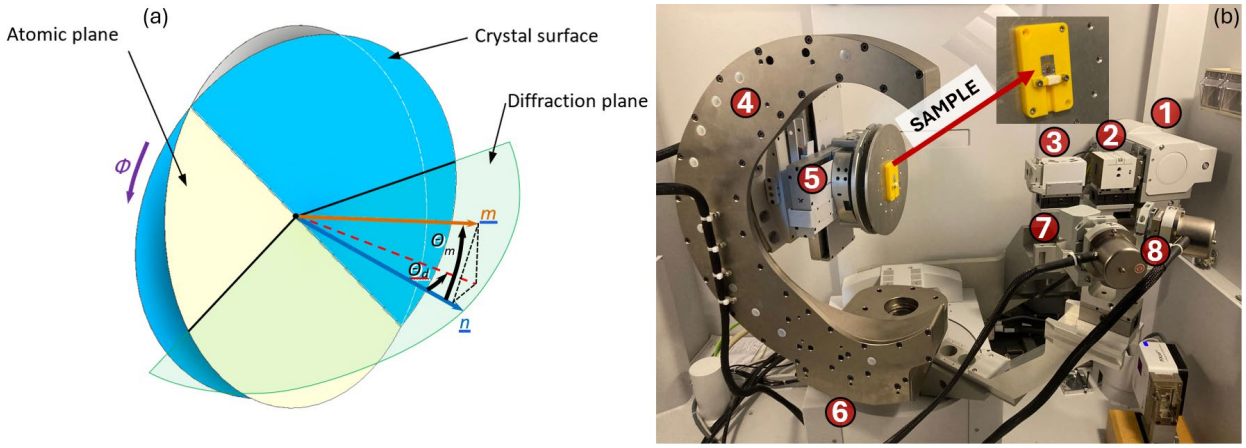

Figure 22 (a) Geometrical model of a crystal illustrating the crystallographic plane (yellow) with its normal m, inclined by the miscut angle Θ_m relative to the surface normal n of the crystal (surface shown in blue). (b) Photograph of the crystal mounted on the high-resolution X-ray diffractometer for the measurement of miscut angles. X-Rays are generated in a conventional x-ray tube (1), collected by a Goebel mirror (2) and directed to a 4-bounce monochromator based on (220) germanium crystals (3). The sample is mounted on a high resolution stage capable of XYZ movements, which is mounted on a Eulerian cradle (4), which is mounted on a high-resolution goniometer (6). Diffracted x-ray beam can be collected by an analyzer crystal based on 3 bounce on (220) germanium (7) and then directed to a detector, or can be directly collected by a detector (8).

The system employs a conventional X-ray tube source, where X-rays are generated by bremsstrahlung radiation produced by electrons incident on a copper anode. The emitted X-rays are subsequently monochromatized and

collimated by a Göbel mirror, followed by a four-bounce monochromator utilizing four successive reflections from (220)-oriented germanium crystals. The setup allows measurements of surface orientation (miscut angle) with accuracy and precision down to 2 µrad, a value ~25000 times better than the requirements (see figure 6b). As an example, Figure 23 shows miscut angle measured on a (111) diamond crystal along different directions.

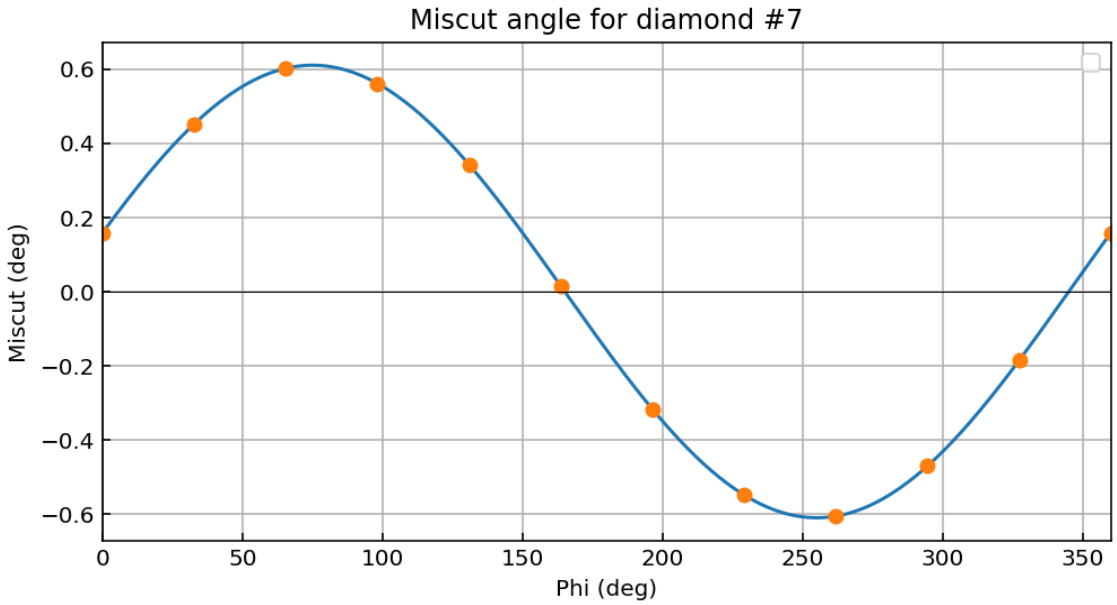

Figure 23: Example of a miscut angle measurement. The measurement was carried out on a diamond crystal with nominal (331) orientation (crystal diamond #7). The experimental data points (in orange) are fitted with a sine function, and the amplitude of the fit—corresponding to the maximum miscut angle—is extracted from the fit parameters. The full set of measured maximum miscut angles is reported in Table 2.

For crystals with nominal (211) and (511) orientation, the use of X-ray radiation at 8 keV does not allow direct excitation of reflections corresponding to the planes parallel to the main crystal surface. In such cases, the surface orientation was determined by analyzing the rocking curves of asymmetric reflections from lattice planes inclined at known angles with respect to the surface normal (see Figure 22a). This approach involves performing X-ray rocking curve measurements by slightly varying the incidence angle (ω) of the X-ray beam around the Bragg diffraction angle corresponding to these asymmetric reflections, thereby accurately determining crystal orientation and lattice alignment.

Funded by
the European Union

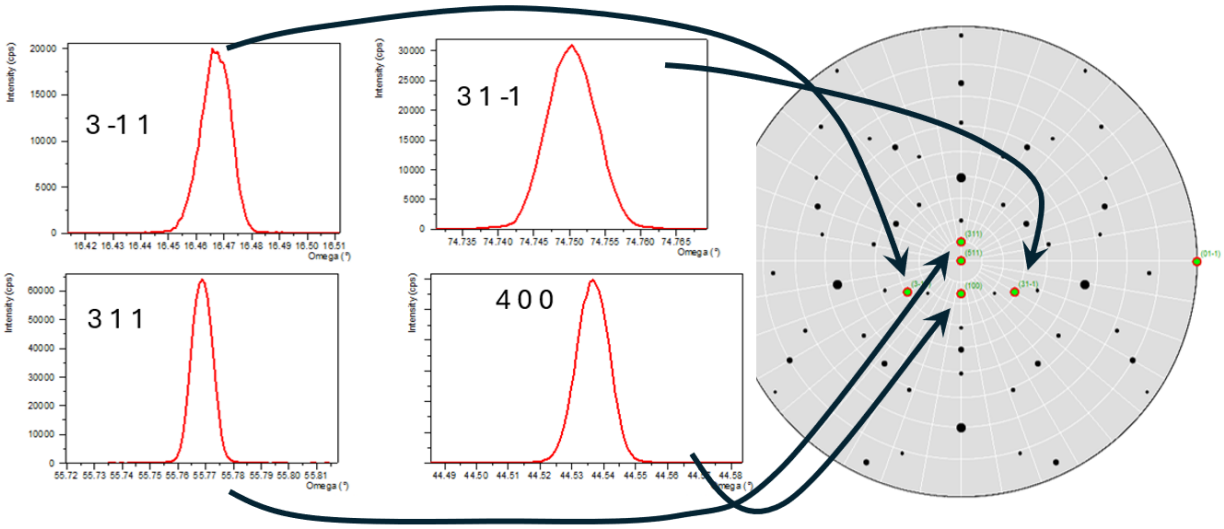

Figure 24. At the photon energy of 8 keV, diffraction from the (511) family of planes is not accessible. To determine the orientation of the crystal surface, asymmetric reflections from the (3-11), (31-1), (311), and (400) planes were measured. The corresponding peaks are shown in the four plots on the left. The angular positions of these reflections were used to reconstruct the crystal stereogram shown on the right. Arrows indicate the association between each measured reflection and its corresponding crystallographic direction in the stereogram. By evaluating the angular separation between the plane normals and the <511> direction, the surface orientation was confirmed to be the (511) plane.

2.4 Diamonds X-ray Topography

X-ray topography is a non-destructive imaging technique based on X-ray diffraction, employed to visualize crystallographic defects and lattice distortions within single crystals with high spatial resolution. Unlike conventional diffraction methods that yield average structural information over large sample volumes, X-ray topography provides spatially resolved images that reveal localized imperfections within the crystal.

In this technique, a monochromatic and collimated X-ray beam is directed onto the crystal. The diffracted X-rays are then recorded on a position-sensitive detector. Variations in the intensity and position of the diffracted beams arise from disruptions in the ideal periodicity of the crystal lattice, such as dislocations, stacking faults, inclusions, or local strain fields. These features are mapped with high sensitivity, allowing for direct observation of internal structural heterogeneities. This characterization was performed at the BM05 beamline of the (European Synchrotron Radiation Facility) (ESRF (European Synchrotron Radiation Facility)), a beamline specifically dedicated to X-ray topography and globally recognized for its outstanding capabilities, and where

personnel has a long lasting experience in characterizing synthetic diamond crystals. The core elements of the setup were an X-Ray beam of energy 20 KeV, a high-resolution goniometer and a detector with spatial resolution of just 11 µm. For each crystal, a pixel-by-pixel rocking curve is recorded, allowing to extract relevant information related to crystal structure.

As an illustrative case, we present the characterization of the (331)-oriented crystal (sample diamond #7). For each pixel, the following parameters were computed from the rocking curve:

- **Full Width at Half Maximum (FWHM):** provides information on the local crystalline perfection. A narrower FWHM indicates a lower degree of lattice distortion or misorientation.
- **Integrated Intensity:** corresponds to the total diffracted signal and is related to the local crystallographic structure and thickness. It can reveal variations in crystal quality or strain.
- **Max Intensity:** reflects the maximum diffracted signal at the optimal angle and is sensitive to local reflectivity and surface quality.
- **Centroid Position:** indicates the angular position of the center of mass of the rocking curve, which can shift due to strain or lattice tilts.

Local imperfections such as dislocations can still be identified through rocking curve analysis. A broadening of the full width at half maximum (FWHM) is indicative of lattice distortions, typically associated with the presence of dislocations. These imperfections induce slight angular misorientations within the otherwise coherent lattice, leading to an increase in the FWHM. Moreover, the centroid position of the rocking curve may vary across the crystal surface, revealing internal strain gradients or subtle lattice tilts. A reduction in peak intensity can also be observed in areas with higher defect density, due to a loss of diffraction efficiency caused by a less perfect crystal structure. Even in a high-quality single crystal, these pixel-by-pixel variations provide valuable insight into the spatial distribution of strain and defect-related phenomena.

Funded by
the European Union

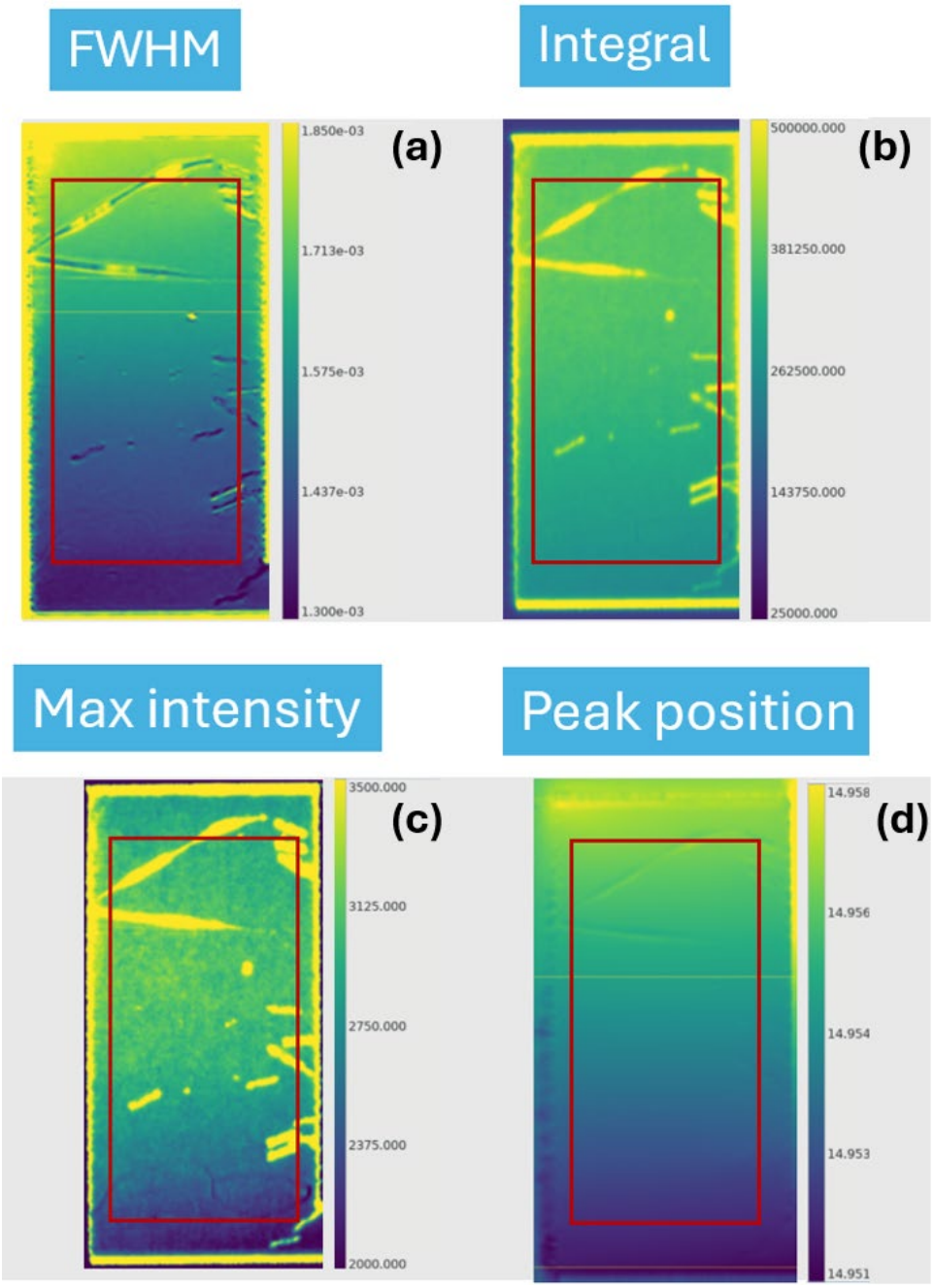

Figure 25. An example of topography, in this case recorded on the (331) oriented crystal. Red rectangle highlights the crystal active region. (a) Full width at half maxim of the rocking curves. (b) Integral or recorded rocking curves. (c-d) Peak intensity and peak positions respectively. Dislocations appear as continuous lines on panes (a), (b) and (c).

Funded by
the European Union

2.5 Diamond crystals individual datasheets

In order to ensure full traceability and facilitate quality assessment, a dedicated datasheet has been compiled for each individual diamond crystal delivered within the scope of this project. These datasheets summarize the key parameters of each crystal, including geometry, thickness, surface roughness, crystallographic orientation, and dislocation count in the active region. Each entry is accompanied by supporting measurements and graphical documentation obtained through white-light interferometry, infrared thickness measurements, high-resolution X-ray diffraction, and synchrotron-based X-ray topography. This systematic approach enables rigorous comparison between supplied items and technical specifications and provides a clear record of compliance for all crystals currently available, and their history.

Funded by
the European Union

2.5.1 Datasheet for crystal diamond #1

MHz-Tomoscopy

Grant Agreement 101046448

Datasheet for the crystal "*Diamond #1*"

The technical specifications for the crystal were established in collaboration with DESY (Dr. Patrik Vagovic and his team) and Lund University (Prof. Pablo Villanueva Perez and his team). These specifications were finalized by DESY in mid-April 2023. Additionally, the design of the metal supports for the crystals was defined in cooperation with SUNA Precision GMBH (Dr. Alke Meents and his team) in early September 2024.

The crystal was purchased by INFN from the company XRNanotech with order dated 14/12/2023 and received by INFN at the end of November 2024.

Crystals geometry

Crystals lateral sizes and thickness are verified through a Fogale TMAP-4 interferometer. The tool does not provide a map of the crystal surface and thickness, but just a report with numerical data. Crystal length was measured to be 5.03 mm, while thickness resulted to be 79.4 µm.

Surface roughness

Surface roughness is measured through a 3D optical profilometer (Zygo NX2) operating at 100X magnification. Measured value is about ~0.7 nm. Measurement is carried out on 20 sites and average value is estimated. Figure 26 shows one of such characterizations

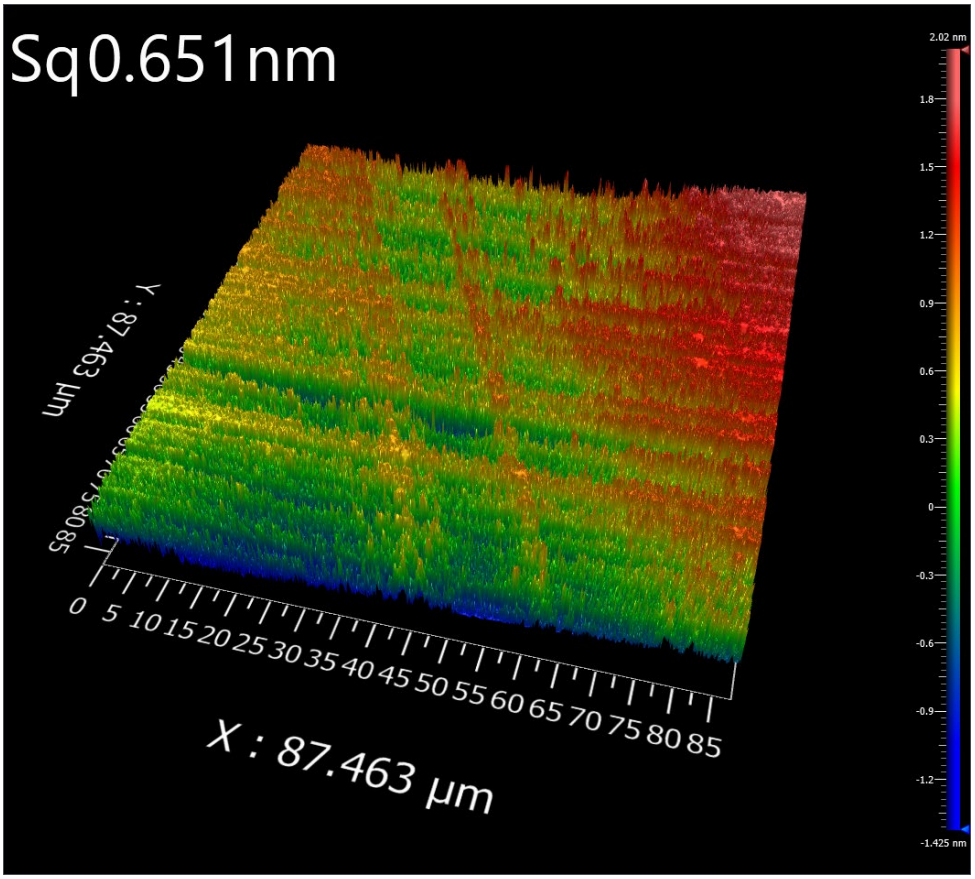

Figure 26: measurement of surface roughness for diamond crystal #1.

Funded by
the European Union

Crystallographic orientation

High-Resolution X-ray Diffraction (Panalytical X'Pert^3 MRD) is used to verify crystallographic orientation.

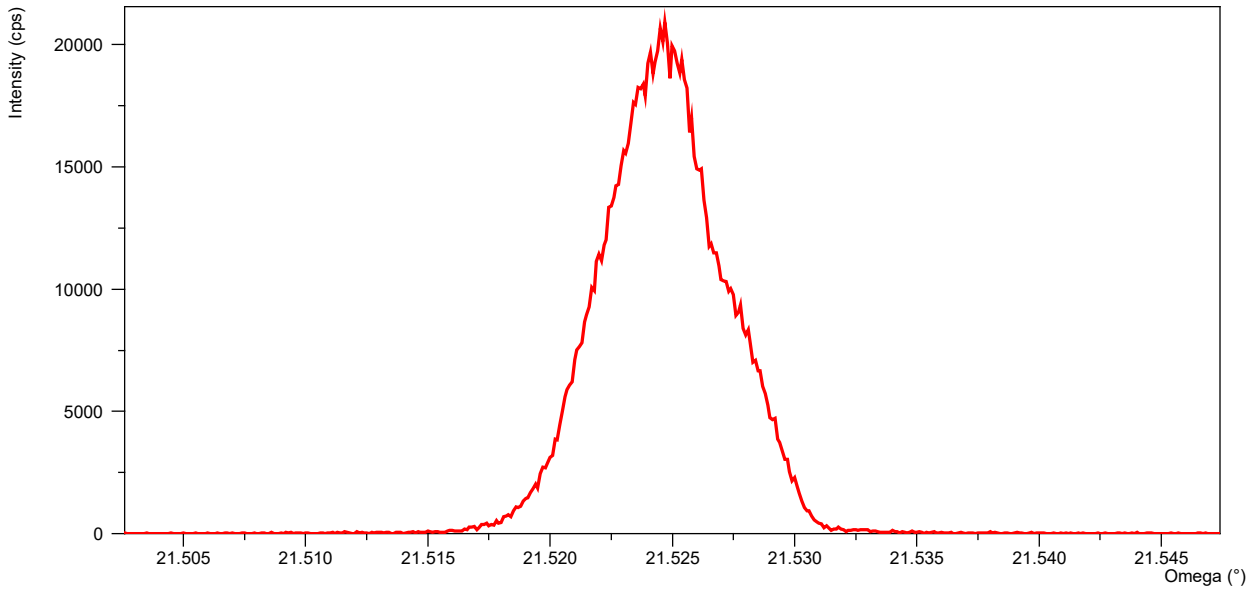

Figure 27. X-Ray rocking curve recorded on the main face of crystal diamond #1 highlights it is (111) oriented. That's worth noting that the beam is wider than the crystal, leading to a tail on the right side of the rocking curve, which is ascribed to the region corresponding to the strain relief cut structure.

The angular position of the rocking curve confirms that the crystal is (111) oriented. Miscut angle, i.e. the angle between the crystal main surface and the atomic planes have been measured through a High-Resolution X-ray Diffraction (Panalytical X'Pert^3 MRD) coupled to a custom-made autocollimator. Results of the measurement are reported in figure 4 and show a maximum value of 1.9811 degrees.

Funded by
the European Union

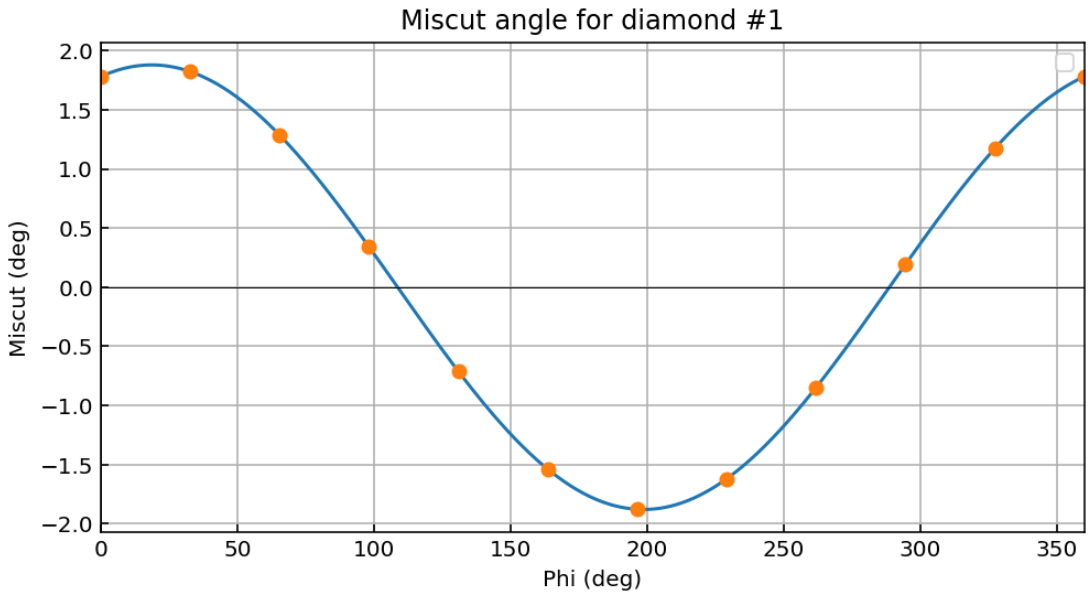

Figure 28. Miscut angle for the sample diamond #1. Maximum value reaches 1.8802 degrees.

Due to a mishandling, the crystal was broken. This occurred prior to topographic characterizations at ESRF, so the number of dislocations in the active area is based on the value provided by the supplier, who characterized the crystal through x-ray topography.

	X-ray topography measurements of the grown crystal. The blue lines indicate the cutout profile of the finished product.	Active area and the number of dislocations
Crystallographic orientation 111 Geometry: 5.67x5.44x1.03mm	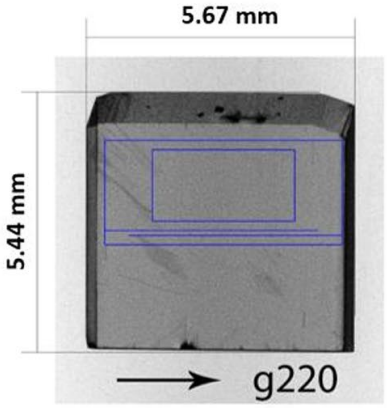	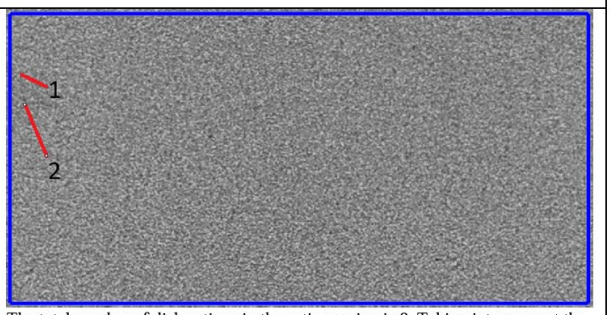 The total number of dislocations in the active region is 2. Taking into account the proportional translation (cutout, thinning and polishing) to the final thickness of the crystal we have 0.14 counts per active region.

Figure 29. X-ray topography characterization of crystal diamond #1, as provided by the supplier.

Table I summarizes the main properties of the crystal diamond #1 and compares them to the tendered specifications.

Technical characteristics			Tender compliance (Yes/No)
Crystal orientation	Orientation	(111)	Yes
Crystal geometry	Length	5.02	Yes
	Thickness, µm	79.4	Yes
Active area	Length x Width, mm	3.00x1.50	Yes
Number of dislocations in the active area	Dislocation count	2	Yes
Angle between the crystal's physical surface and the atomic plane	Degrees	1.8802	Yes

Table 1: comparison between expected main crystal features and characterizations.

Funded by the European Union

2.5.2 Datasheet for crystal diamond #2

MHz-Tomoscopy

Grant Agreement 101046448

Datasheet for the crystal "*Diamond #2*"

The technical specifications for the crystal were established in collaboration with DESY (Dr. Patrik Vagovic and his team) and Lund University (Prof. Pablo Villanueva Perez and his team). These specifications were finalized by DESY in mid-April 2023. Additionally, the design of the metal supports for the crystals was defined in cooperation with SUNA Precision GMBH (Dr. Alke Meents and his team) in early September 2024.

The crystal was purchased by INFN from the company XRNanotech with order dated 14/12/2023 and received by INFN at the end of November 2024.

Crystals geometry

Crystals lateral sizes and thickness are verified through a 3D optical profilometer (Zygo NX2), whose working principle relies on white-light interferometry. Crystal length is 5.04 mm. Average thickness of the active region measured through white light interferometry is 79.20 µm, in agreement with measurement through low coherence infrared interferometry (Fogale TMAP-4) which delivered a value of 79.3 µm.

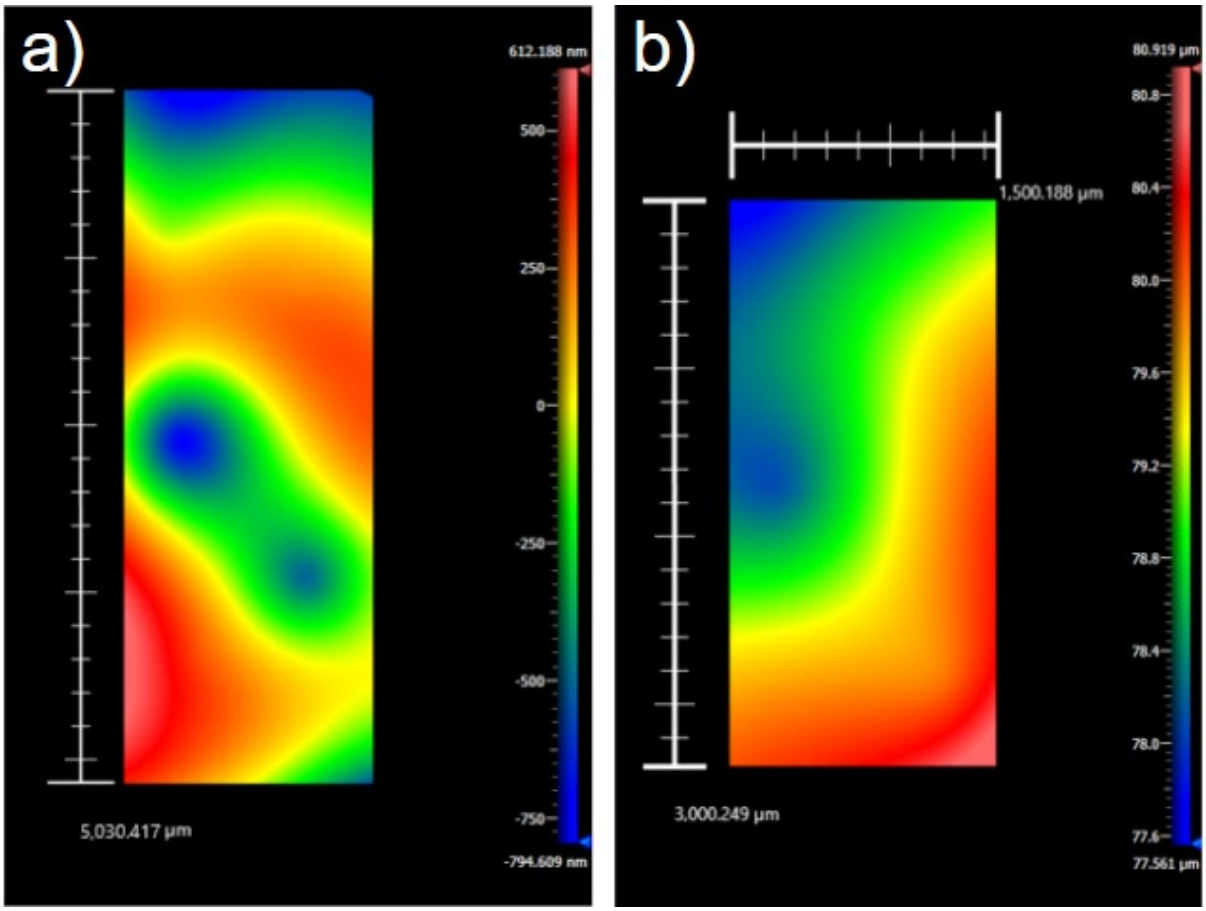

Figure 30: (a) interferometric characterization of the surface of the crystal diamond #2, used to determine the crystal length. (b) Thickness profile of the crystal active region.

Funded by
the European Union

Surface roughness

Surface roughness is measured through a 3D optical profilometer (Zygo NX2) operating at 100X magnification. Measured value is about ~0.7 nm. Measurement is carried out on 20 sites and average value is estimated. Figure 31 shows one of such characterizations

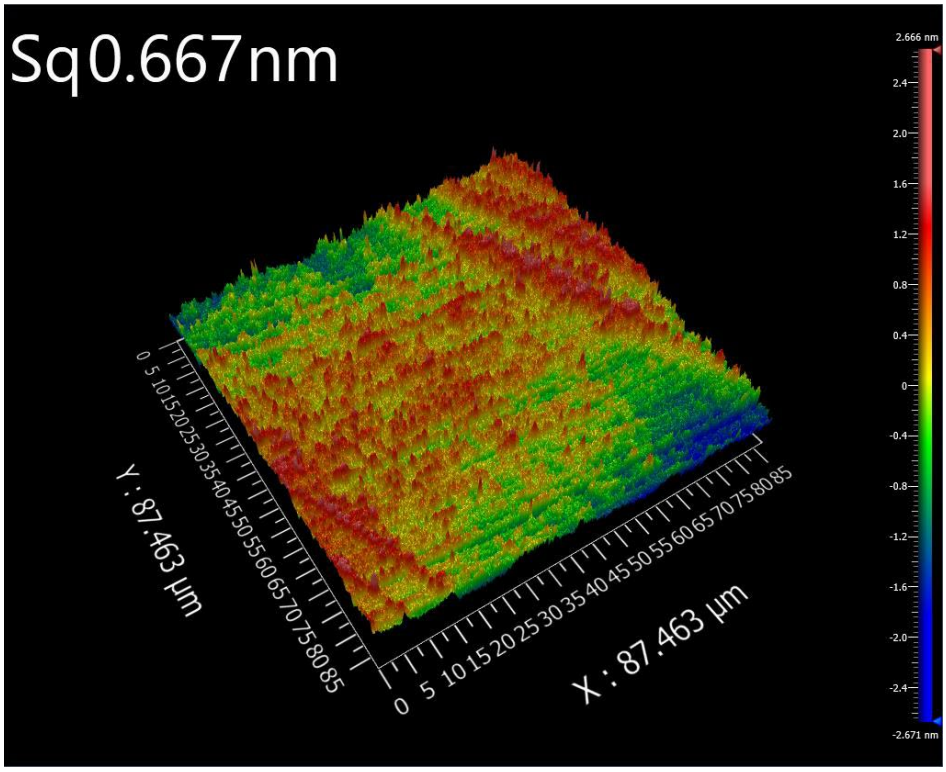

Figure 31: measurement of surface roughness for diamond crystal #2.

Funded by
the European Union

Crystallographic orientation

High-Resolution X-ray Diffraction (Panalytical X'Pert^3 MRD) is used to verify crystallographic orientation.

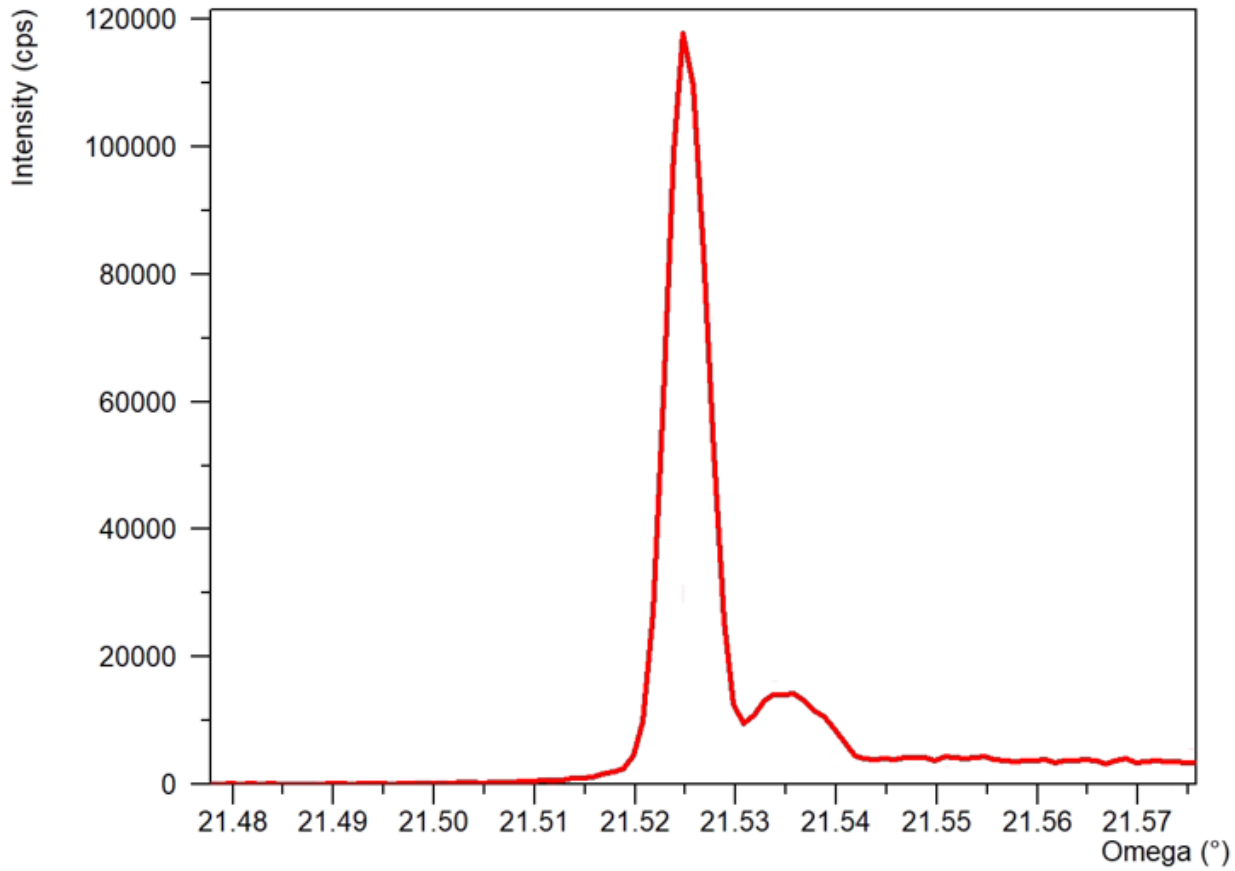

Figure 32. X-Ray rocking curve recorded on the main face of crystal diamond #2 highlight it is (111) oriented. That's worth noting that the beam is wider than the crystal, leading to a tail on the right side of the rocking curve, which is ascribed to the region corresponding to the strain relief cut structure.

The angular position of the rocking curve confirms that the crystal is (111) oriented, as expected.

Miscut angle, i.e. the angle between the crystal main surface and the atomic planes have been measured through a High-Resolution X-ray Diffraction (Panalytical X'Pert^3 MRD) coupled to a custom-made autocollimator. Results of the measurement are reported in figure 4 and show a maximum value of 1.9811 degrees.

Funded by
the European Union

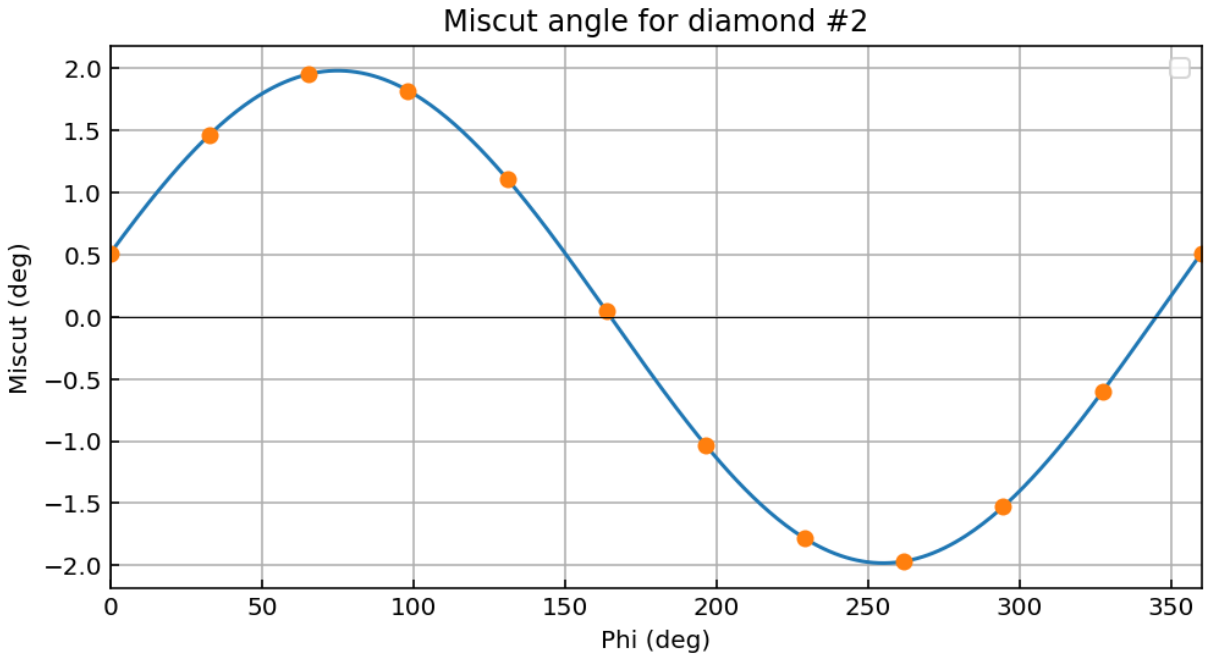

Figure 33. Miscut angle for the sample diamond #2. Maximum value reaches 1.9811 degree.

Funded by
the European Union

X-ray Topography

X-ray Topography has been carried out at BM05 beamline at ESRF (European Synchrotron Radiation Facility). Results of the characterization shows 1 dislocations over the active are of the sample in terms of (a) Full-width half maximum of the rocking curve (b) Integral of the rocking curves (c) Rocking curve peak intensity (d) Centroid peak position.

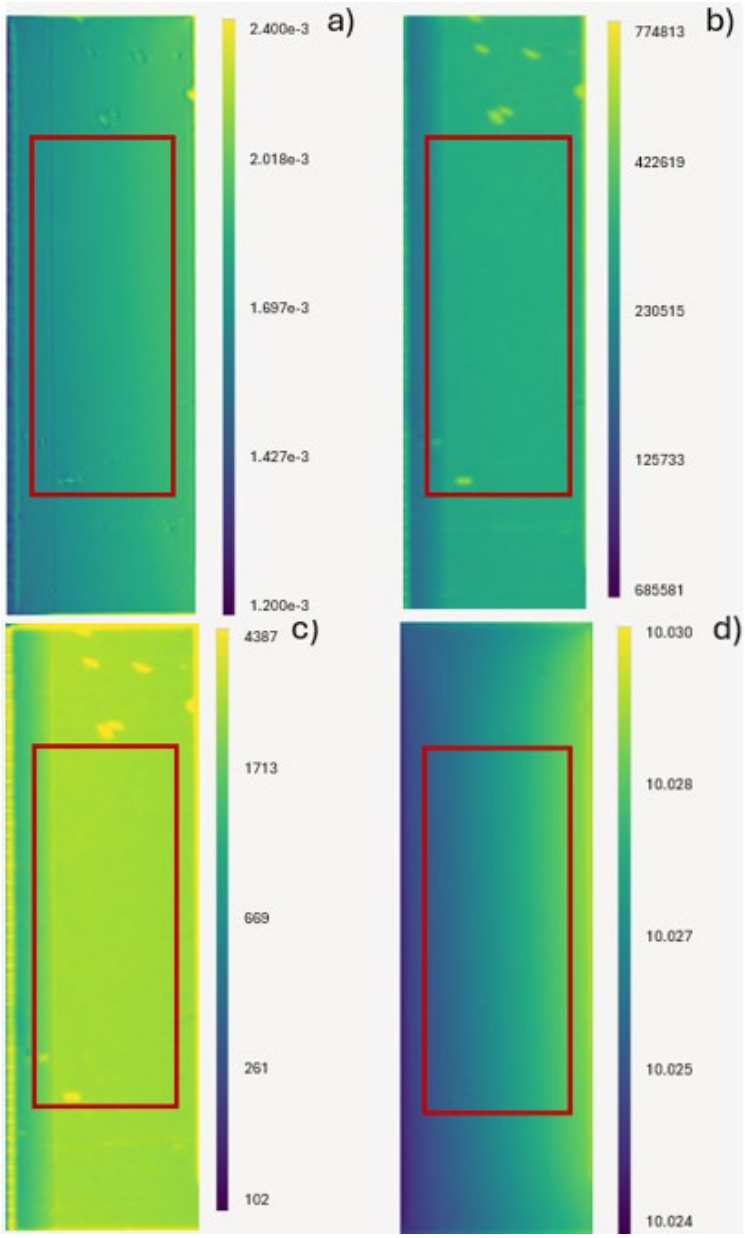

Figure 34. X-Ray topographies recorded at BM05 facility of ESRF (European Synchrotron Radiation Facility). (a) Full-width half maximum of the rocking curve (b) Integral of the rocking curves (c) Rocking curve peak intensity (d) Centroid peak position.

Funded by
the European Union

Table I summarizes the main properties of the crystal diamond #2 and compares them to the tendered specifications.

Technical characteristics			Tender compliance (Yes/No)
Crystal orientation	Orientation	(111)	Yes
Crystal geometry	Length	5.04	Yes
	Thickness, µm	79.2	Yes
Active area	Length x Width, mm	3.00x1.50	Yes
Number of dislocations in the active area	Dislocation count	1	Yes
Angle between the crystal's physical surface and the atomic plane	Degrees	1.9811	Yes

Table 1: comparison between expected main crystal features and characterizations.

Funded by the European Union

2.5.3 Datasheet for crystal diamond #3

MHz-Tomoscopy

Grant Agreement 101046448

Datasheet for the crystal "*Diamond #3*"

The technical specifications for the crystal were established in collaboration with DESY (Dr. Patrik Vagovic and his team) and Lund University (Prof. Pablo Villanueva Perez and his team). These specifications were finalized by DESY in mid-April 2023. Additionally, the design of the metal supports for the crystals was defined in cooperation with SUNA Precision GMBH (Dr. Alke Meents and his team) in early September 2024.

The crystal was purchased by INFN from the company XRNanotech with order dated 14/12/2023 and received by INFN at the end of November 2024.

Crystals geometry

Crystals lateral sizes and thickness are verified through a 3D optical profilometer (Zygo NX2), whose working principle relies on white-light interferometry. Crystal length is 4.02 mm. Average thickness of the active region measured through white light interferometry is 96.85 µm, in agreement with measurement through low coherence infrared interferometry (Fogale TMAP-4) which delivered a value of 96.8 µm.

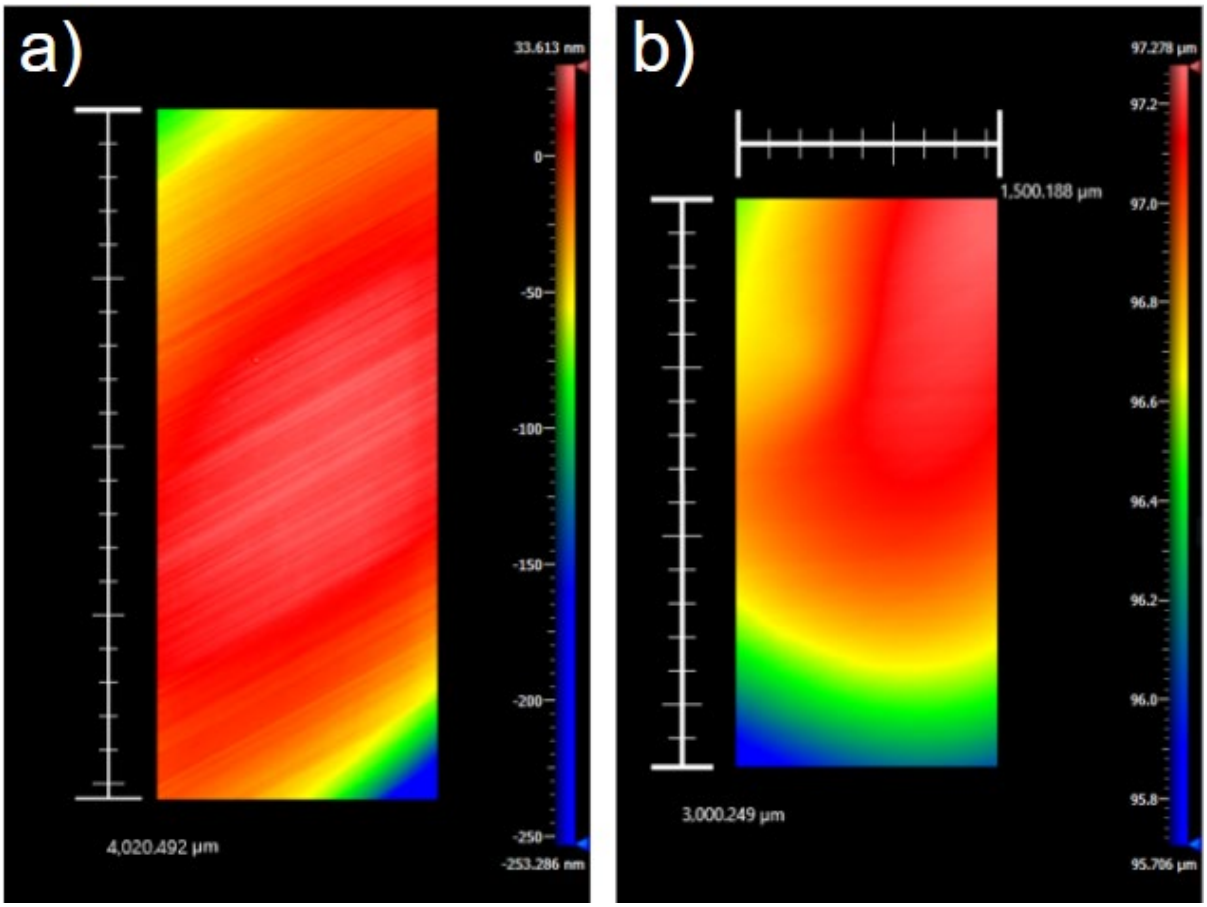

Figure 35: (a) interferometric characterization of the surface of the crystal diamond #3, used to determine the crystal length. (b) Thickness profile of the crystal active region.

Funded by
the European Union

Surface roughness

Surface roughness is measured through a 3D optical profilometer (Zygo NX2) operating at 100X magnification. Measured value is about ~3.9 nm. Measurement is carried out on 20 sites and average value is estimated. Figure 36 shows one of such characterizations

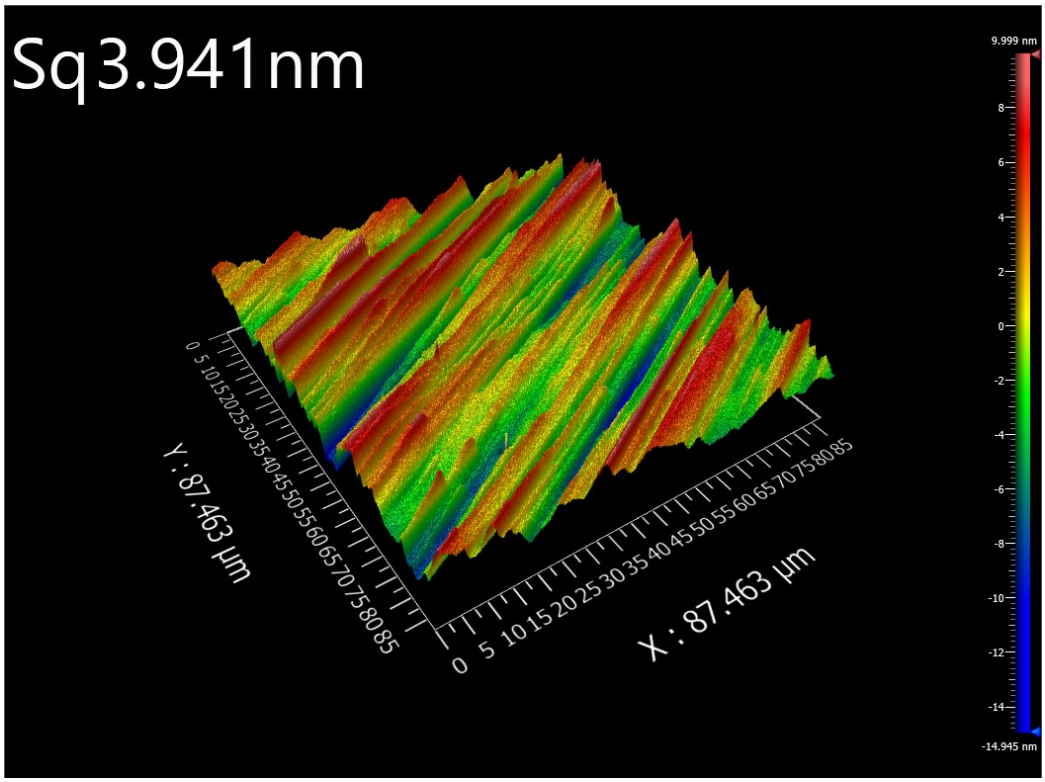

Figure 36: measurement of surface roughness for diamond crystal #3.

Crystallographic orientation

High-Resolution X-ray Diffraction (Panalytical X'Pert^3 MRD) is used to verify crystallographic orientation.

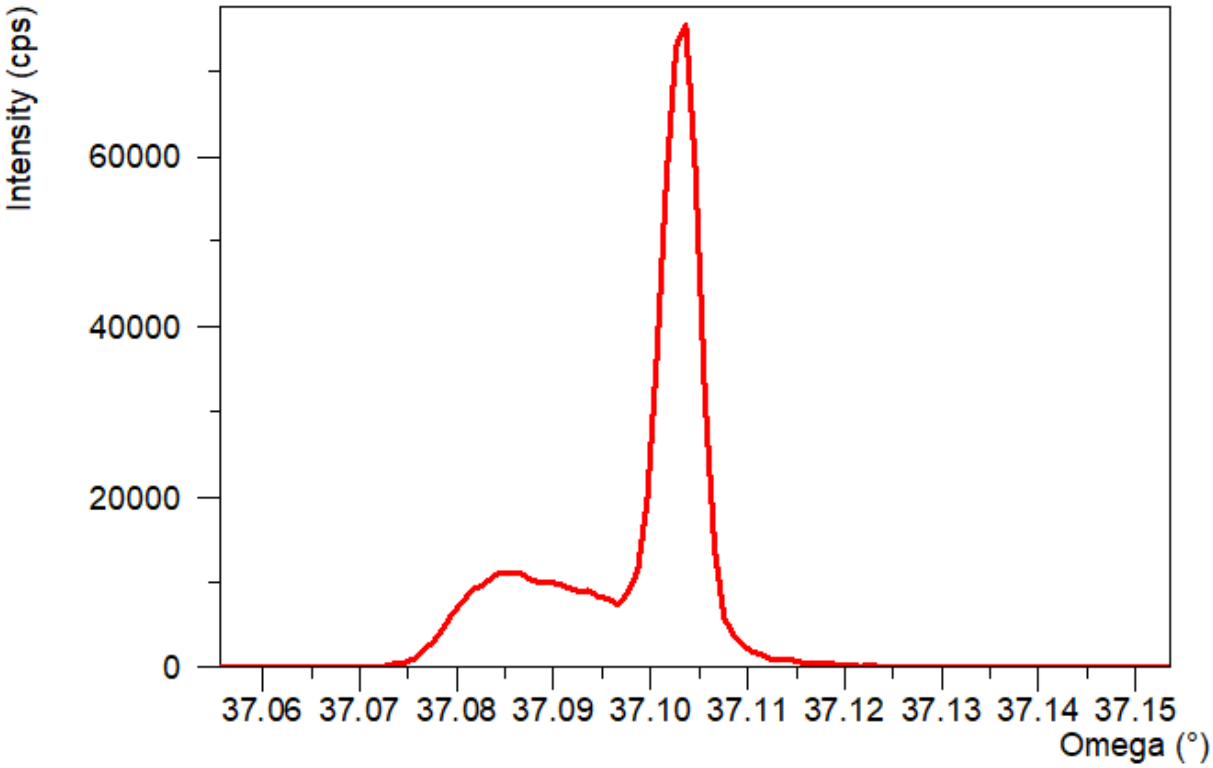

Figure 37. X-Ray rocking curve recorded on the main face of crystal diamond #3 highlight it is (110) oriented. That's worth noting that the beam is wider than the crystal, leading to a tail on the left side of the rocking curve, which is ascribed to the region corresponding to the strain relief cut structure.

The angular position of the rocking curve confirms that the crystal is (110) oriented. Miscut angle, i.e. the angle between the crystal main surface and the atomic planes have been measured through a High-Resolution X-ray Diffraction (Panalytical X'Pert^3 MRD) coupled to a custom-made autocollimator. Results of the measurement are reported in figure 4 and show a maximum value of 0.9012 degrees.

Funded by
the European Union

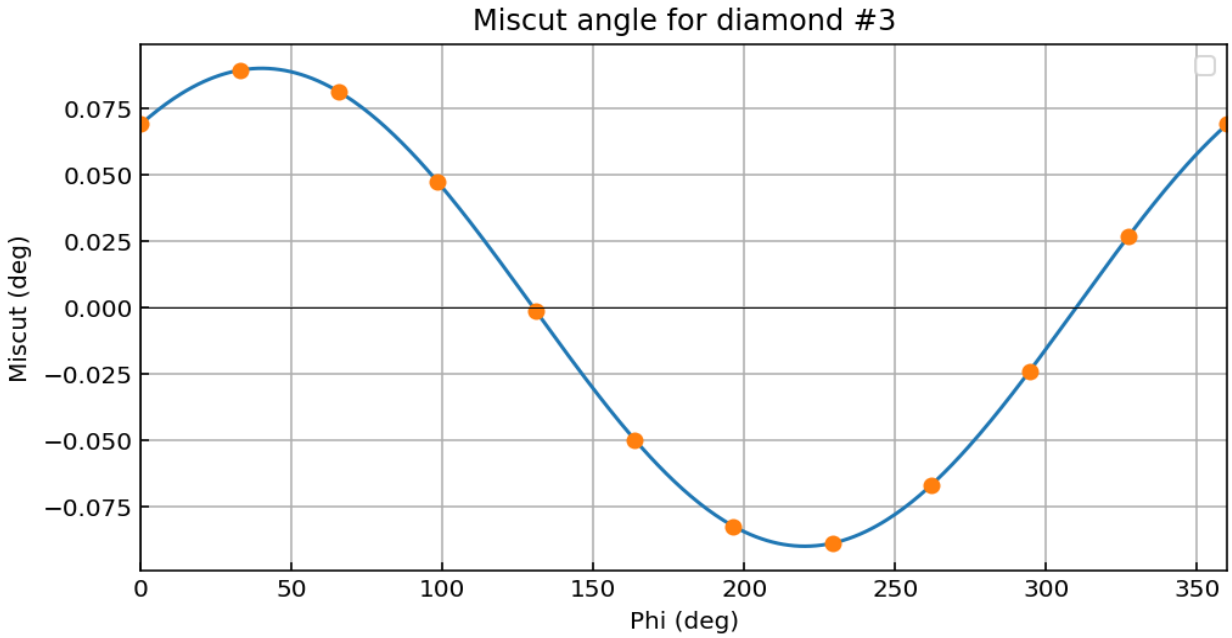

Figure 38. Miscut angle for sample diamond #3. Maximum value reaches 0.9012 degrees.

Funded by
the European Union

X-ray Topography

X-ray Topography has been carried out at BM05 beamline at ESRF (European Synchrotron Radiation Facility). Results of the characterization shows 1 dislocations over the active are of the sample in terms of (a) Full-width half maximum of the rocking curve (b) Integral of the rocking curves (c) Rocking curve peak intensity (d) Centroid peak position.

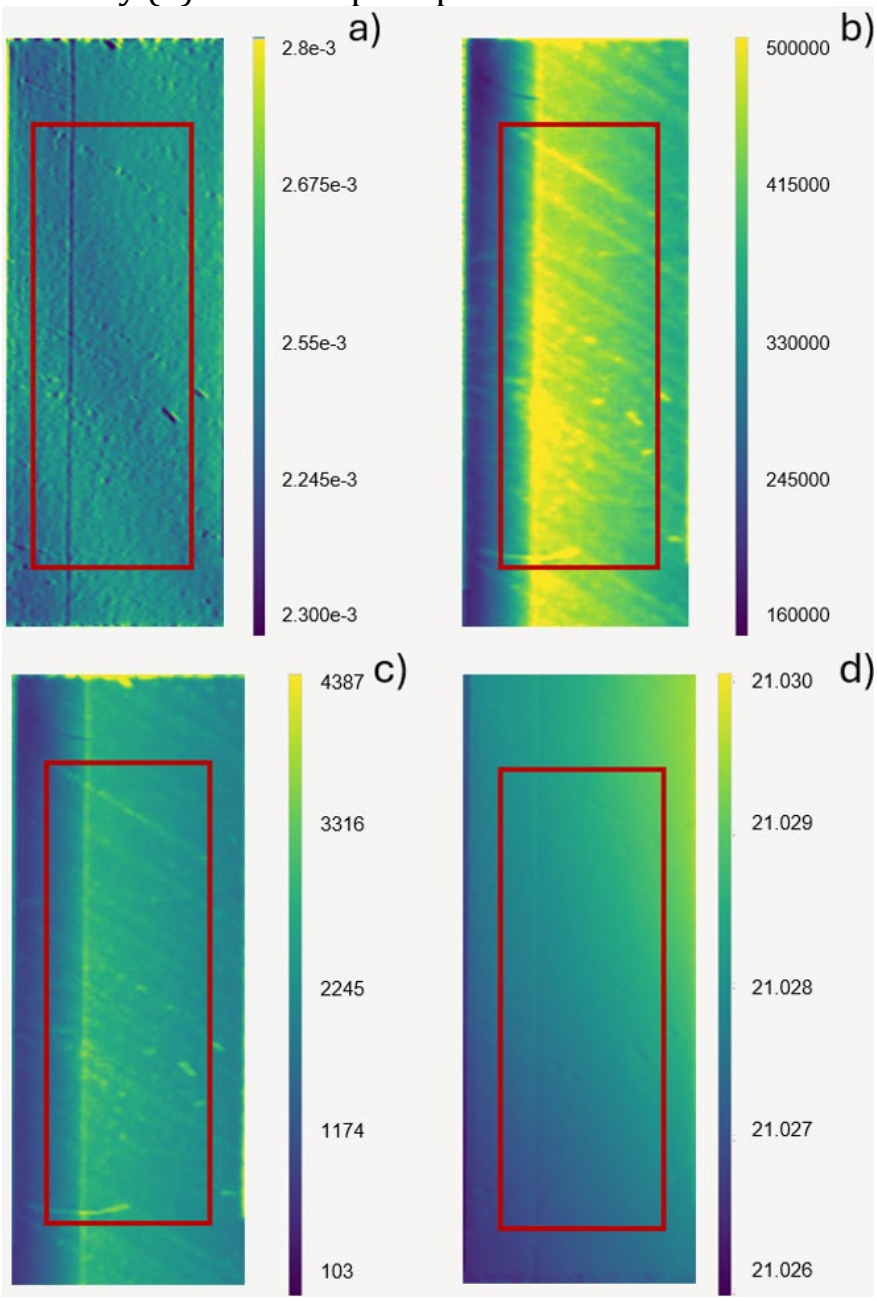

Figure 39. X-Ray topographies recorded at BM05 facility of ESRF (European Synchrotron Radiation Facility). (a) Full-width half maximum of the rocking curve (b) Integral of the rocking curves (c) Rocking curve peak intensity (d) Centroid peak position.

Funded by
the European Union

Table I summarizes the main properties of the crystal diamond #3 and compares them to the tendered specifications.

Technical characteristics			Tender compliance (Yes/No)
Crystal orientation	Orientation	(110)	Yes
Crystal geometry	Length	4.02	Yes
	Thickness, µm	96.85	Yes
Active area	Length x Width, mm	3.00x1.50	Yes
Number of dislocations in the active area	Dislocation count	1	Yes
Angle between the crystal's physical surface and the atomic plane	Degrees	0.9012	Yes

Table 1: comparison between expected main crystal features and characterizations.

Funded by the European Union

2.5.4 Datasheet for crystal diamond #4

MHz-Tomoscopy

Grant Agreement 101046448

Datasheet for the crystal "*Diamond #4*"

The technical specifications for the crystal were established in collaboration with DESY (Dr. Patrik Vagovic and his team) and Lund University (Prof. Pablo Villanueva Perez and his team). These specifications were finalized by DESY in mid-April 2023. Additionally, the design of the metal supports for the crystals was defined in cooperation with SUNA Precision GMBH (Dr. Alke Meents and his team) in early September 2024.

The crystal was purchased by INFN from the company XRNanotech with order dated 14/12/2023 and received by INFN at the end of November 2024.

Crystals geometry

Crystals lateral sizes and thickness are verified through a 3D optical profilometer (Zygo NX2), whose working principle relies on white-light interferometry. Crystal length is 4.03 mm. Average thickness of the active region measured through white light interferometry is 98.97 µm, in agreement with measurement through low coherence infrared interferometry (Fogale TMAP-4) which delivered a value of 98.8 µm.

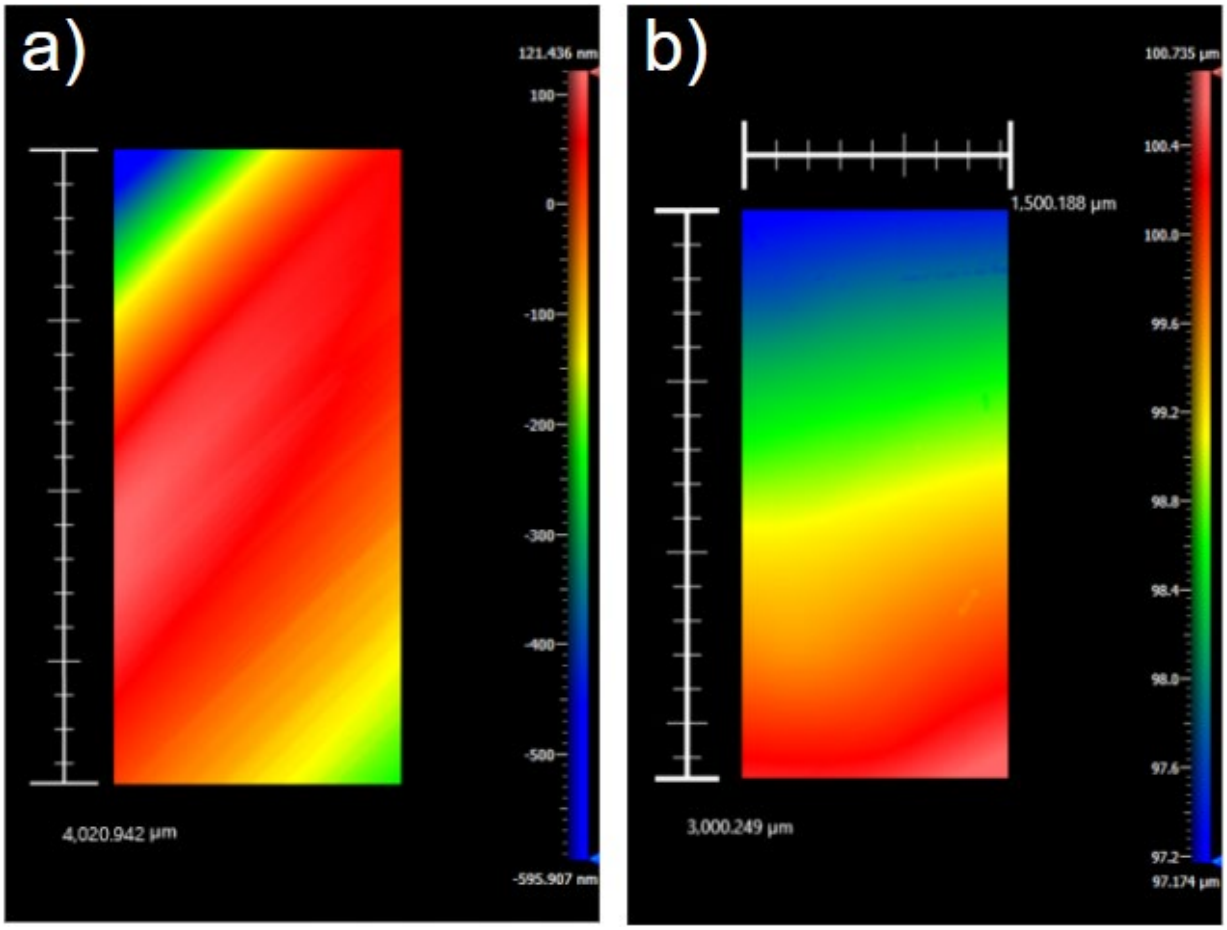

Figure 40: (a) interferometric characterization of the surface of the crystal diamond #4, used to determine the crystal length. (b) Thickness profile of the crystal active region.

Funded by
the European Union

Surface roughness

Surface roughness is measured through a 3D optical profilometer (Zygo NX2) operating at 100X magnification. Measured value is about ~0.4 nm. Measurement is carried out on 20 sites and average value is estimated. Figure 41 shows one of such characterizations.

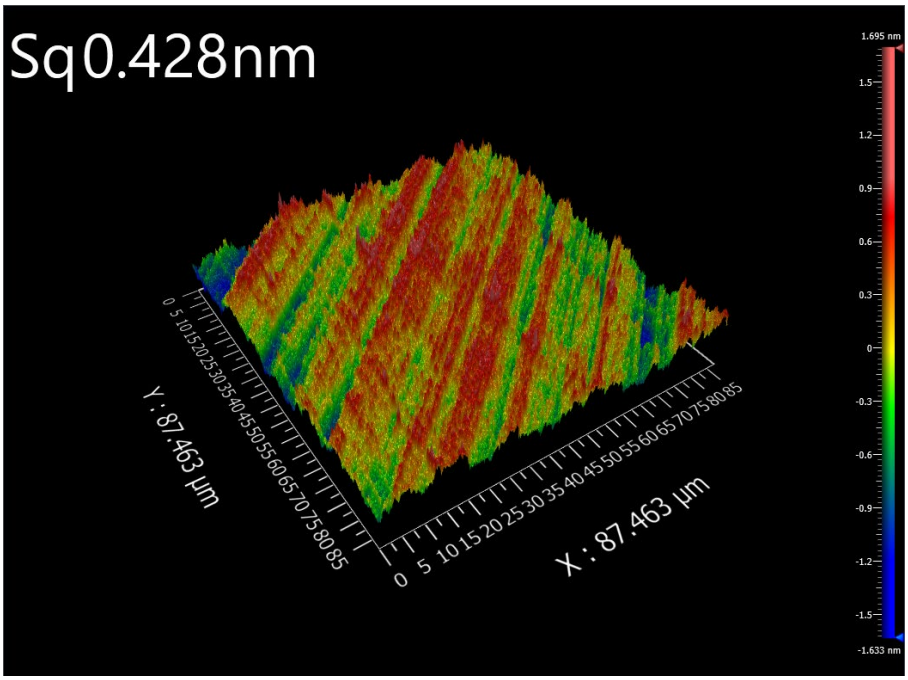

Figure 41: measurement of surface roughness for diamond crystal #4.

Funded by
the European Union

Crystallographic orientation

High-Resolution X-ray Diffraction (Panalytical X'Pert^3 MRD) is used to verify crystallographic orientation.

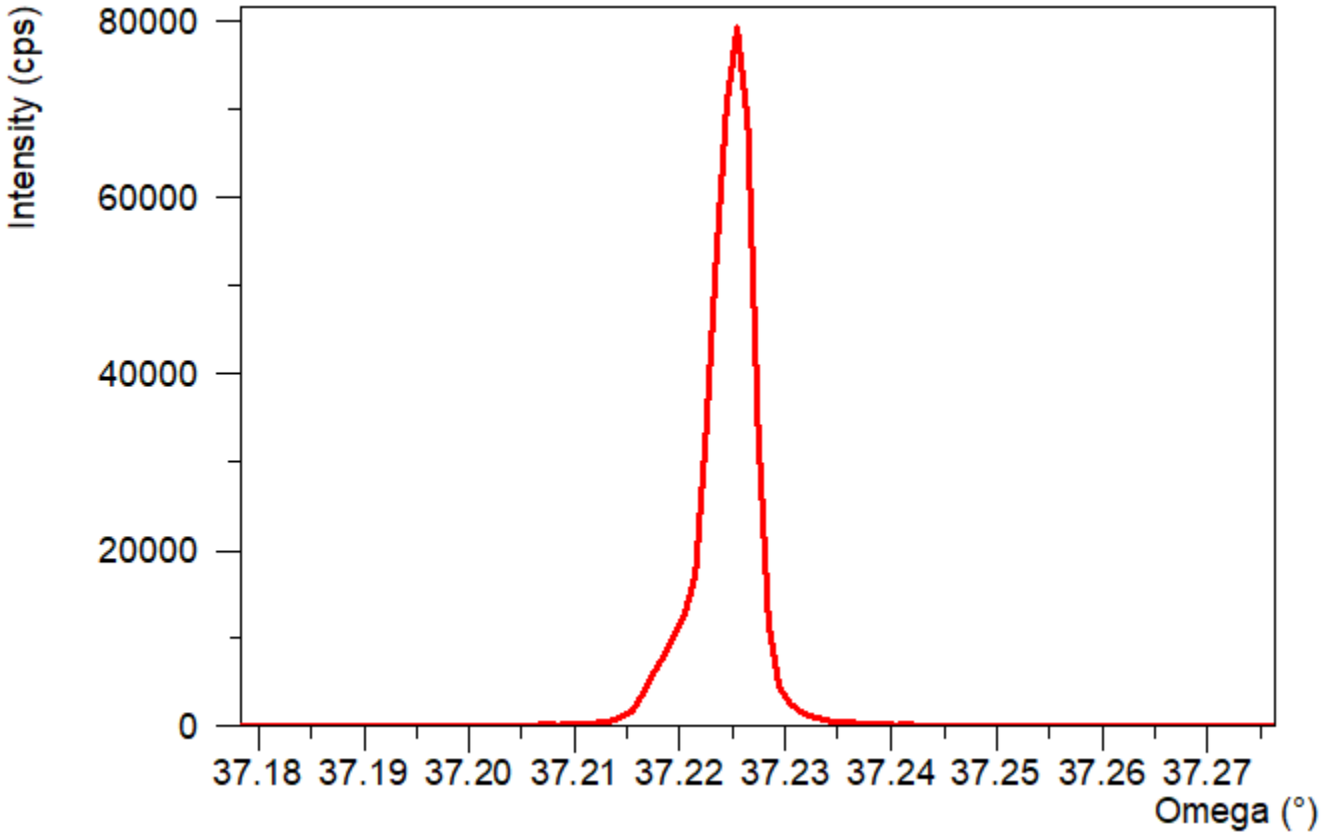

Figure 42. X-Ray rocking curve recorded on the main face of crystal diamond #2 highlight it is (110) oriented.

The angular position of the rocking curve confirms that the crystal is (110) oriented. Miscut angle, i.e. the angle between the crystal main surface and the atomic planes have been measured through a High-Resolution X-ray Diffraction (Panalytical X'Pert^3 MRD) coupled to a custom-made autocollimator. Results of the measurement are reported in figure 4 and show a maximum value of 0.1112 degrees.

Funded by
the European Union

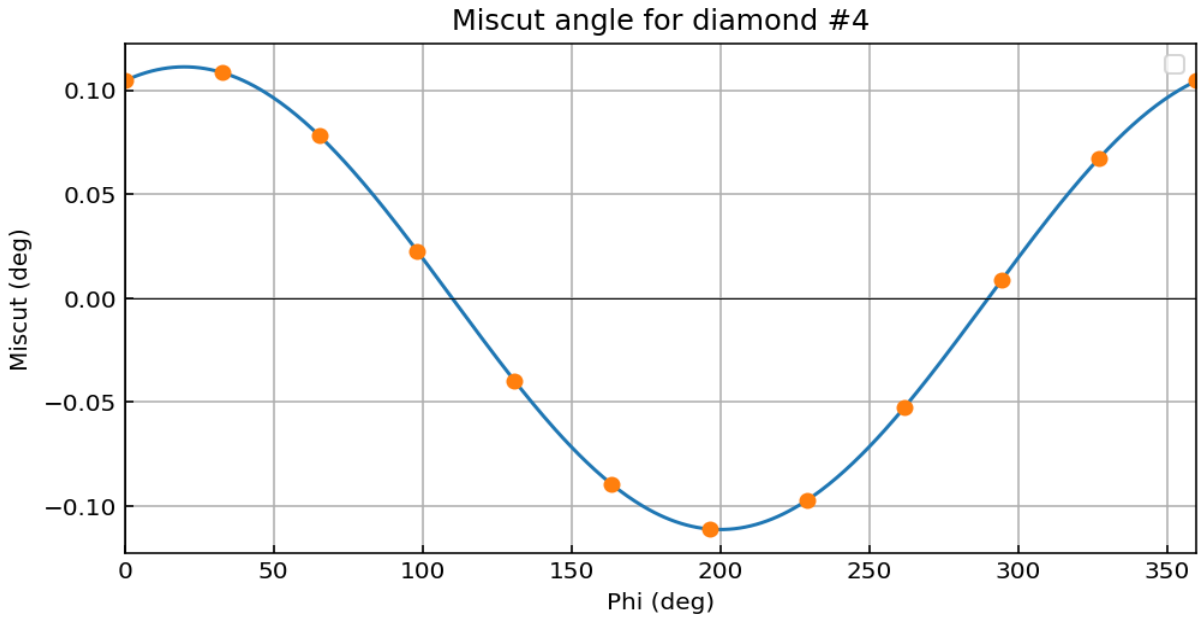

Figure 43. Miscut angle for sample diamond #4. Maximum value reaches 0.1112 degrees.

Funded by
the European Union

X-ray Topography

X-ray Topography has been carried out at BM05 beamline at ESRF (European Synchrotron Radiation Facility). Results of the characterization shows 1 dislocations over the active are of the sample in terms of (a) Full-width half maximum of the rocking curve (b) Integral of the rocking curves (c) Rocking curve peak intensity (d) Centroid peak position.

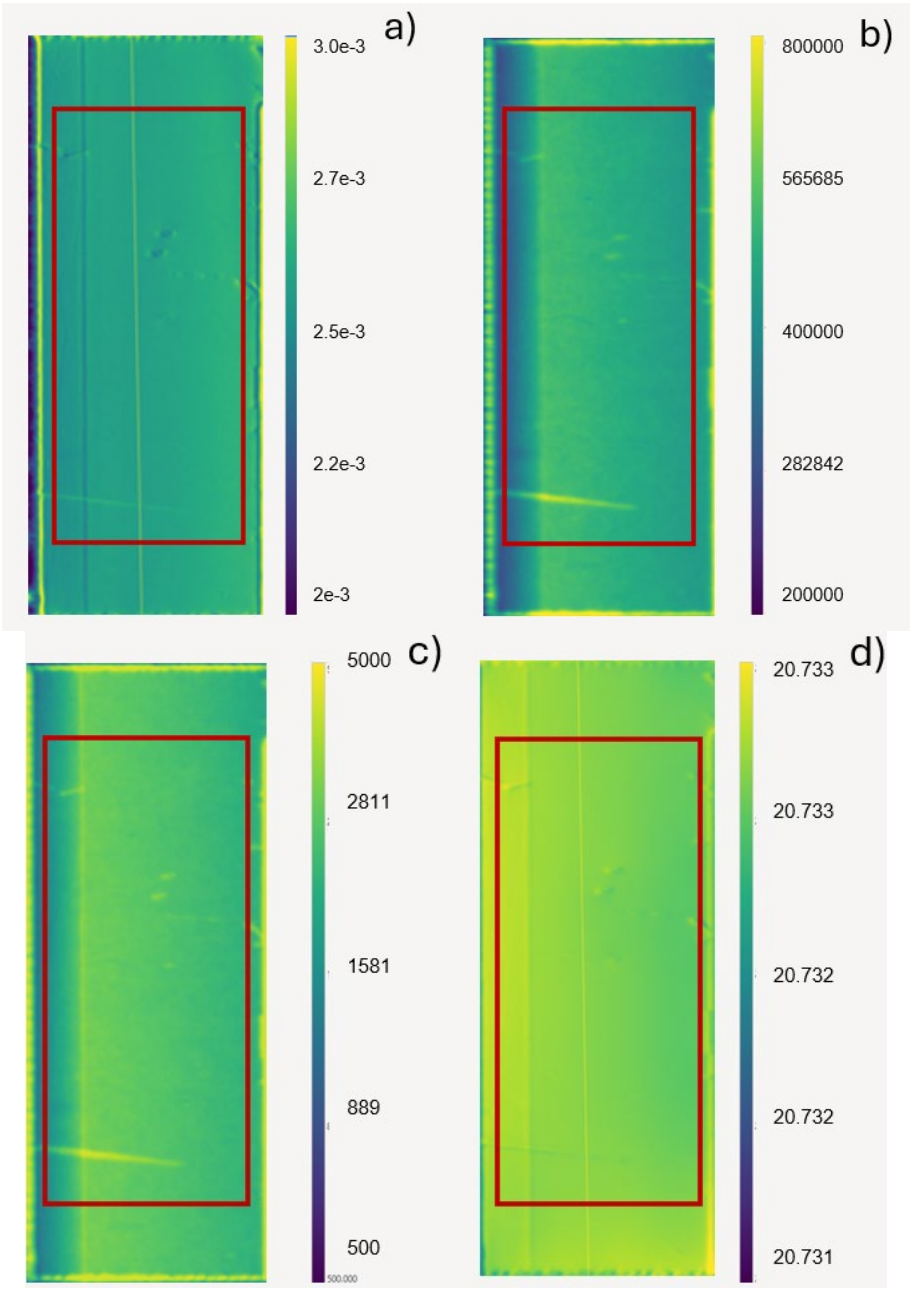

Figure 44. X-Ray topographies recorded at BM05 facility of ESRF (European Synchrotron Radiation Facility). (a) Full-width half maximum of the rocking curve (b) Integral of the rocking curves (c) Rocking curve peak intensity (d) Centroid peak position.

Table I summarizes the main properties of the crystal diamond #4 and compares them to the tendered specifications.

Technical characteristics			Tender compliance (Yes/No)
Crystal orientation	Orientation	(110)	Yes
Crystal geometry	Length	4.03	Yes
	Thickness, µm	98.97	Yes
Active area	Length x Width, mm	3.00x1.50	Yes
Number of dislocations in the active area	Dislocation count	3	Yes
Angle between the crystal's physical surface and the atomic plane	Degrees	0.1112	Yes

Table 1: comparison between expected main crystal features and characterizations.

Funded by the European Union

2.5.5 Datasheet for crystal diamond #5

MHz-Tomoscopy

Grant Agreement 101046448

Datasheet for the crystal "*Diamond #5*"

The technical specifications for the crystal were established in collaboration with DESY (Dr. Patrik Vagovic and his team) and Lund University (Prof. Pablo Villanueva Perez and his team). These specifications were finalized by DESY in mid-April 2023. Additionally, the design of the metal supports for the crystals was defined in cooperation with SUNA Precision GMBH (Dr. Alke Meents and his team) in early September 2024.

The crystal was purchased by INFN from the company XRNanotech with order dated 14/12/2023 and received by INFN at the end of November 2024.

Crystals geometry

Crystals lateral sizes and thickness are verified through a 3D optical profilometer (Zygo NX2), whose working principle relies on white-light interferometry. Crystal length is 4.12 mm. Average thickness of the active region measured through white light interferometry is 99.3 µm, in agreement with measurement through low coherence infrared interferometry (Fogale TMAP-4) which delivered a value of 99.2 µm.

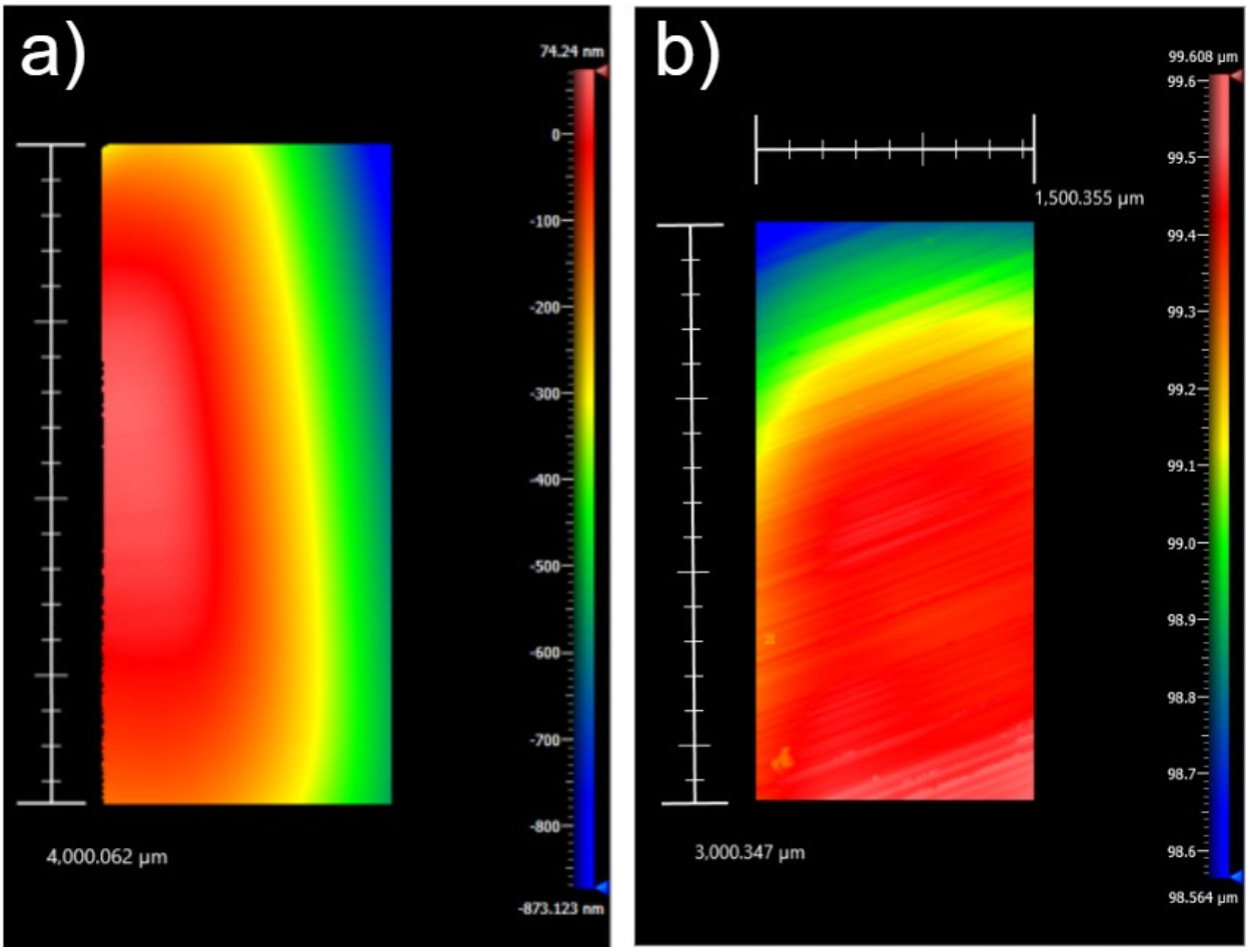

Figure 45: (a) interferometric characterization of the surface of the crystal diamond #5, used to determine the crystal length. (b) Thickness profile of the crystal active region.

Funded by
the European Union

Surface roughness

Surface roughness is measured through a 3D optical profilometer (Zygo NX2) operating at 100X magnification. Measured value is about ~0.4 nm. Measurement is carried out on 20 sites and average value is estimated. Figure 46 shows one of such characterizations.

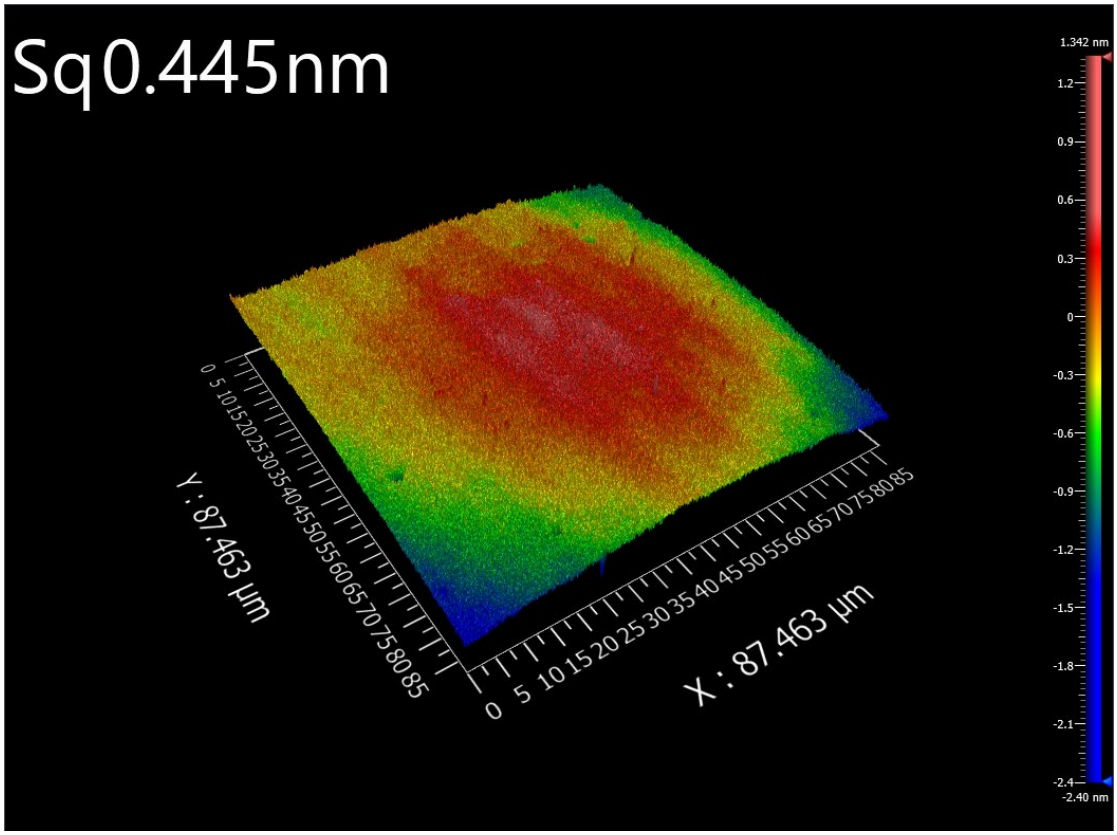

Figure 46: measurement of surface roughness for diamond crystal #5.

Funded by
the European Union

Crystallographic orientation

High-Resolution X-ray Diffraction (Panalytical X'Pert^3 MRD) is used to verify crystallographic orientation.

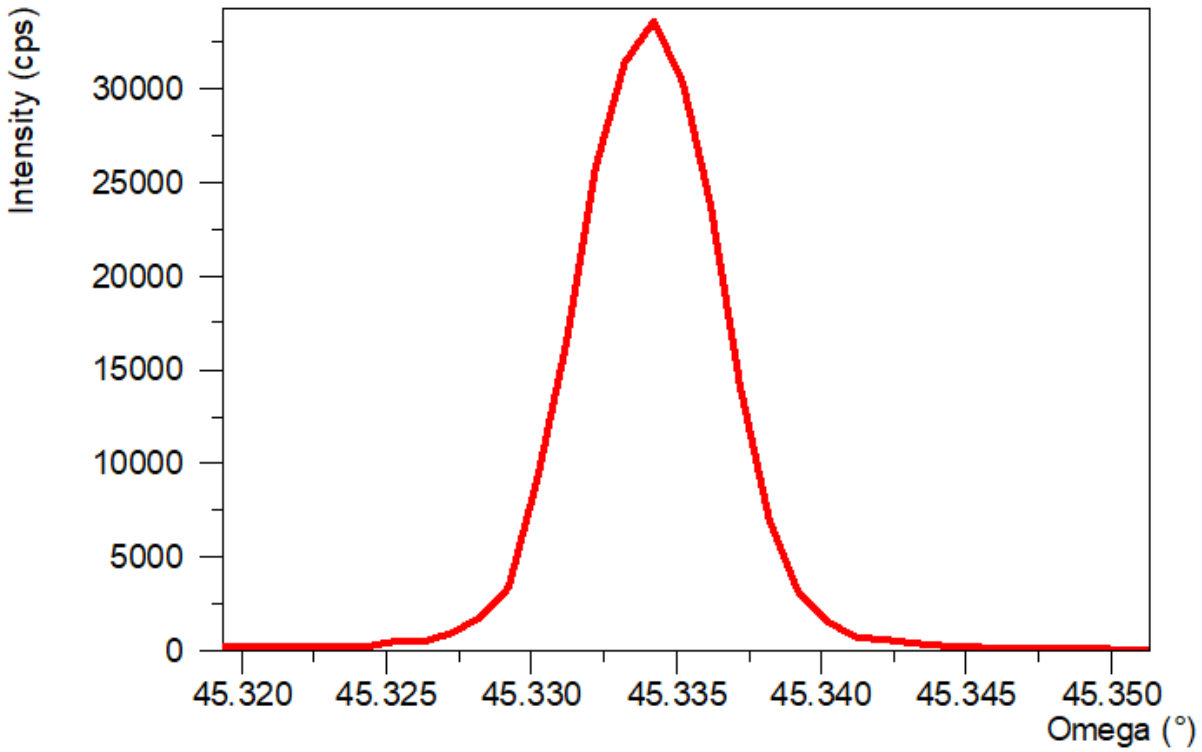

Figure 47. X-Ray rocking curve recorded on the main face of crystal diamond #5 highlight it is (311) oriented.

The angular position of the rocking curve confirms that the crystal is (311) oriented, as expected. Miscut angle, i.e. the angle between the crystal main surface and the atomic planes have been measured through a High-Resolution X-ray Diffraction (Panalytical X'Pert^3 MRD) coupled to a custom-made autocollimator. Results of the measurement are reported in figure 4 and show a maximum value of 0.0912 degrees.

Funded by
the European Union

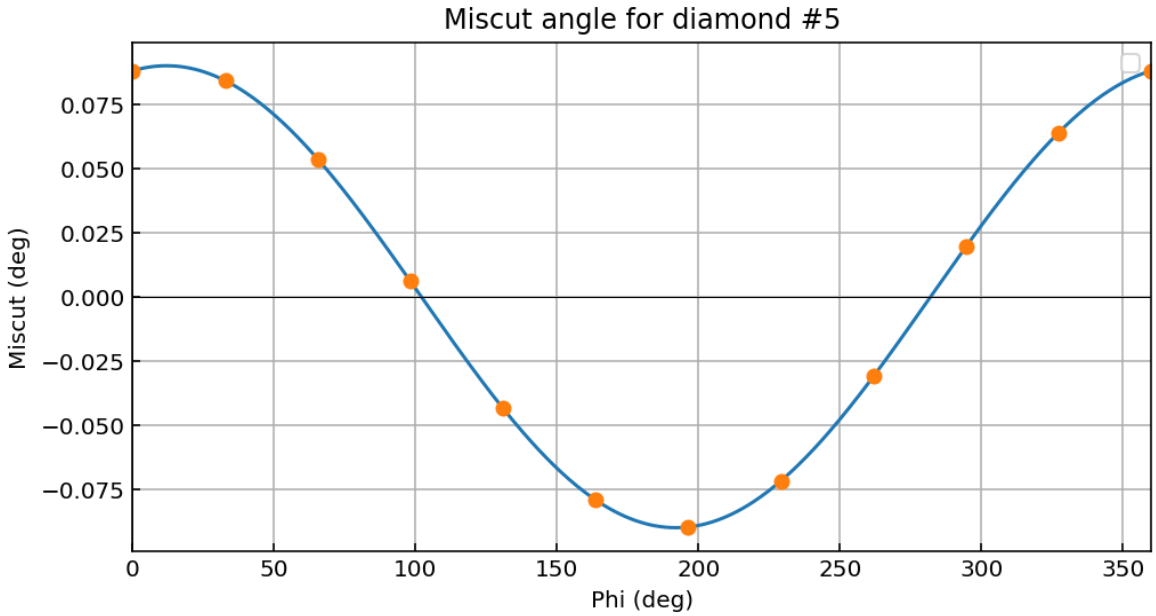

Figure 48. Miscut angle for diamond sample #5. Maximum value reaches 0.0912 degrees.

Funded by
the European Union

X-ray Topography

X-ray Topography has been carried out at BM05 beamline at ESRF (European Synchrotron Radiation Facility) and results are shown in figure 5, reporting in (a) Full-width half maximum of the rocking curves (b) Integral of the rocking curves (c) Rocking curve peak intensity (d) Centroid peak position. That is worth noting that signal of pictures (b) and (d), which are typically used to confirm presence of dislocations in the crystal bulk, in this case is dominated by slight imperfections arising from the signal coming from the crystal surface. Merging the information collected from figures (a) and (d) and the topographic data provided by the supplier (see appendix 1) we conclude that the number of dislocations over the active area is compatible with 0.

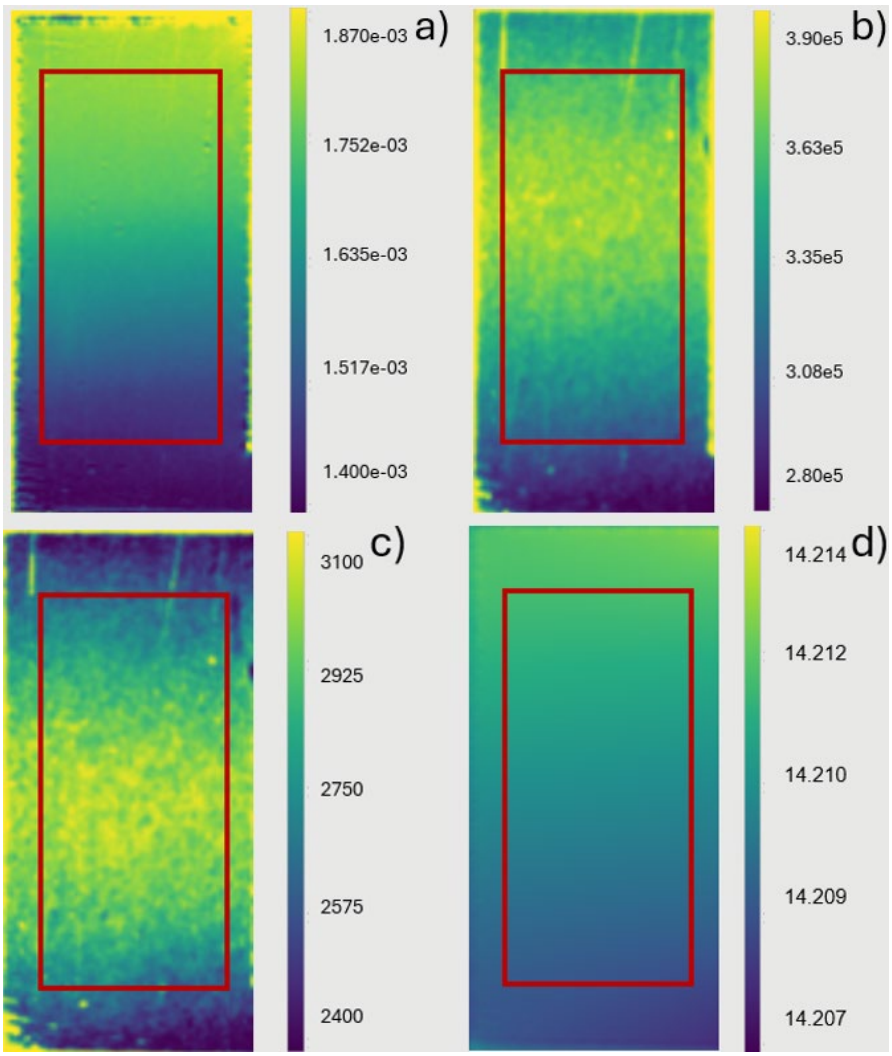

Figure 49. X-Ray topographies recorded at BM05 facility of ESRF (European Synchrotron Radiation Facility). (a) Full-width half maximum of the rocking curve (b) Integral of the rocking curves (c) Rocking curve peak intensity (d) Centroid peak position.

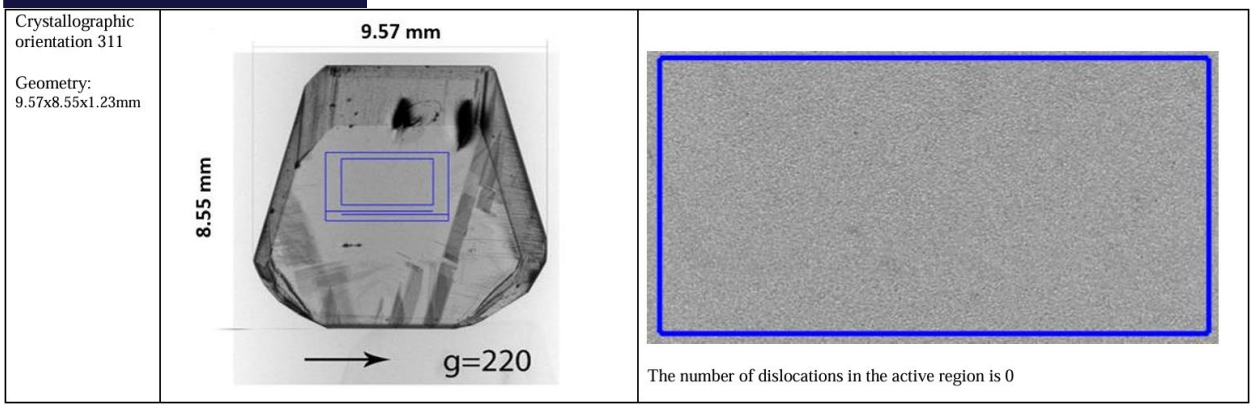

Figure 50 X-Ray topography collected by XRnanotech, the supplier of the crystal. The topography is collected on the crystal gem prior to cutting, polishing and machining to the final size.

Table I summarizes the main properties of the crystal diamond #5 and compares them to the tendered specifications.

Technical characteristics			Tender compliance (Yes/No)
Crystal orientation	Orientation	(311)	Yes
Crystal geometry	Length	4.12	Yes
	Thickness, µm	99.12	Yes
Active area	Length x Width, mm	3.00x1.50	Yes
Number of dislocations in the active area	Dislocation count	0	Yes
Angle between the crystal's physical surface and the atomic plane	Degrees	0.0912	Yes

Table 1: comparison between expected main crystal features and characterizations.

Funded by the European Union

2.5.6 Datasheet for crystal diamond #6

MHz-Tomoscopy

Grant Agreement 101046448

Datasheet for the crystal "*Diamond #6*"

The technical specifications for the crystal were established in collaboration with DESY (Dr. Patrik Vagovic and his team) and Lund University (Prof. Pablo Villanueva Perez and his team). These specifications were finalized by DESY in mid-April 2023. Additionally, the design of the metal supports for the crystals was defined in cooperation with SUNA Precision GMBH (Dr. Alke Meents and his team) in early September 2024.

The crystal was purchased by INFN from the company XRNanotech with order dated 14/12/2023 and received by INFN at the end of November 2024.

Crystals geometry

Crystals lateral sizes and thickness are verified through a 3D optical profilometer (Zygo NX2), whose working principle relies on white-light interferometry. Crystal length is 4.02 mm. Average thickness of the active region measured through white light interferometry is 77.12 µm, in agreement with measurement through low coherence infrared interferometry (Fogale TMAP-4) which delivered a value of 77.1 µm.

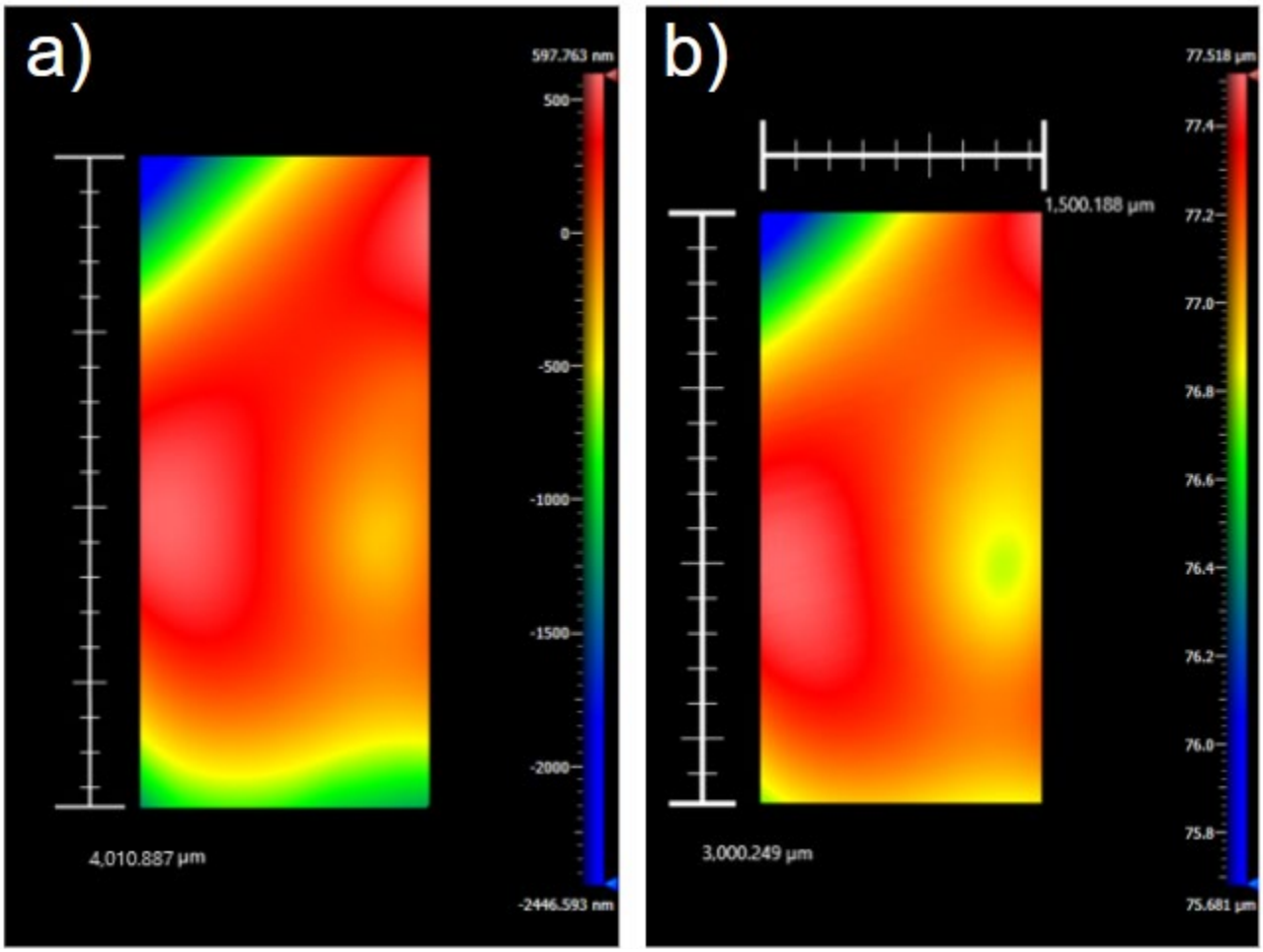

Figure 51: (a) interferometric characterization of the surface of the crystal diamond #6, used to determine the crystal length. (b) Thickness profile of the crystal active region.

Funded by
the European Union

Surface roughness

Surface roughness is measured through a 3D optical profilometer (Zygo NX2) operating at 100X magnification. Measured value is about ~1.1 nm. Measurement is carried out on 20 sites and average value is estimated. Figure 52 shows one of such characterizations. Small spikes are ascribed to residues left from evaporation of drops of water used to clean the crystal by the manufactured after polishing operations.

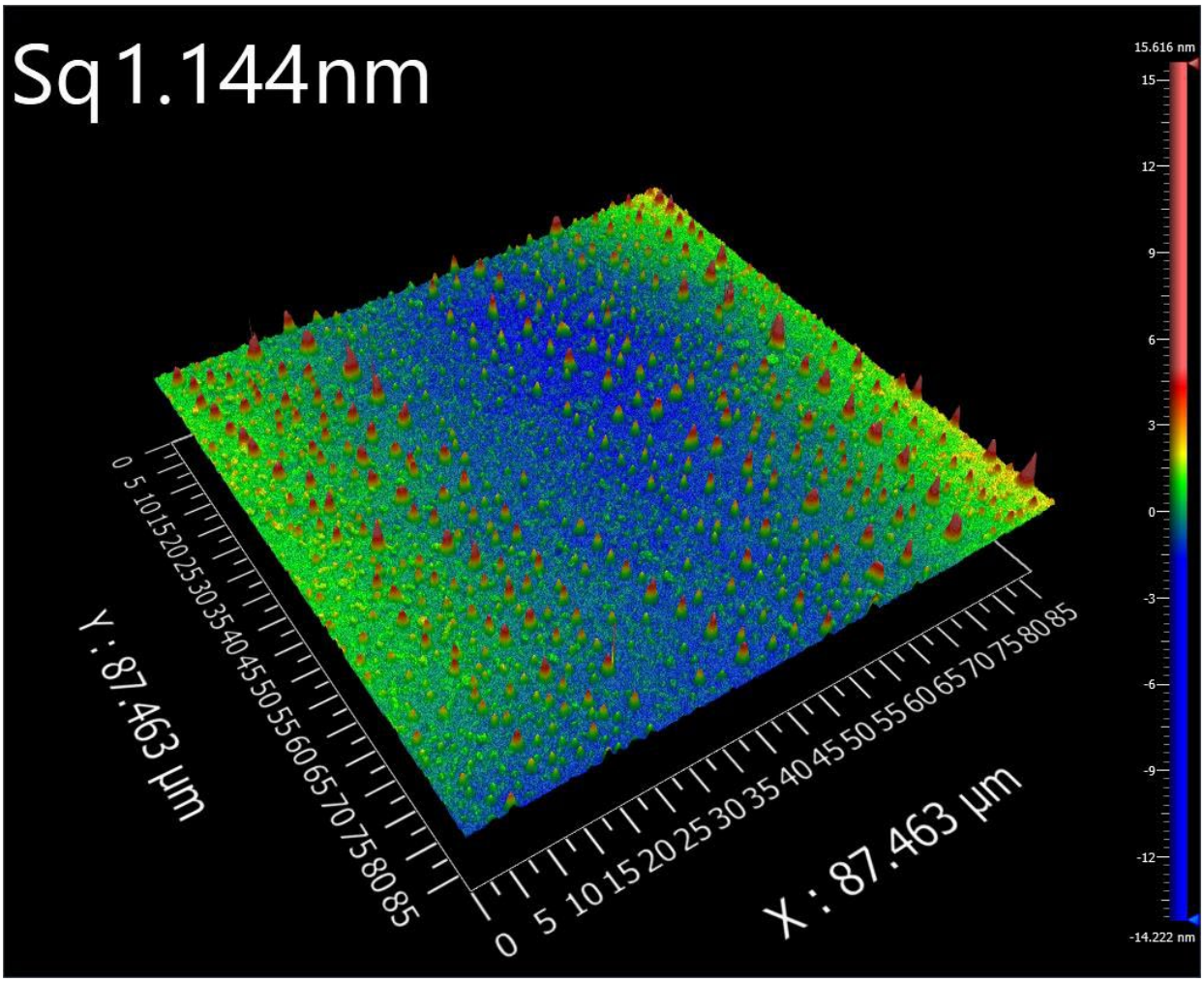

Figure 52: measurement of surface roughness for diamond crystal #6. The observed spikes are attributed to residues left by drying water following the cleaning process.

Funded by
the European Union

Crystallographic orientation

For crystals with nominal (211) and (511) orientation, the use of X-ray radiation at 8 keV does not allow direct excitation of reflections corresponding to the planes parallel to the main crystal surface. In such cases, the surface orientation was determined by analyzing the rocking curves of asymmetric reflections from lattice planes inclined at known angles with respect to the surface normal (see Figure 53). This approach involves performing X-ray rocking curve measurements by slightly varying the incidence angle (ω) of the X-ray beam around the Bragg diffraction angle corresponding to these asymmetric reflections, thereby accurately determining crystal orientation and lattice alignment.

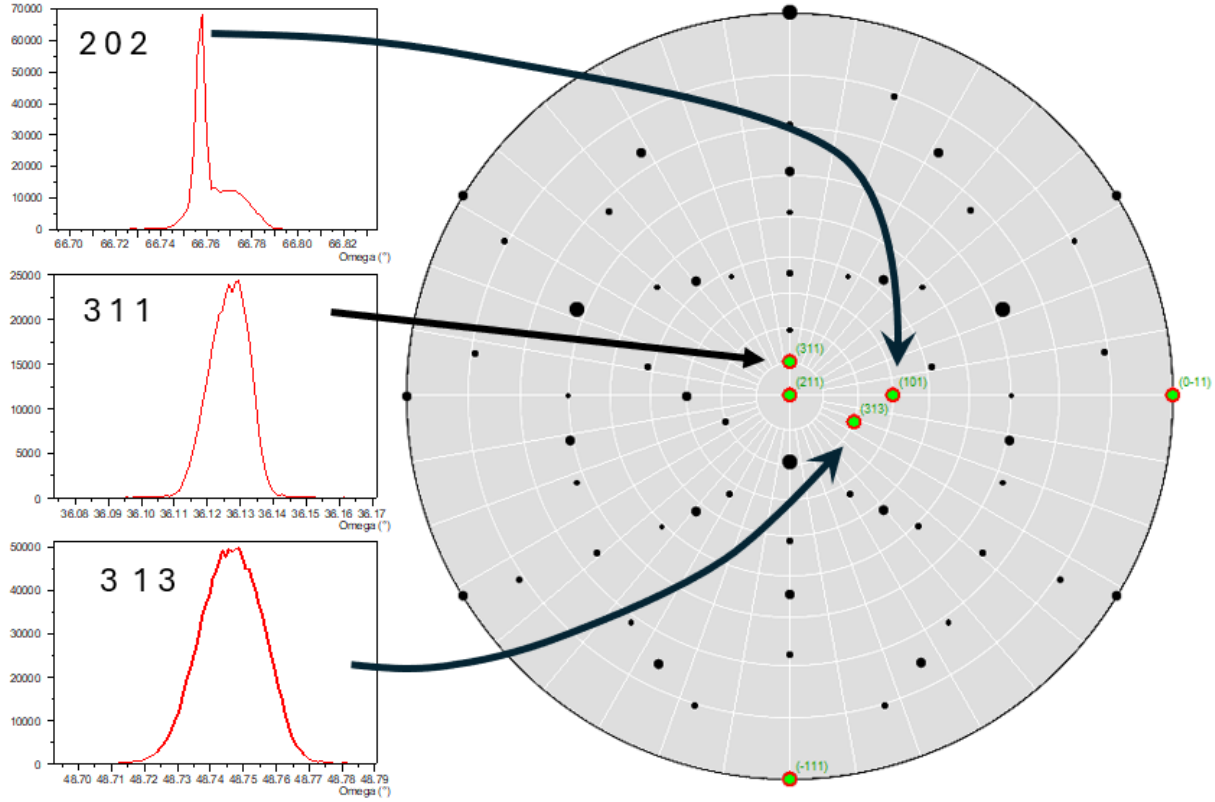

Figure 53. At the photon energy of 8 keV, diffraction from the (211) family of planes is not accessible. To determine the orientation of the crystal surface, asymmetric reflections from the (202), (311), (313), planes were measured. The corresponding peaks are shown in the four plots on the left. The angular positions of these reflections were used to reconstruct the crystal stereogram shown on the right. Arrows indicate the association between each measured reflection and its corresponding crystallographic direction in the stereogram. By evaluating the angular separation between the plane normals and the <211> direction, the surface orientation was confirmed to be the (211) plane.

Angular position of the rocking curve confirms that the crystal is (211) oriented, as expected.

Funded by
the European Union

Miscut angle, i.e. the angle between the crystal main surface and the atomic planes have been measured through a High-Resolution X-ray Diffraction (Panalytical X'Pert^3 MRD) coupled to a custom-made autocollimator. Results of the measurement are reported in figure 4 and show a maximum value of 0.1923 degrees.

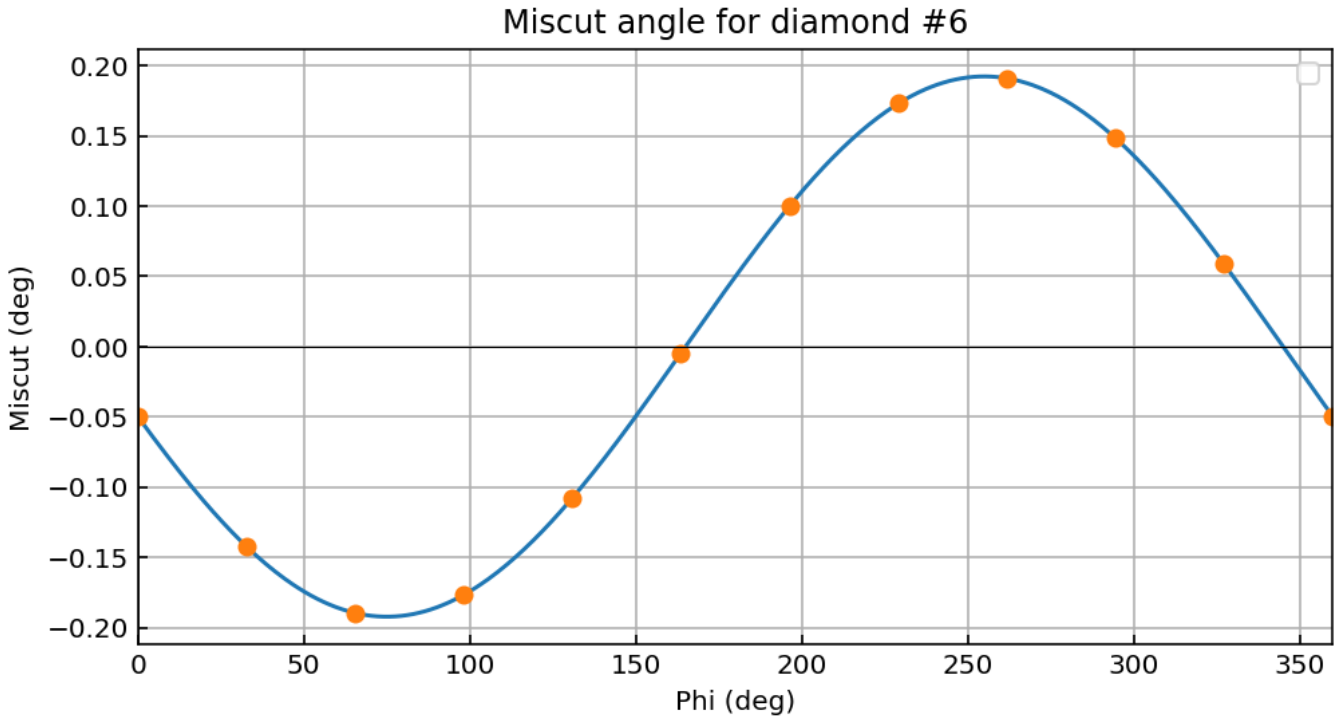

Figure 54. Miscut angle for sample diamond #6 oriented crystal. Maximum value reaches 0.1923 degree.

X-ray Topography

X-ray Topography has been carried out at BM05 beamline at ESRF (European Synchrotron Radiation Facility). Results of the characterization shows 1 dislocations over the active are of the sample in terms of (a) Full-width half maximum of the rocking curve (b) Integral of the rocking curves (c) Rocking curve peak intensity (d) Centroid peak position.

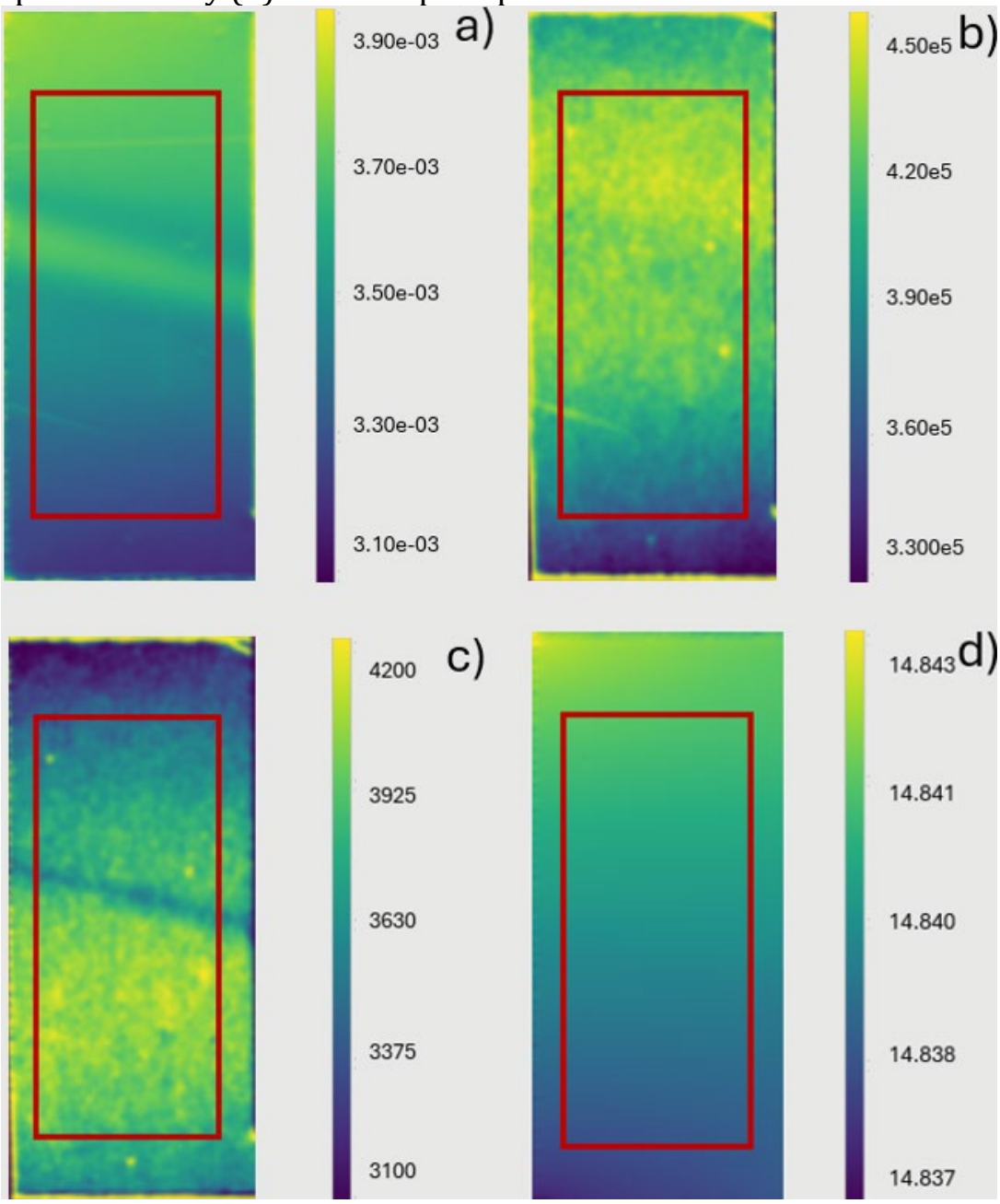

Figure 55. X-Ray topographies recorded at BM05 facility of ESRF (European Synchrotron Radiation Facility). (a) Full-width half maximum of the rocking curve (b) Integral of the rocking curves (c) Rocking curve peak intensity (d) Centroid peak position.

Funded by
the European Union

Table I summarizes the main properties of the crystal diamond #6 and compare them to the tendered specifications.

Technical characteristics			Tender compliance (Yes/No)
Crystal orientation	Orientation	(211)	Yes
Crystal geometry	Length	4.03	Yes
	Thickness, µm	77.12	Yes
Active area	Length x Width, mm	3.00x1.50	Yes
Number of dislocations in the active area	Dislocation count	1	Yes
Angle between the crystal's physical surface and the atomic plane	Degrees	0.1923	Yes

Table 1: comparison between expected main crystal features and characterizations.

Funded by the European Union

2.5.7 Datasheet for crystal diamond #7

MHz-Tomoscopy

Grant Agreement 101046448

Datasheet for the crystal "*Diamond #7*"

The technical specifications for the crystal were established in collaboration with DESY (Dr. Patrik Vagovic and his team) and Lund University (Prof. Pablo Villanueva Perez and his team). These specifications were finalized by DESY by mid-April 2023. Additionally, the design of the metal supports for the crystals was defined in cooperation with SUNA Precision GMBH (Dr. Alke Meents and his team) in early September 2024.

The crystal was purchased by INFN from the company XRNanotech with order dated 14/12/2023 and received by INFN at the end of November 2024.

The crystal is mounted on an aluminum frame and its geometry is characterized by a strain relief cut assuring that stress coming from mount does not propagate to the active region of the crystal.

Crystals geometry

Crystals lateral sizes and thickness are verified through a 3D optical profilometer (Zygo NX2), whose working principle relies on white-light interferometry. Crystal length is 4.03 mm. Average thickness of the active region measured through white light interferometry is 99.1 µm, in agreement with measurement through low coherence infrared interferometry (Fogale TMAP-4) which delivered a value of 99.2 µm.

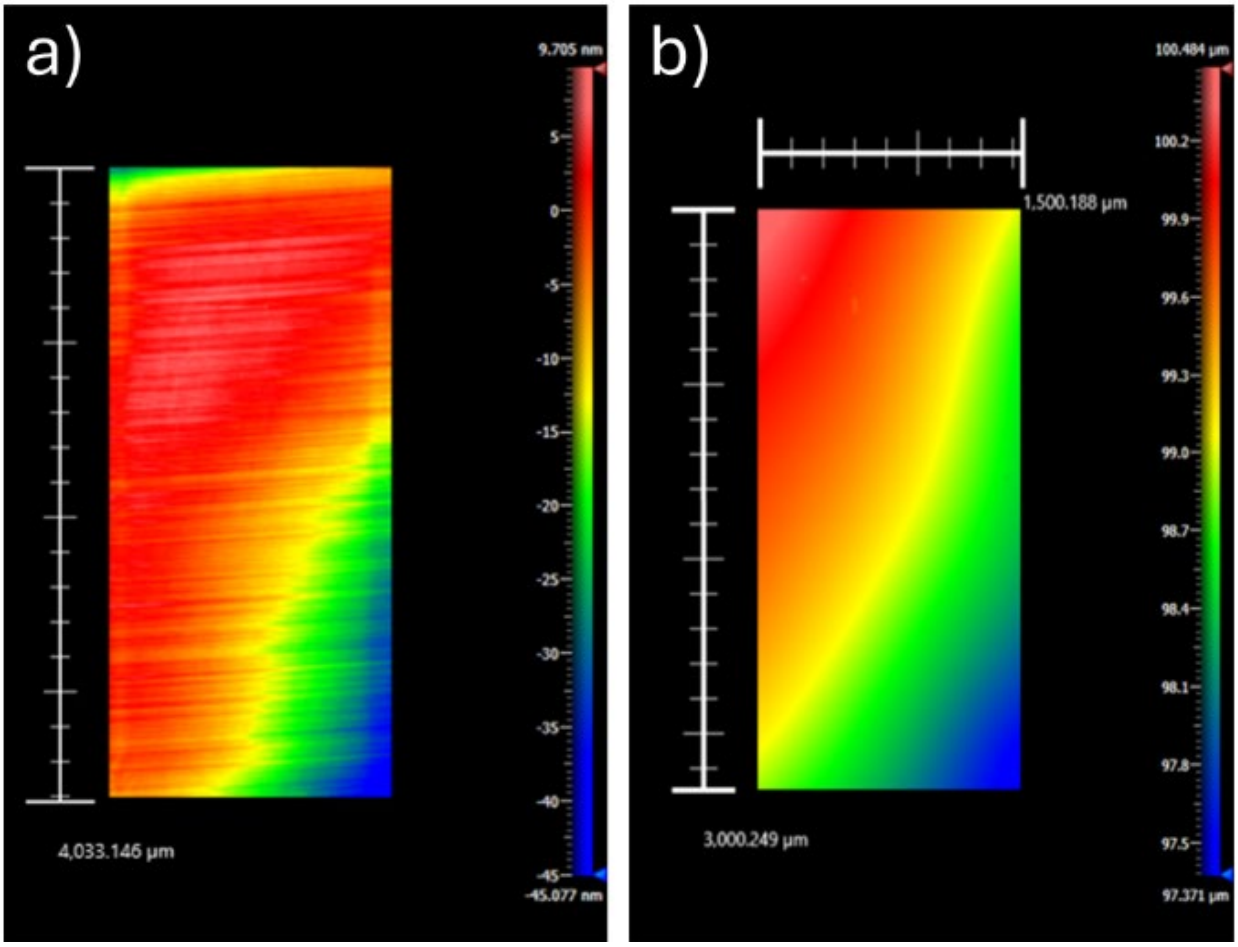

Figure 56: (a) interferometric characterization of the surface of the crystal diamond #7, used to determine the crystal length. (b) Thickness profile of the crystal active region.

Funded by
the European Union

Surface roughness

Surface roughness is measured through a 3D optical profilometer (Zygo NX2) operating at 100X magnification. Measured value is about ~2.8 nm. Measurement is carried out on 20 sites and average value is estimated. Figure 57 shows one of such characterizations.

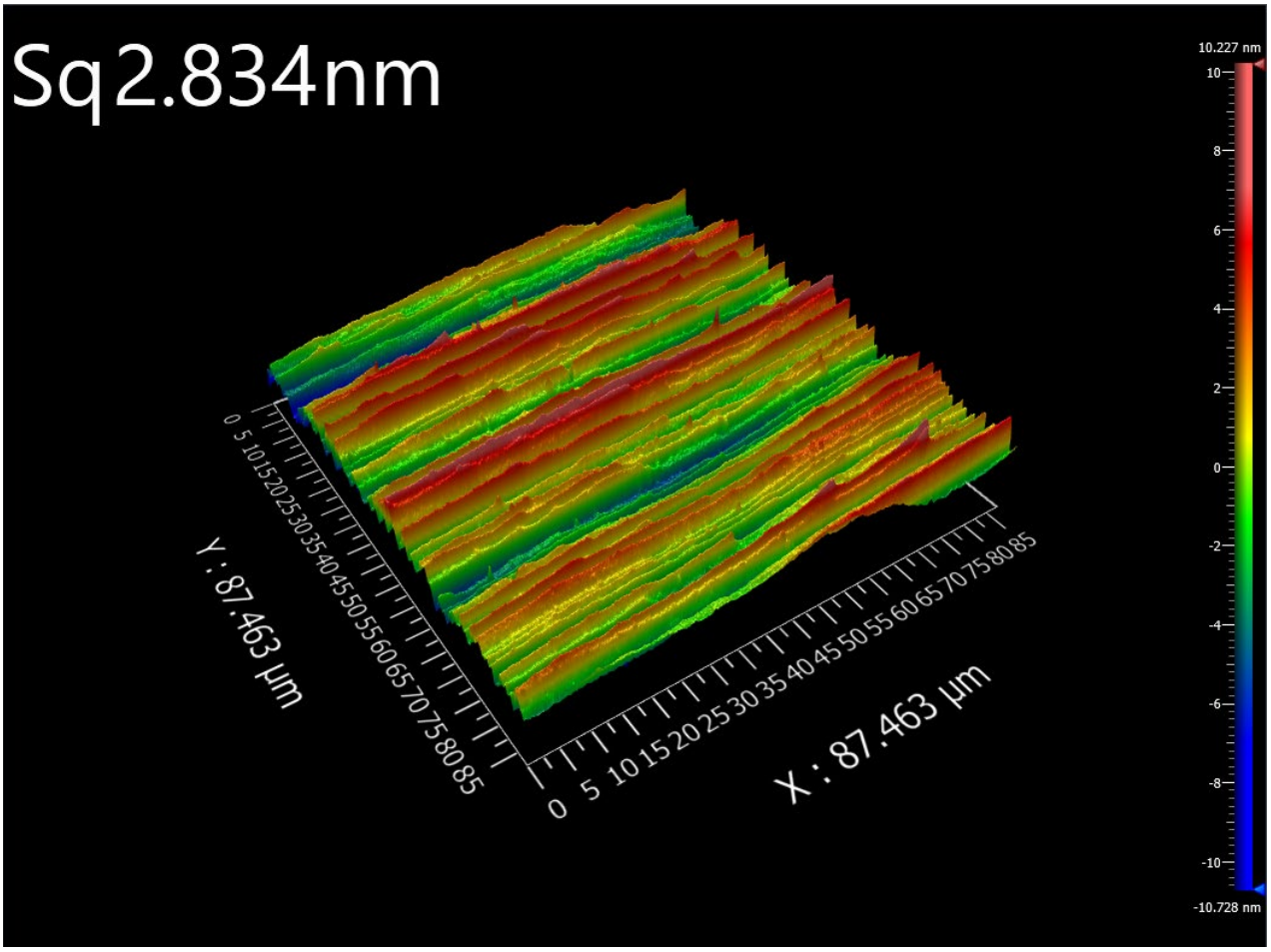

Figure 57: measurement of surface roughness for diamond crystal #7.

Funded by
the European Union

Crystallographic orientation

High-Resolution X-ray Diffraction (Panalytical X'Pert^3 MRD) is used to verify crystallographic orientation.

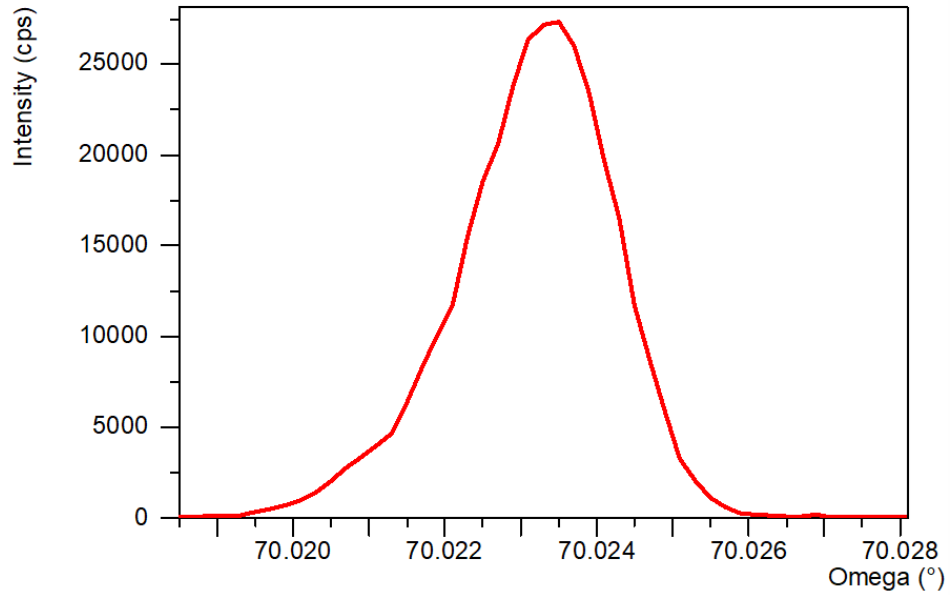

Figure 58. X-Ray rocking curve recorded on the main face of crystal diamond #7 highlight it is (331) oriented. That's worth noting that the beam is wider than the crystal, leading to a tail on the left side of the rocking curve, which is ascribed to the region corresponding to the strain relief cut structure.

The angular position of the rocking curve confirms that the crystal is (331) oriented. Miscut angle, i.e. the angle between the crystal main surface and the atomic planes have been measured through a High-Resolution X-ray Diffraction (Panalytical X'Pert^3 MRD) coupled to a custom-made autocollimator. Results of the measurement are reported in figure 4 and show a maximum value of 0.6124 degrees.

Funded by
the European Union

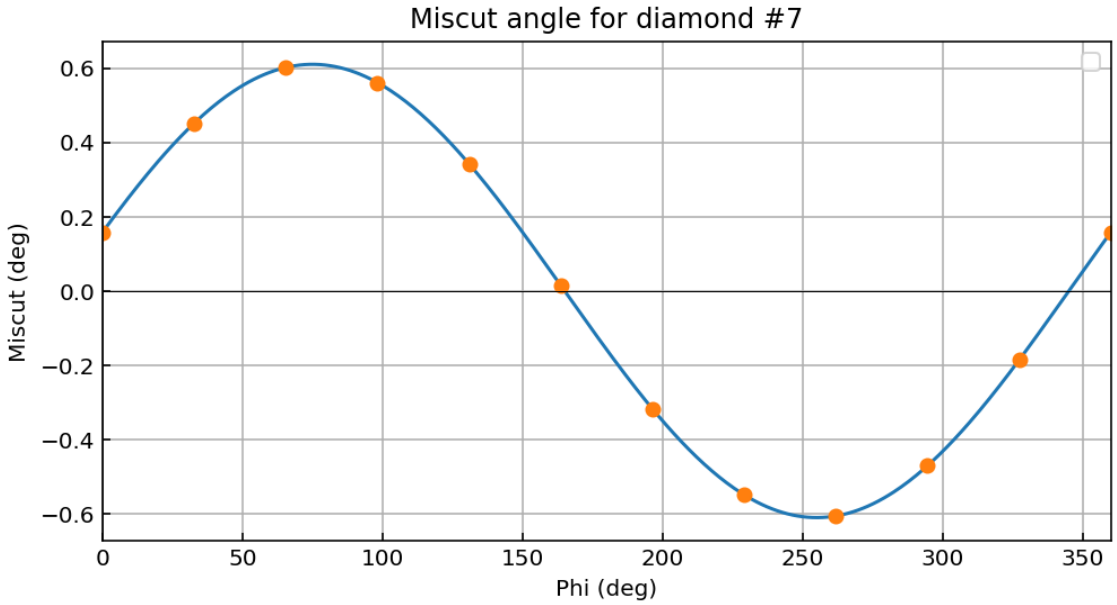

Figure 59. Miscut angle for sample diamond #7. Maximum value reaches 0.6134 degree.

Funded by
the European Union

X-ray Topography

X-ray Topography has been carried out at BM05 beamline at ESRF (European Synchrotron Radiation Facility). Results of the characterization shows 1 dislocations over the active are of the sample in terms of (a) Full-width half maximum of the rocking curve (b) Integral of the rocking curves (c) Rocking curve peak intensity (d) Centroid peak position.

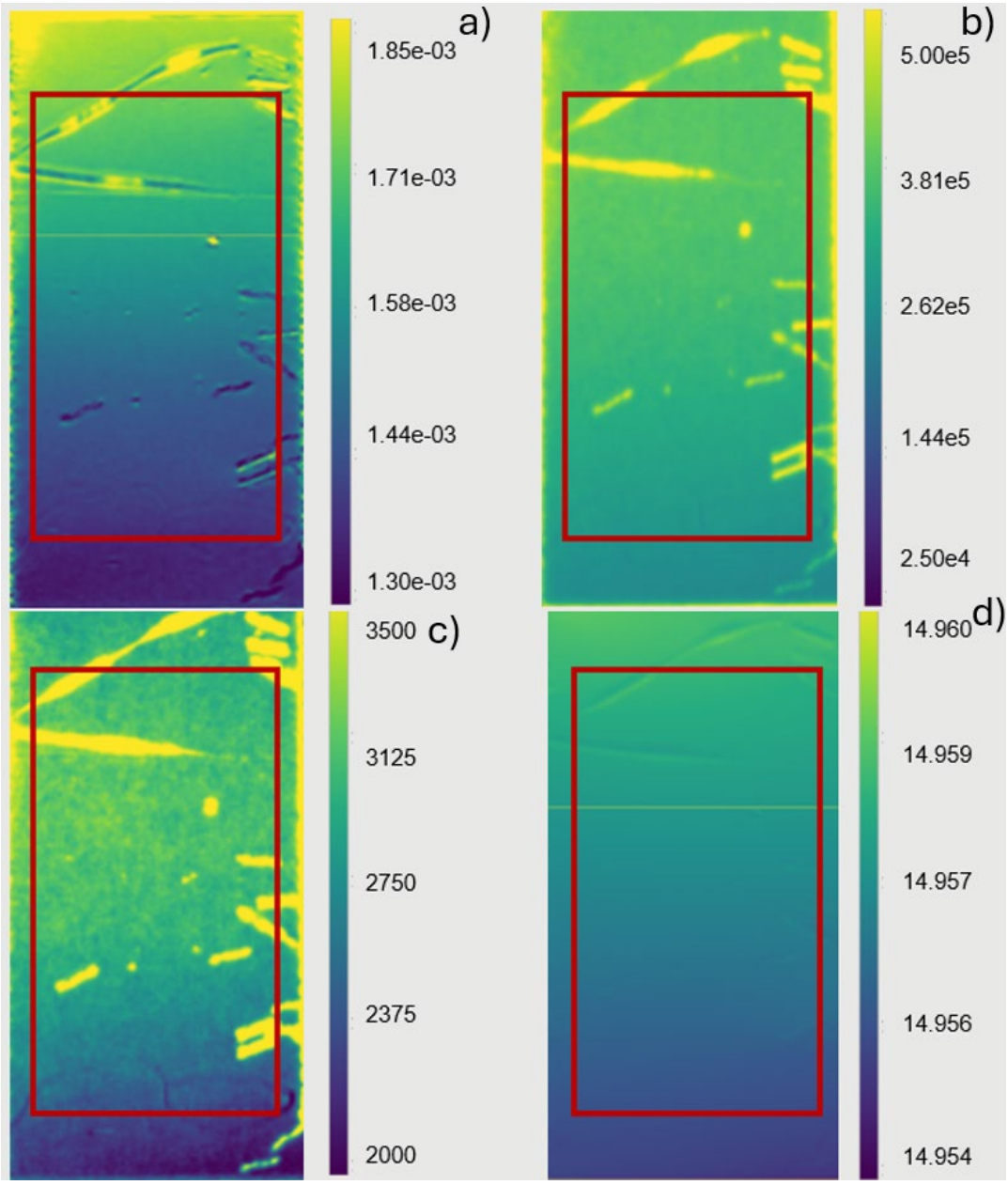

Figure 60. X-Ray topographies recorded at BM05 facility of ESRF (European Synchrotron Radiation Facility). (a) Full-width half maximum of the rocking curve (b) Integral of the rocking curves (c) Rocking curve peak intensity (d) Centroid peak position.

Table I summarizes the main properties of the crystal diamond #7 and compare them to the tendered specifications.

Technical characteristics			Tender compliance (Yes/No)
Crystal orientation	Orientation	(331)	Yes
Crystal geometry	Length	4.03	Yes
	Thickness, µm	99.1	Yes
Active area	Length x Width, mm	3.00x1.50	Yes
Number of dislocations in the active area	Dislocation count	10	Yes
Angle between the crystal's physical surface and the atomic plane	Degrees	0.6124	Yes

Table 1: comparison between expected main crystal features and characterizations.

Funded by the European Union

2.5.8 Datasheet for crystal diamond #8

MHz-Tomoscopy

Grant Agreement 101046448

Datasheet for the crystal "*Diamond #8*"

The technical specifications for the crystal were established in collaboration with DESY (Dr. Patrik Vagovic and his team) and Lund University (Prof. Pablo Villanueva Perez and his team). These specifications were finalized by DESY in mid-April 2023. Additionally, the design of the metal supports for the crystals was defined in cooperation with SUNA Precision GMBH (Dr. Alke Meents and his team) in early September 2024.

The crystal was purchased by INFN from the company XRNanotech with order dated 14/12/2023 and received by INFN at the end of November 2024.

Crystals geometry

Crystals lateral sizes and thickness are verified through a 3D optical profilometer (Zygo NX2), whose working principle relies on white-light interferometry. Crystal length is 4.01 mm. Average thickness of the active region measured through white light interferometry is 97.8 µm, in agreement with measurement through low coherence infrared interferometry (Fogale TMAP-4) which delivered a value of 97.9 µm.

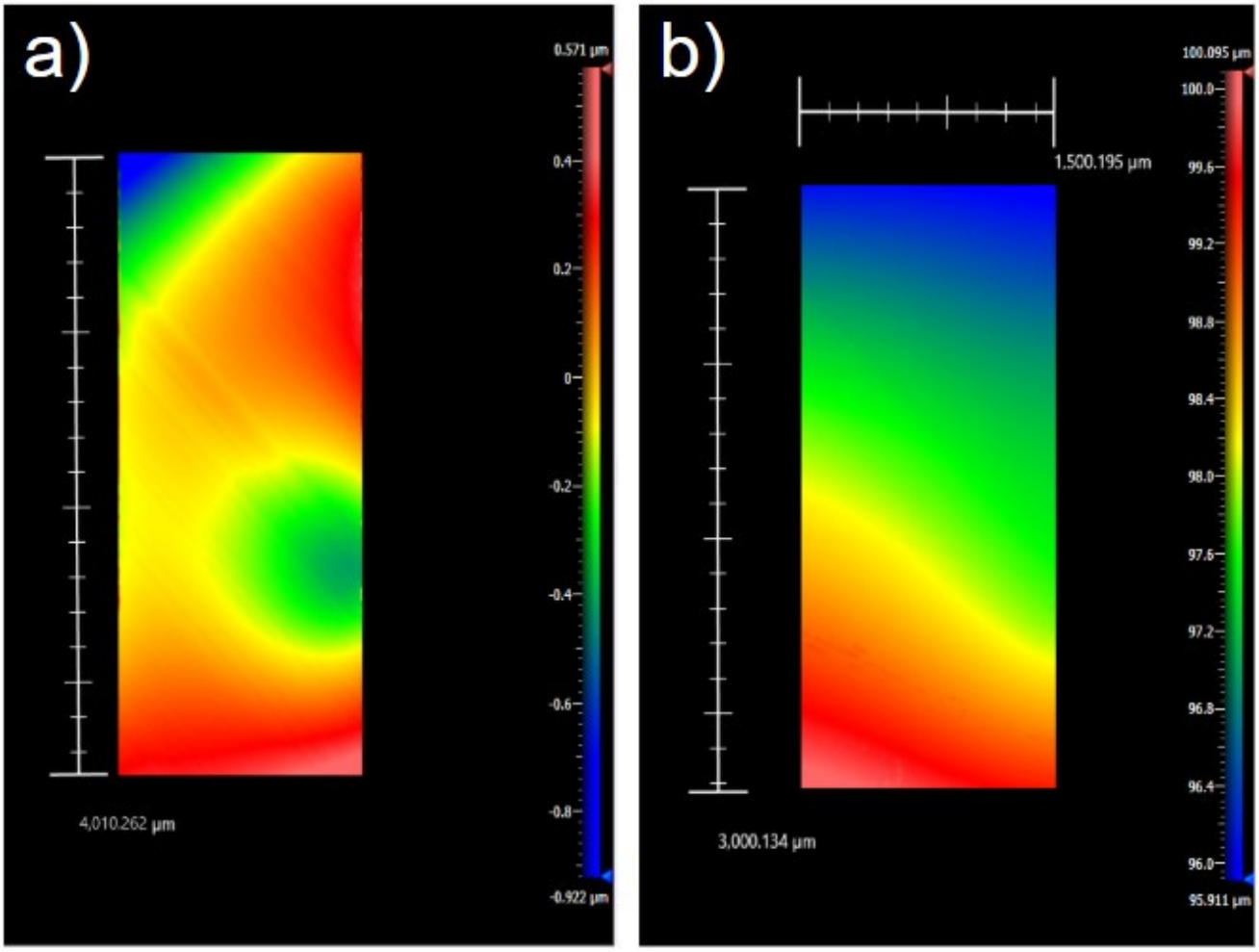

Figure 61: (a) interferometric characterization of the surface of the crystal diamond #8, used to determine the crystal length. (b) Thickness profile of the crystal active region.

Funded by
the European Union

Surface roughness

Surface roughness is measured through a 3D optical profilometer (Zygo NX2) operating at 100X magnification. Measured value is about ~2.7nm. Measurement is carried out on 20 sites and average value is estimated.

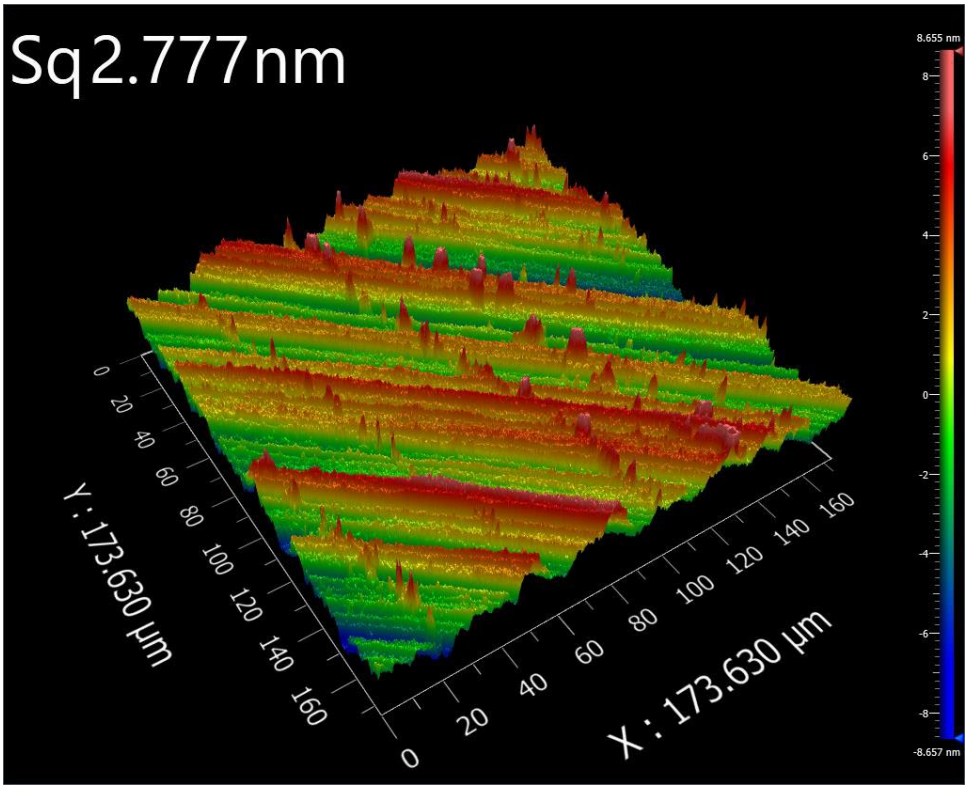

Figure 62: measurement of surface roughness for diamond crystal #8.

Funded by
the European Union

Crystallographic orientation

High-Resolution X-ray Diffraction (Panalytical X'Pert^3 MRD) is used to verify crystallographic orientation. The use of X-ray radiation at 8 keV does not allow direct excitation of reflections corresponding to the planes (511), nominally parallel to the main crystal surface. The surface orientation was determined by analyzing the rocking curves of asymmetric reflections from lattice planes inclined at known angles with respect to the surface normal (see Figure 63). This approach involves performing X-ray rocking curve measurements by slightly varying the incidence angle (ω) of the X-ray beam around the Bragg diffraction angle corresponding to these asymmetric reflections, thereby accurately determining crystal orientation and lattice alignment.

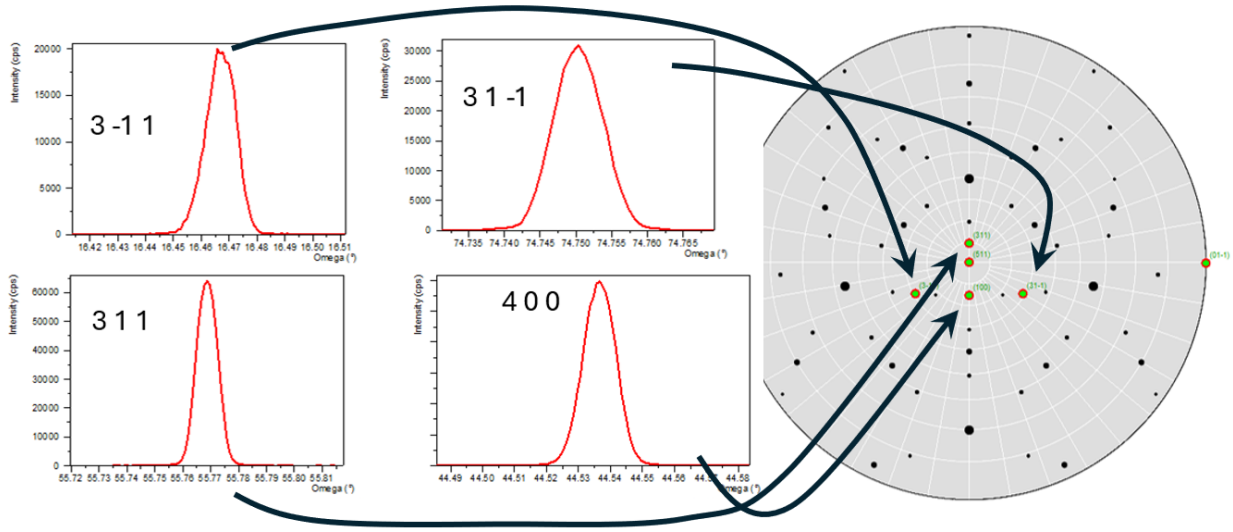

Figure 63. At the photon energy of 8 keV, diffraction from the (511) family of planes is not accessible. To determine the orientation of the crystal surface, asymmetric reflections from the (3-11), (31-1), (311), and (400) planes were measured. The corresponding peaks are shown in the four plots on the left. The angular positions of these reflections were used to reconstruct the crystal stereogram shown on the right. Arrows indicate the association between each measured reflection and its corresponding crystallographic direction in the stereogram. By evaluating the angular separation between the plane normals and the <511> direction, the surface orientation was confirmed to be the (511) plane.

Angular position of the rocking curve confirms that the crystal is (511) oriented, as expected.

Miscut angle, i.e. the angle between the crystal main surface and the atomic planes have been measured through a High-Resolution X-ray Diffraction (Panalytical X'Pert^3 MRD) coupled to a custom-made autocollimator. In this case also the miscut of the (511) surface was determined through analysis of

Funded by
the European Union

asymmetric reflections. Results of the measurement are reported in figure 4 and show a maximum value of 0.4241 degrees.

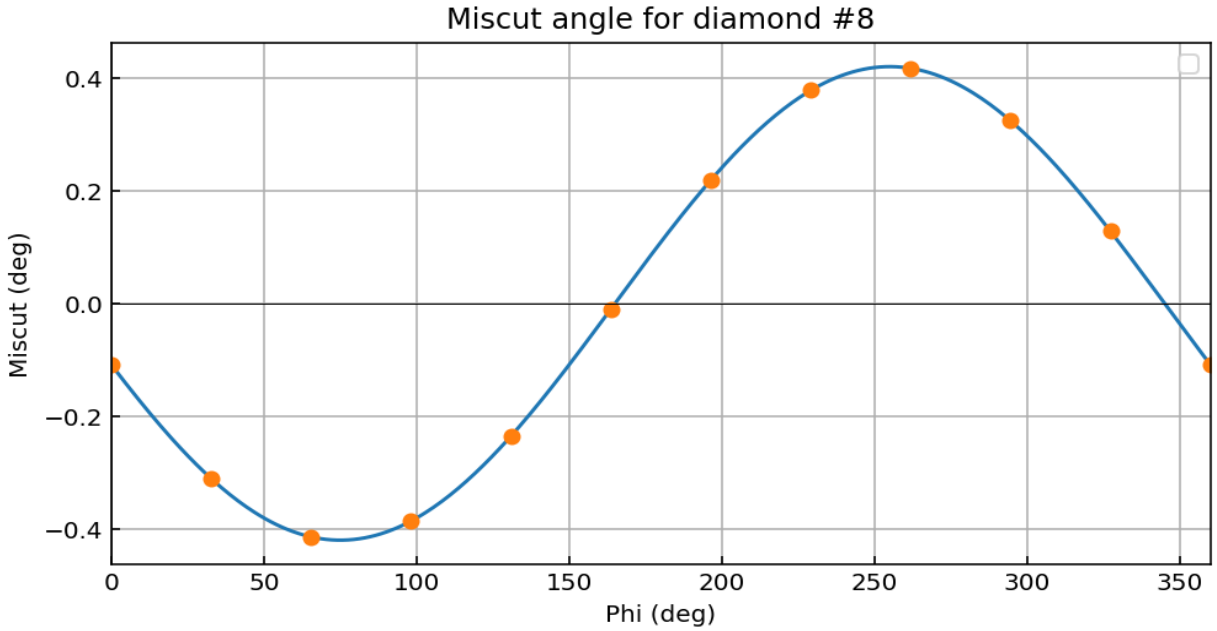

Figure 64. Miscut angle for sample diamond #8. Maximum value reaches 0.4241 degree.

Funded by
the European Union

X-ray Topography

X-ray Topography has been carried out at BM05 beamline at ESRF (European Synchrotron Radiation Facility). Results of the characterization show 3 dislocations over the active are of the sample. That's worth noting that also in this case x-ray diffraction signal from the surface plays a major role in determining the result of the integral of the rocking curves (figure 5b) and the rocking curve peak intensity (figure 5d)

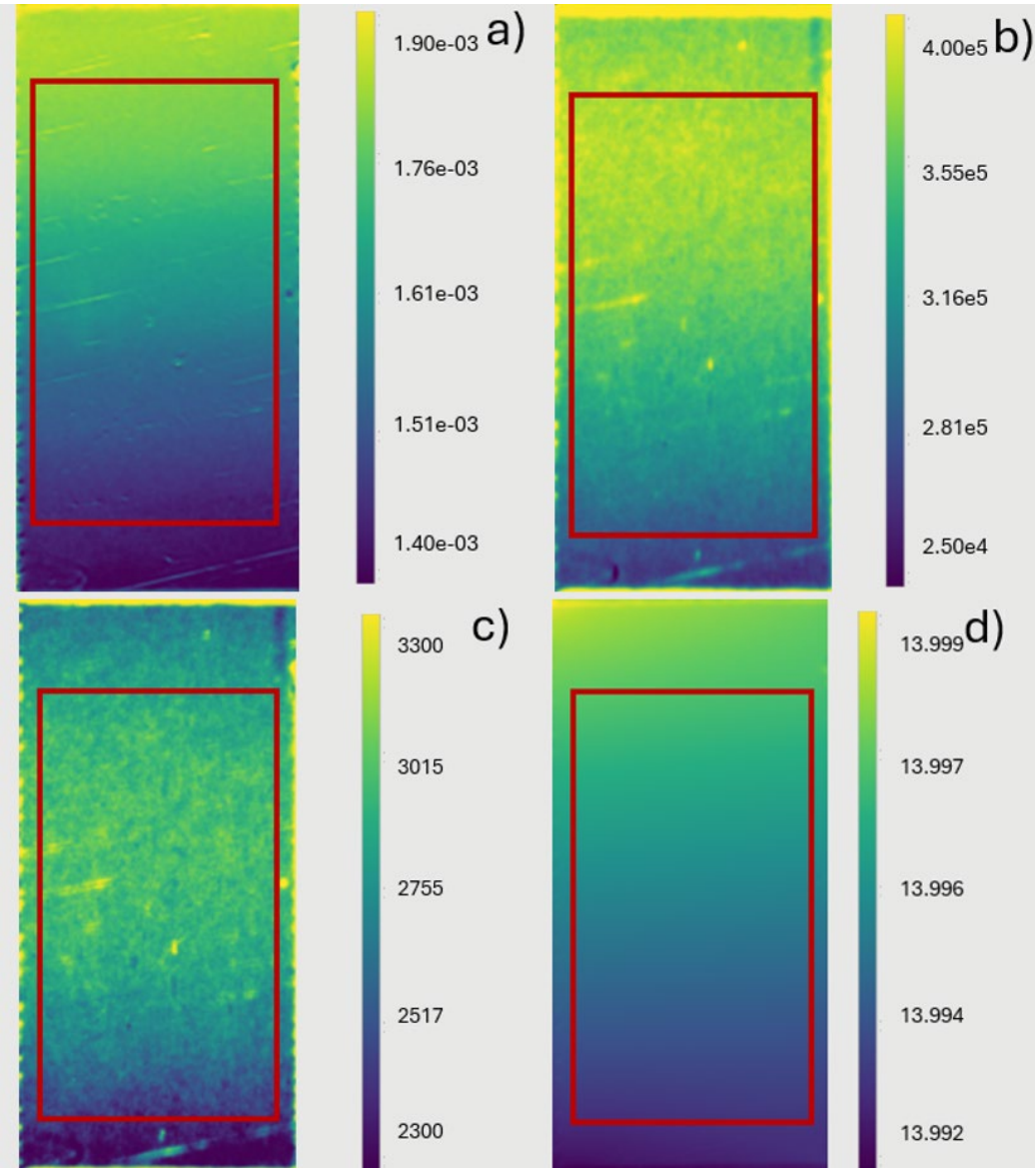

Figure 65. X-Ray topographies recorded at BM05 facility of ESRF (European Synchrotron Radiation Facility). (a) Full-width half maximum of the rocking curve (b) Integral of the rocking curves (c) Rocking curve peak intensity (d) Centroid peak position.

Funded by
the European Union

Table I summarizes the main properties of the crystal diamond #8 and compares them to the tendered specifications.

Technical characteristics			Tender compliance (Yes/No)
Crystal orientation	Orientation	(511)	Yes
Crystal geometry	Length	4.01	Yes
	Thickness, µm	97.8	Yes
Active area	Length x Width, mm	3.00x1.50	Yes
Number of dislocations in the active area	Dislocation count	3	Yes
Angle between the crystal's physical surface and the atomic plane	Degrees	0.4241	Yes

Table 1: comparison between expected main crystal features and characterizations.

Funded by the European Union

3. Bibliography

1. Mazzolari, A., et al., *Silicon crystals for steering high-intensity particle beams at ultrahigh-energy accelerators.* Physical Review Research, 2021. **3**(1): p. 013108.
2. Qu, Z., Y. Ma, and J. Wu, *Exploring mounting solutions for cryogenically cooled thin crystal optics in high power density x-ray free electron lasers.* Review of Scientific Instruments, 2024. **95**(5).
3. de Groot, P., *Principles of interference microscopy for the measurement of surface topography.* Advances in Optics and Photonics, 2015. **7**(1): p. 1-65.
4. de Groot, P., X. Colonna de Lega, and J. Liesener, *Model-based white light interference microscopy for metrology of transparent film stacks and optically-unresolved structures*, in *Fringe 2009: 6th International Workshop on Advanced Optical Metrology*, W. Osten and M. Kujawinska, Editors. 2009, Springer Berlin Heidelberg: Berlin, Heidelberg. p. 1-8.

Funded by
the European Union

4. Annex 1

Annex 1 is the certificate INFN has received from the supplier of the crystals (XRnanotech).

Funded by
the European Union

XRnanotech AG
Parkstrasse 1
B1.O3.01
CH 5234 Villigen
Tel: +41 56 5080 264

PRODUCT DOCUMENTATION OF SINGLE-CRYSTAL DIAMONDS WITH EXTREMELY LOW DENSITY OF DISLOCATIONS FOR THE MHZ-TOMOSCOPY PROJECT

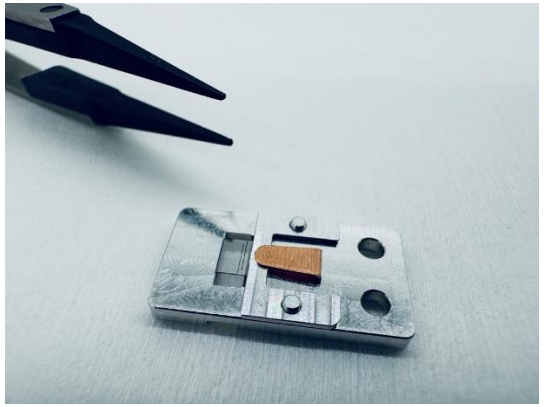

TECHNICAL REQUIREMENTS FOR THE SUPPLY

1) **Crystal Growth Method**: High Pressure High Temperature (HPHT).
2) **Purity Grade**: IIa (as defined by the International Institute of Diamond Grading & Research).
3) **Angle between the crystal's physical surface and the atomic plane**: The crystallographic orientation of the main surface is indicated in Table 1: the major surfaces of the crystal are parallel to the atomic planes of the crystal within 3 degrees along any direction.
4) **Surface Roughness of both major surfaces (Ra)**: < 50 nm.
5) **Active Area**: each crystal has an 'active area' in the relative position (within the crystal geometry) and with the dimensions given in Table 1. This area exhibits a dislocation count below 10.
6) **Crystal Geometry and Crystallographic Orientation**: the geometry and crystallographic orientation of the crystals are given in Table 1.
7) **Strain relief cuts:** Each crystal has two strain relief cuts according to the specs.
8) **Supports for the Crystals**: Each crystal has been accompanied by an aluminum frame that ensures the ability to handle the crystal.
9) **Crystal Assembly**: Each crystal was mounted in its respective frame made of aluminum. The assembly was carried out in such a way that only the region beneath the "strain relief cuts" is in contact with the frame itself.

XRnanotech AG
Parkstrasse 1
B1.O3.01
CH 5234 Villigen
Tel: +41 56 5080 264

COMPLIANCE OF PARAMETERS OF DIAMOND SINGLE CRYSTALS HPHT-GROWN TYPE IIA WITH THE TECHNICAL REQUIREMENTS

Technical characteristics		Crystallographic Orientation							
		{111}	{111}	{110}	{110}	{311}	{211}	{331}	{511}
Crystal geometry	Length x Width, mm	5.00x3.20	5.00x3.20	4.00x3.20	4.00x3.20	4.00x3.20	4.00x3.20	4.00x3.20	4.00x3.20
	Thickness, mm	0.074	0.080	0.097	0.100	0.100	0.077	0.100	0.100
Active area	Length x Width, mm	3.00x1.50	3.00x1.50	3.00x1.50	3.00x1.50	3.00x1.50	3.00x1.50	3.00x1.50	3.00x1.50
Number of dislocations in the active area	Dislocation count	<2	<1	<7	<7	0	<2	<10	0
Angle between the crystal's physical surface and the atomic plane	Degrees	2.0	2.1	0.1	0.1	0.4	0.2	0.6	0.4

XRnanotech AG
Parkstrasse 1
B1.O3.01
CH 5234 Villigen
Tel: +41 56 5080 264

X-RAY TOPOGRAPHY MEASUREMENTS

	X-ray topography measurements of the grown crystal. The blue lines indicate the cutout profile of the finished product.	Active area and the number of dislocations
Crystallographic orientation 111 Geometry: 5.67x5.44x1.03mm	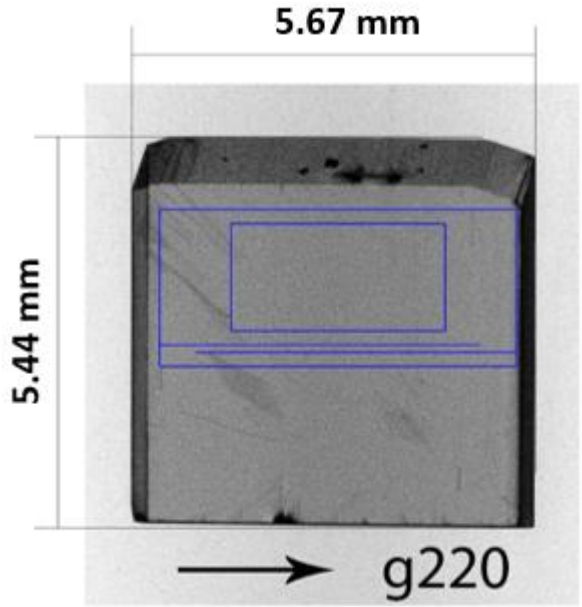	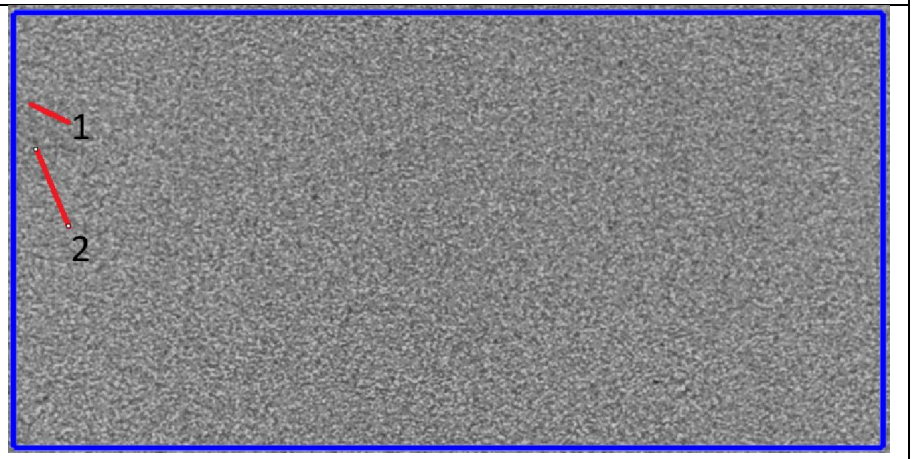 The total number of dislocations in the active region is 2. Taking into account the proportional translation (cutout, thinning and polishing) to the final thickness of the crystal we have 0.14 counts per active region.

XRnanotech AG
Parkstrasse 1
B1.O3.01
CH 5234 Villigen
Tel: +41 56 5080 264

Crystallographic orientation 111 Geometry: 6.04x4.42x1.22mm	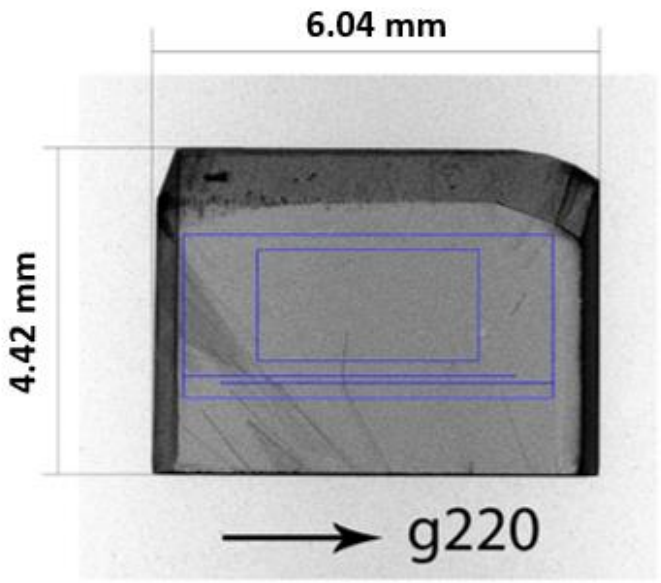	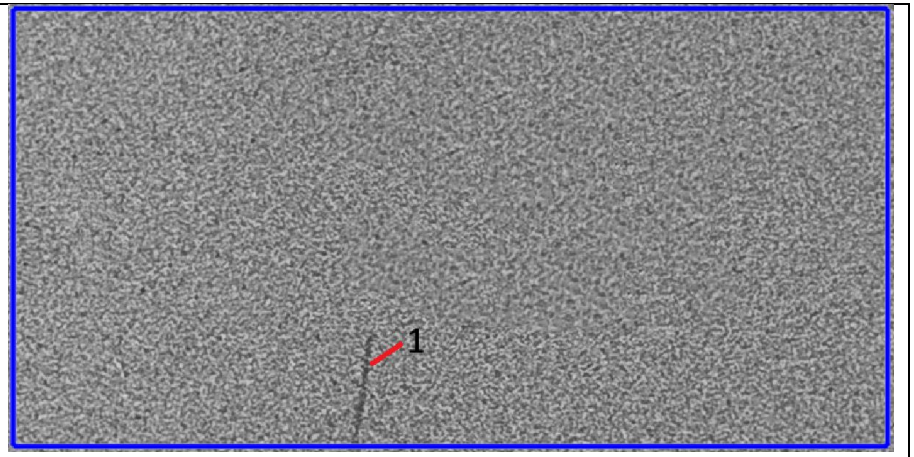 The number of dislocations in the active region is 1. Taking into account translation of dislocation density to the final thickness of the crystal we have 0.065 counts per active region

XRnanotech AG
Parkstrasse 1
B1.O3.01
CH 5234 Villigen
Tel: +41 56 5080 264

Crystallographic orientation 110 Geometry: 5.86x4.76x1.12mm	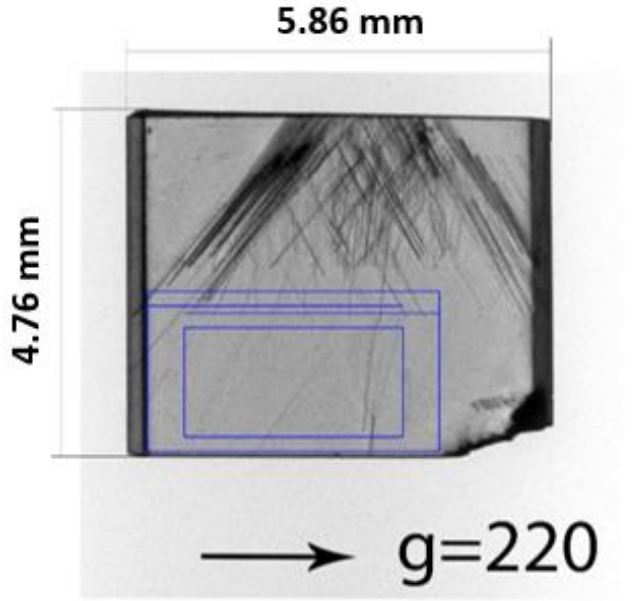	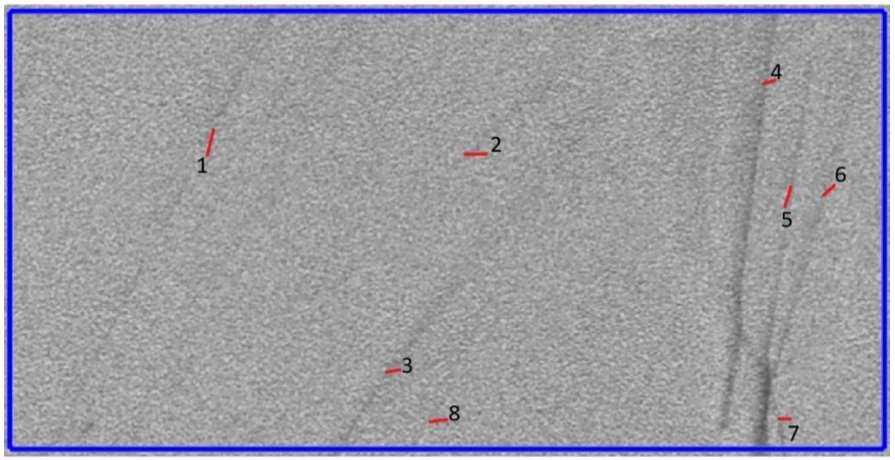 The total number of dislocations in the active region is less than 10 at the crystal thickness of 1.12 mm. Proportional calculation of dislocation density when the crystal thickness is reduced to 0.097 mm gives a value of 0.69 counts per active region.

XRnanotech AG
Parkstrasse 1
B1.O3.01
CH 5234 Villigen
Tel: +41 56 5080 264

Crystallographic orientation 110 Geometry: 5.86x4.76x1.12mm	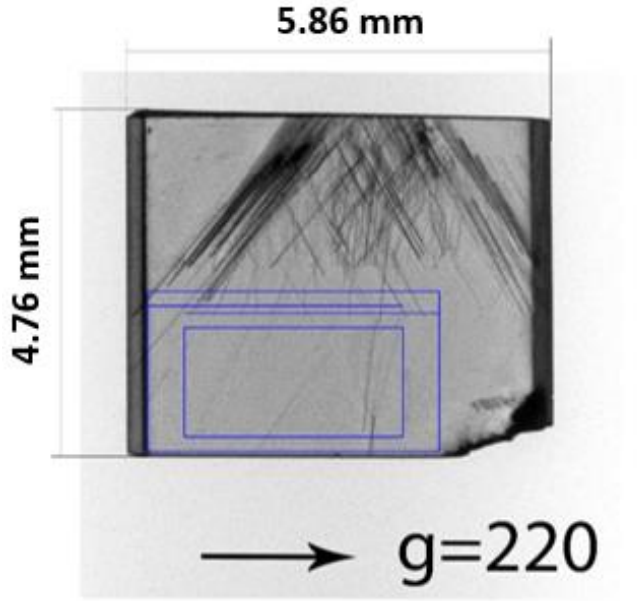	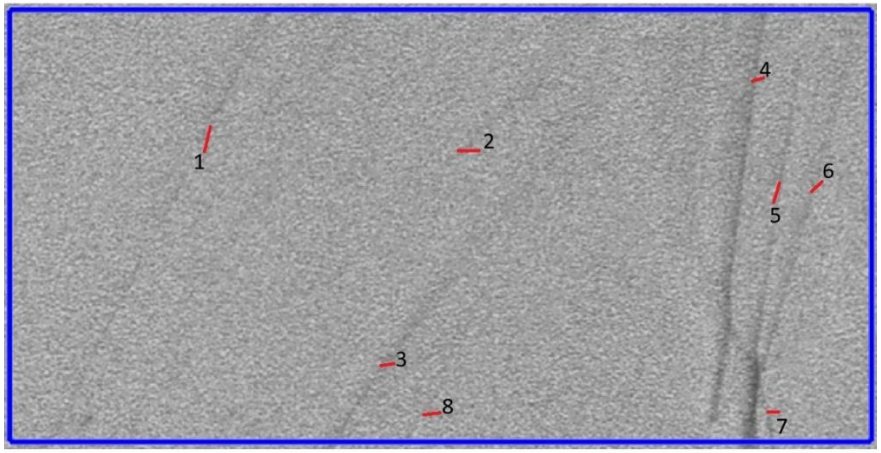 The total number of dislocations in the active region is less than 10 at the crystal thickness of 1.12 mm. Proportional calculation of dislocation density when the crystal thickness is reduced to 0.097 mm gives a value of 0.69 counts per active region

XRnanotech AG
Parkstrasse 1
B1.O3.01
CH 5234 Villigen
Tel: +41 56 5080 264

Crystallographic orientation 211 Geometry: 9.52x6.64x1.48mm	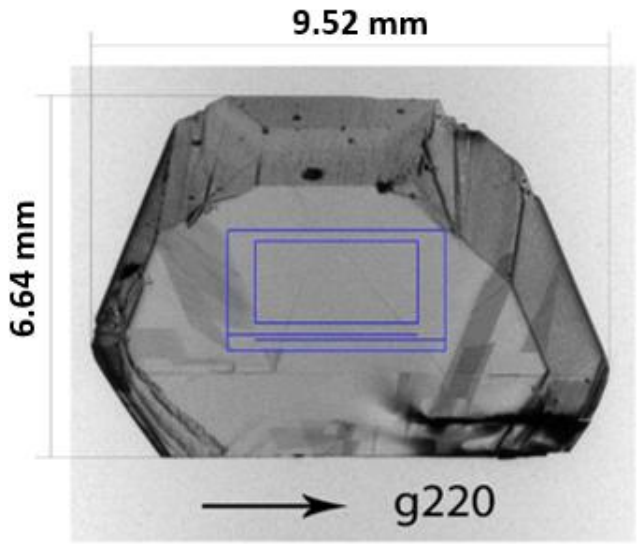	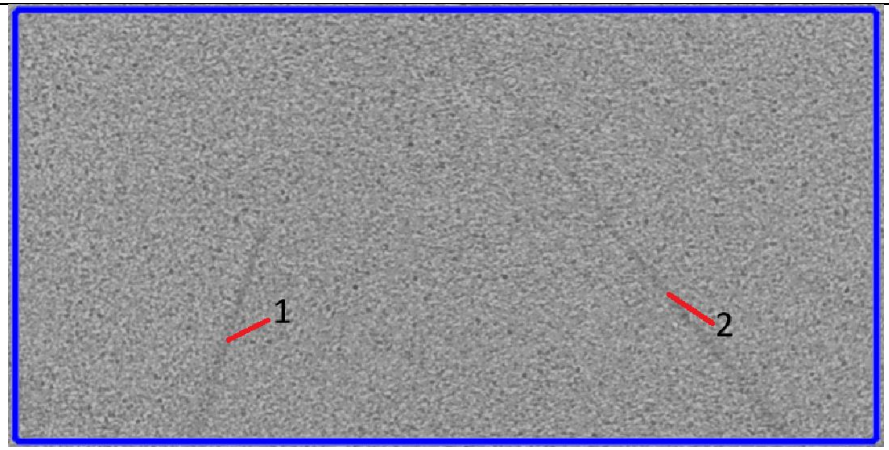 The number of dislocations in the active region is 2. Taking into account the proportional change of dislocation density from the crystal thickness, we have 0.1 counts per active region.

XRnanotech AG
Parkstrasse 1
B1.O3.01
CH 5234 Villigen
Tel: +41 56 5080 264

Crystallographic orientation 311 Geometry: 9.57x8.55x1.23mm	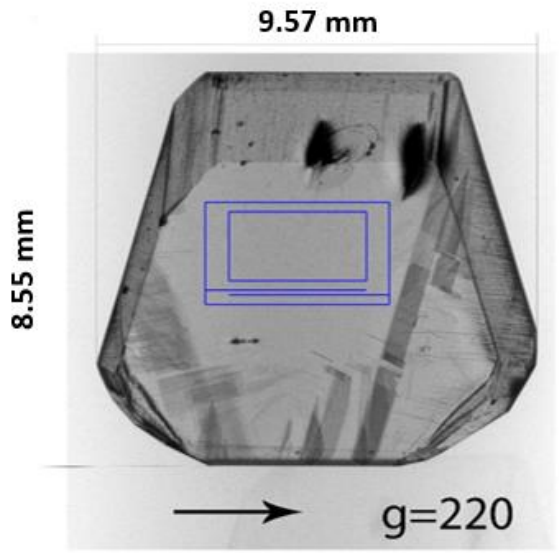	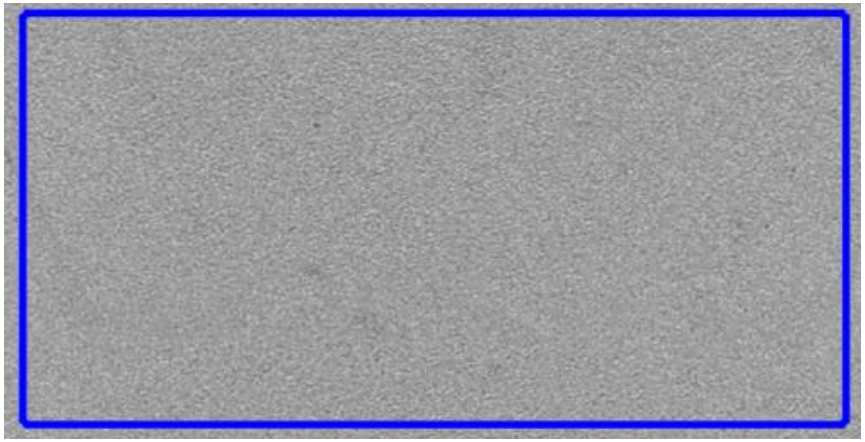 The number of dislocations in the active region is 0

XRnanotech AG
Parkstrasse 1
B1.O3.01
CH 5234 Villigen
Tel: +41 56 5080 264

Crystallographic orientation 331 Geometry: 5.83x4.61x1.34mm	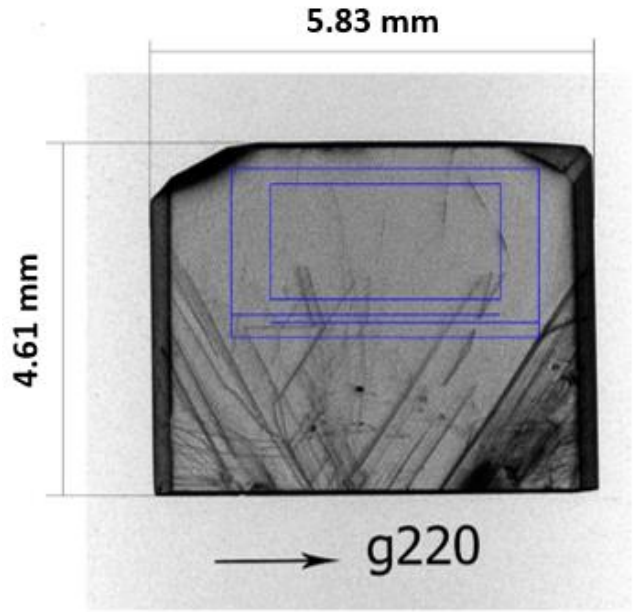	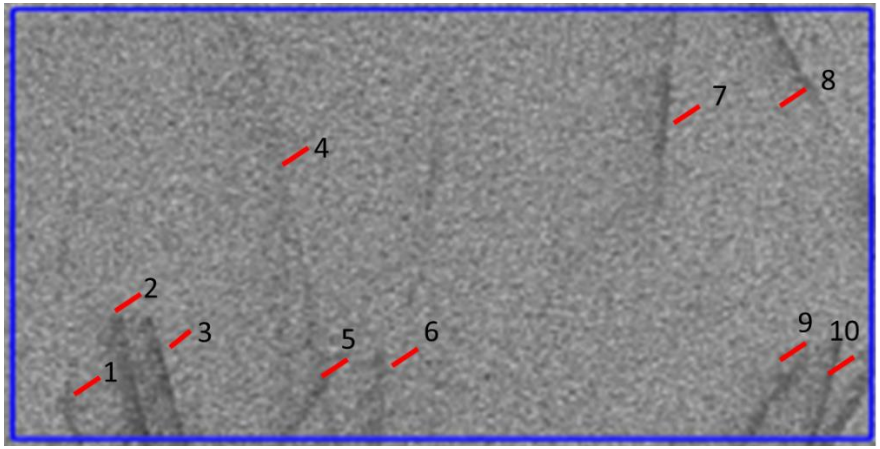 The number of dislocations in the active region is 10. Taking into account the proportional change of dislocation density from the crystal thickness, we have 0.63 counts per active region.

XRnanotech AG
Parkstrasse 1
B1.O3.01
CH 5234 Villigen
Tel: +41 56 5080 264

Crystallographic orientation 511 Geometry: 9.56x7.44x1.1mm	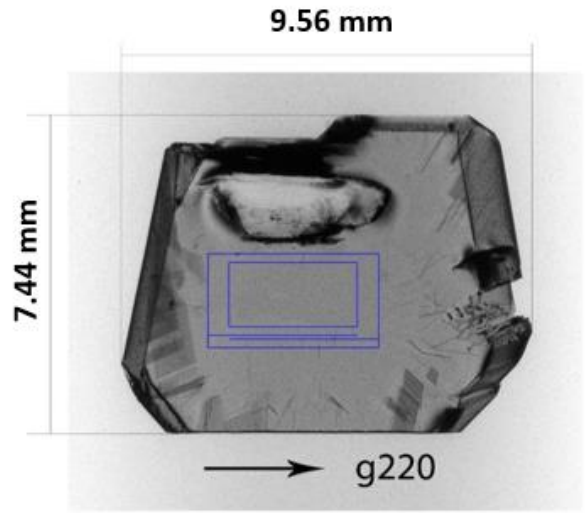	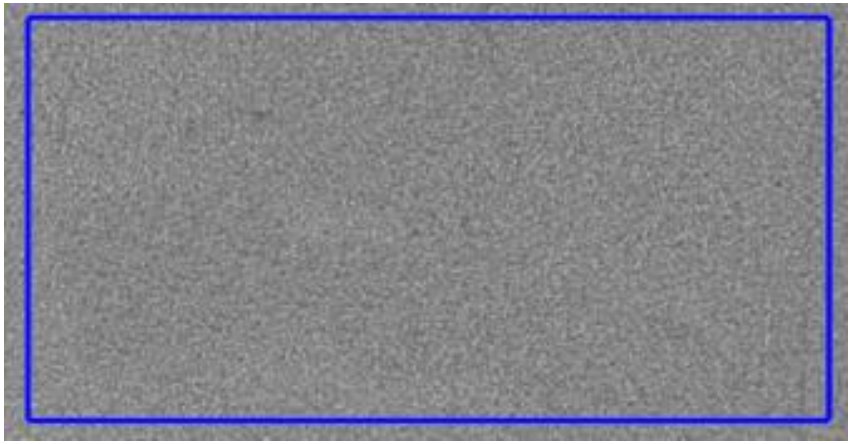 The number of dislocations in the active region is 0.